THE GEOLOGY OF THE ACID PHASE OF THE BUSHVELD COMPLEX, NORTH OF PRETORIA - A GEOCHEMICAL/STATISTICAL APPROACH

by

HENDRIK DE BRUIYN

Submitted in fulfilment of the requirements
for the degree of

PHILOSOPHIA DOCTOR

in the
Faculty of Science,
Department of Geology,
University of the Orange Free State

DECEMBER, 1980

DR. G.J. GERINGER

ABSTRACT

A petrographical and geochemical study of the acid phase of the Bushveld Complex, north of Pretoria, was undertaken with the aim to identify the different rock units, to determine their interrelationships and to classify the rocks as well as describing their geochemistry.

The oldest geological formation in the area is the Rooiberg Group which is subdivided into two units, namely the Kwaggasnek (lower) and Schrikkloof (upper) Formations. Petrographical, mineralogical and geochemical data are submitted for the different units. From the data it can be deduced that these units formed as products of a single parental magma, while statistical manipulation of the geochemical data indicates that these formations differ significantly from the Damwal Formation farther to the east. The gradational contact relationships between the felsites and underlying granophyre are described and explained in the text.

The various granophyre occurrences of the Rashoop Granophyre Suite are classified and described. The mineralogical, petrographical and geochemical data indicate a limited differentiation trend from the felsites into the granophyre. This may indicate that the granophyre in part resulted from the rapid crystallization of the parental magma of the Rooiberg Group. A model for the origin and formation of the Rashoop Granophyre Suite, based on petrographical and geochemical evidence, is proposed.

The granites are subdivided according to age and field relationships, as well as mineralogical, petrographical and geochemical characteristics into the Sekhukhuni, Verena, Makhutso, Klipvoor and Klipkloof granites. The mode of intrusion as well as the mineralogical, petrological and geochemical composition of each type are discussed. A petrochemical investigation of the granites indicate that the various granites, with the exception of the Klipkloof granite, represent the differentiation products of a single parental magma. A similar study on the Makhutso and Verena granites indicates that leptite assimilation influenced the final differentiation trend in these granites, causing enrichment in certain elements and depletion in others.

Chemical variation diagrams, corroborated by statistical parameters, strongly suggest that the felsite of the Kwaggasnek and Schrikkloof Formations, the granophyre of the Rashoop Granophyre Suite and the various granites are genetically related to one another and most probably represent the differentiation products of a single differentiated parental magma. Geochemical evidence pointed out that the Klipkloof granites, however, represent a separate granitic intrusion.

A structural analysis of the area indicates tectonic instability and relative movement during and after emplacement of the Bushveld granite, resulting in structural highs and lows in the granite floor; some of the graben-like structures serve as depositional basins for the deposition of the Karoo Sequence in the area.

A genetic model for the acid phase of the Bushveld Complex is proposed.

CONTENTS

PAGE

LIST OF FIGURES

LIST OF TABLES

LIST OF APPENDICES

1 INTRODUCTION

1.1 GENERAL

The Bushveld Complex, which is situated in the central part of the Transvaal basin, occupies a total area of approximately 67 340 km^2 (Hunter, 1975). It consists of four synformal lobes which are arranged about two axes to form a cruciform outline (Fig. 1.1).

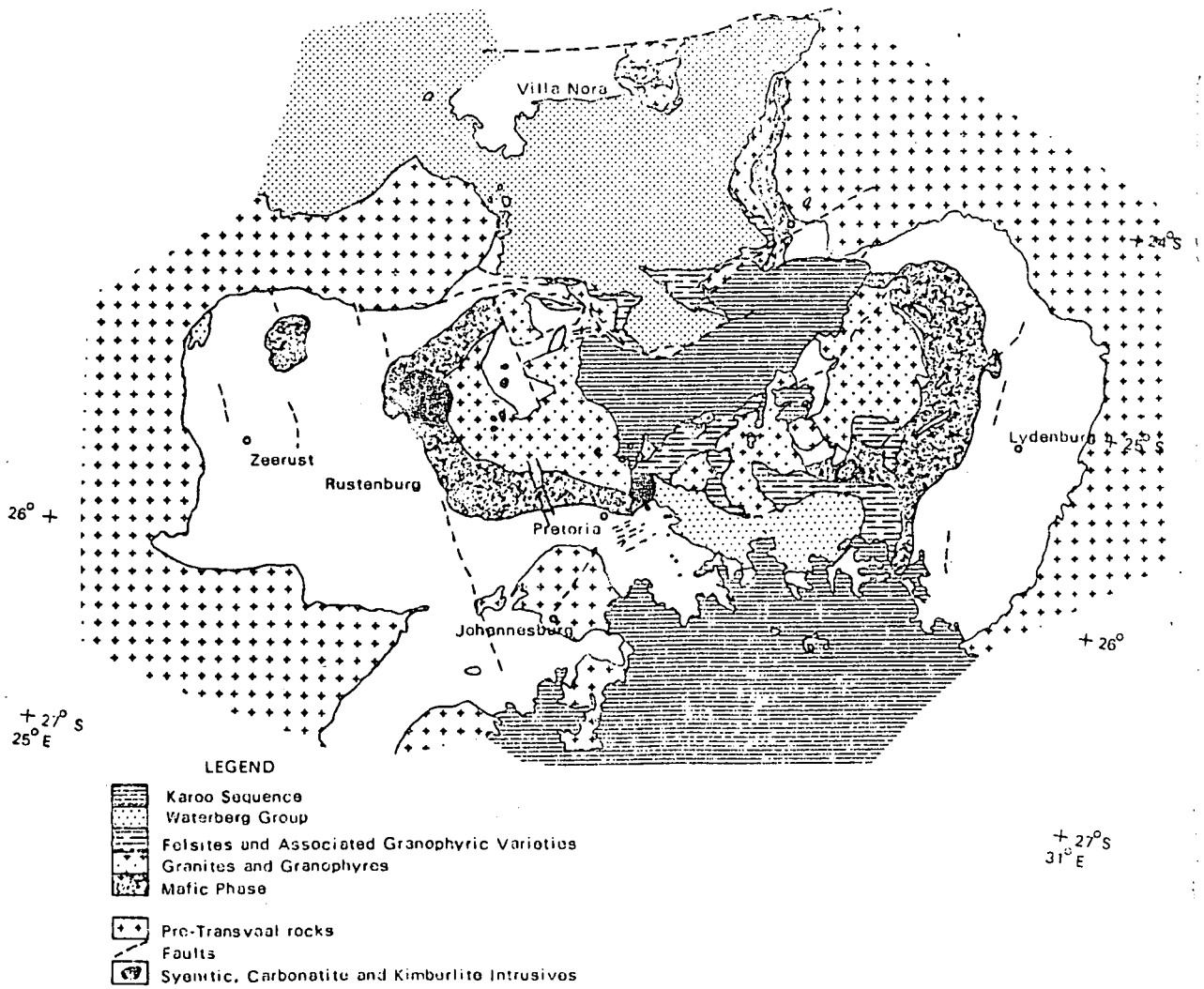

Fig. 1.1. Simplified geological map of the Bushveld Complex (after Hunter, 1975).

Bushveld granite and felsite are largely confined within the four main lobes of mafic rocks. The granites exhibit stratiform layering which consists of coarse-grained grey granite, medium-grained grey and red granite, with younger granites showing intrusive relationships with the former types. Granophyric granite to granophyre are commonly associated with the granite/felsite contacts and overlying Transvaal sediments.

The felsites form the roof-rocks of the Complex in many instances. Flow-banded varieties, massive rocks and sedimentary intercalations are part of the rocks confined to the basin structure of the Complex. Their stratigraphic position remains uncertain; they have been regarded as the terminal phase of the Transvaal Sequence, or as an extrusive event co-genetic with the Bushveld Complex (Hunter, 1975).

1.2 AIM OF STUDY AND PRESENT INVESTIGATION

The acid phase of the Bushveld Complex has received considerable attention from a great number of investigators. The genetic relationships of the granitic, granophyric and felsitic rocks, however, still remain problematic. The present investigation was, therefore, conducted to contribute to our knowledge and understanding of the genetic relationships of these rock suites.

The goals set for the present investigation were :

(1) To map an area in which both granitic and granophyric rocks are closely related and to classify the various granitic bodies which form part of the Acid Phase within the study area.

(2) To study the relationships between the various granitic rocks, the granophyric rocks and the roof-rocks, which in this area, consist mainly of the rocks belonging to the Rooiberg Group.

(3) To establish a possible relationship between the various magmas which gave rise to the different entities.

(4) To postulate a tectonic model for the origin and emplacement of the acid phase of that part of the Bushveld Complex.

The work was initially performed as a project of the Geological Survey while the author was attached to that organization. Mapping was done on aerial photographs (scale 1 : 30 000), from which the data were transferred to topographical maps (scale 1 : 50 000) by means of a proportional compass and a Map-O-Graph. These maps were reduced to a scale of 1 : 100 000 for publication by the Geological Survey (Folder 1).

The laboratory investigations were carried out at the Geological Survey until June, 1974, and thereafter at the University of the North and the University of the Orange Free State. Chemical analyses were carried out by Bergström and Bakker using XRF- and gravimetrical methods, while the statistical reduction of the data was performed by means of computer programmes on a Univac Computer at the University of the Orange Free State.

1.3 PREVIOUS WORK

Previous work in and around the area mapped, was mainly restricted to the prominent geological features such as the Roodeplaat Complex and the Pretoria salt pan in the south, while the felsic rocks in the central part of the area were mapped on a regional scale.

The Geological Survey sheet 2 (Pienaarsrivier), of which the explanation was prepared by Kynaston (1907), was first mapped by Mellor and Hall in the period 1904 to 1906. A great deal of attention was paid to the area around Roodeplaat, which was first mapped and described by Kynaston in 1907 and consequently revised by Lombaard (1929), who first used the term 'centrocline' for the Roodeplaat structure. The volcano was reinvestigated by Teichmann, then a member of the Geological Survey, in 1962. Numerous other investigators, for instance Shand (1921, 1922), Venter (1933), Truter (1949), Van Biljon (1949), Toens (1952), Coertze (1962) and Verwoerd (1967) also contributed to the knowledge regarding this feature.

The Pretoria salt pan has been described by authors such as Cohen (1896), Wagner (1920, 1922, 1929), Kynaston and Mellor (1905), Hall (1932), Koen (1955) and Verwoerd (1967).

Portions of the Pienaarsrivier sheet were reinvestigated by Spies (1952) and Snyman (1953). Their work was incorporated into the Geological Map of the Union of South Africa of 1955.

The western half of the old sheet 18 (Moosrivier), which is now part of the 1 : 250 000 Pretoria sheet, was previously surveyed by Hall (1904), Jorissen (1905), Gau (1906) and Wagner (1927). Lombaard (1931) completed the mapping, compiled their work and prepared the explanation for this sheet. Truter (1943) described a dome-shaped granite body in the vicinity of Witnek within the study area. This dome is now known as the Makhutso Granite (De Bruiyn & Rhodes, 1975). In 1956 Glatthaar investigated the pyroclastic rocks of the Rust de Winter area, while Van Zijl (1965) described the geophysics of the Albert Silver Mine on Roodepoortje 250 JR.

The work of other investigators will be referred to where appropriate.

2 LOCALITY AND PHYSIOGRAPHY

The geology of an area just north of Pretoria and to the south of Warmbad between longitudes 28° and 29° east and latitudes 25° and 25° 30′ south (Fig. 2.1) was investigated. It comprises a total area of approximately 5 000 km^2, of which about 2 500 km^2 is underlain by acidic rocks of the Bushveld Complex.

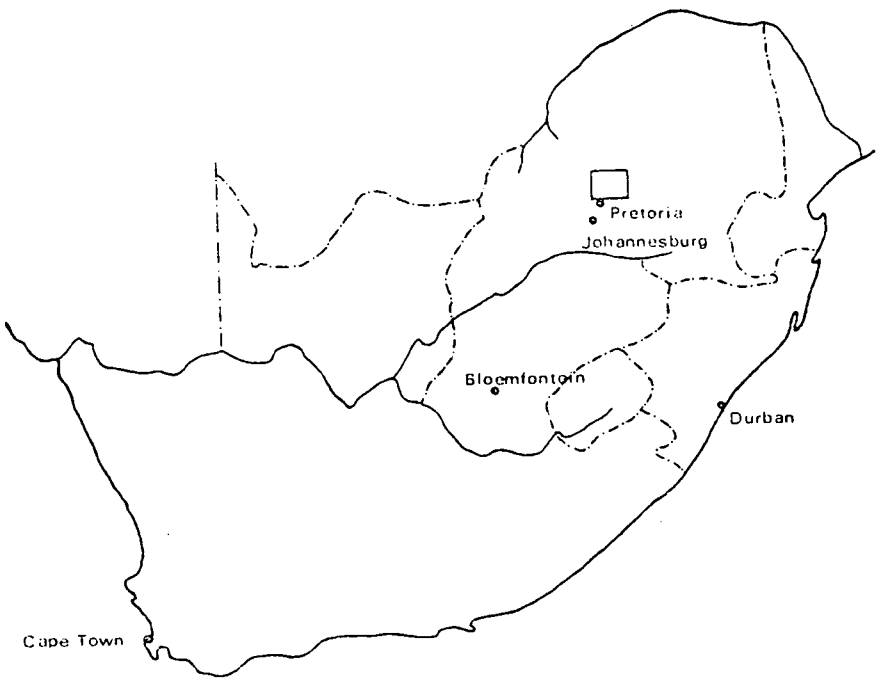

Fig. 2.1. Locality map of the study area.

2.1 TOPOGRAPHY

The area in the south-east is marked by an undulating topography, which extends northwards to an escarpment, coinciding with a geological boundary formed by the younger Karoo rocks (Lombaard, 1931). The south-eastern portion was classified as the plateau region by Lombaard (1931) (Fig. 2.2).

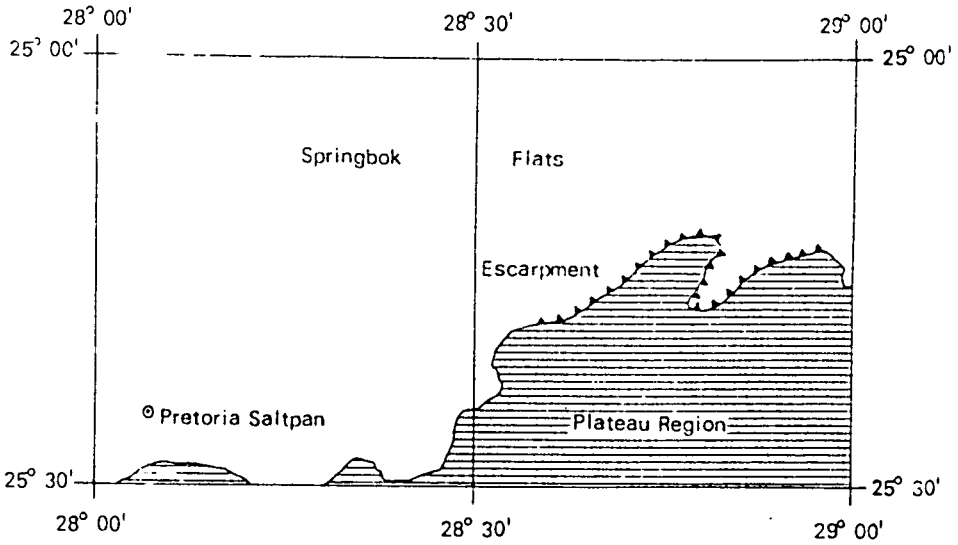

Fig. 2.2. Topographical subdivision of the area north of Pretoria (modified after Lombaard, 1931).

The escarpment extends from Pieterskraal 190 JR in the east to Buffelsdrift 179 JR in the west. It attains a maximum height of 300 m at Zaagkuilfontein 204 JR (Fig. 2.3), while lower relief is, however, more common.

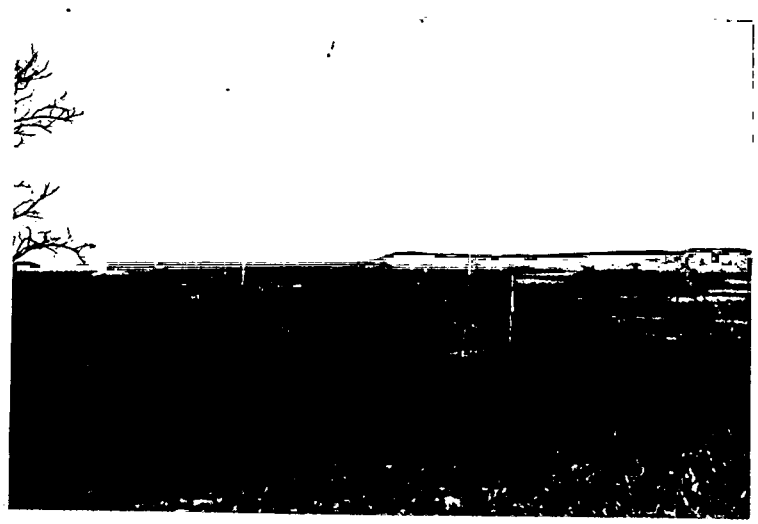

Fig. 2.3. The escarpment at Zaagkuilfontein 204 JR formed by the Karoo/Acid Phase contact in the background.

Another range of steep hills occurs to the south of the Pretoria Salt Pan. These hills consist of granophyre while the plains immediately to the north are underlain by granite. To the north of the escarpments, the topography is gently undulating with only small erosion relicts of Waterberg and Karoo sediments projecting above the plain, forming an adult landscape.

The Pretoria Salt Pan is a crater-like feature which rises to a height of more than 50 m above the surrounding plain. The centre of the crater is approximately 100 m below the rim, therefore about 50 m below the landscape surrounding the pan.

2.2 DRAINAGE

Three major rivers, namely the Pienaars River (with its major tributary the Boekenhoutspruit), the Apies River (with the Plat River as major tributary) and the Elands River (with its tributaries the Enkeldoornspruit, Gifspruit and Kameel River) drain the area. The Moses River, itself a tributary of the Olifants River, drains the eastern part of the area. A simplified drainage map of the area is shown in Figure 2.4.

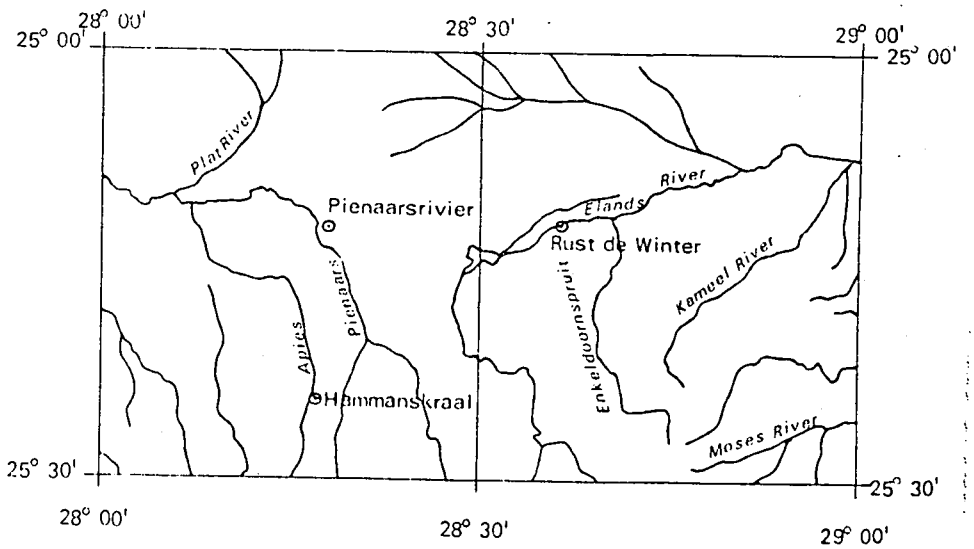

Fig. 2.4. Simplified drainage map of the study area.

The rivers in the southern part of the area are short and numerous, whereas those in the north are longer and the drainage pattern more open. This could in part be attributed to the virtual peneplained surface of the landscape in the north.

Lombaard (1931) stated that the drainage of this area is superimposed from the overlying Karoo rocks, presently represented by outliers. This could well be the case in the Springbok Flats area, but the lower order stream segments (Strahler, 1952) in the south are too numerous and too short for this to be the case. The drainage in the southern part of this area indicates that the area is still juvenile in its erosion cycle.

The meandering of the Elands River in the vicinity of Bezuidenhoutkraal 166 JR is explained by the river flowing over easily weathered sediments and then being superimposed over more resistant felsite and granite, thus stemming the flow and causing it to meander (Lombaard, 1931). This could, however, not be the cause of the meandering of both the Apies and Pienaars Rivers, as no such disturbances were observed in their vicinities. The meandering of these two rivers is, therefore, interpreted as being the result of a mature landscape through which they flow.

The drainage pattern of the rivers is typically dendritic with numerous first, second and higher order streams. In a drainage analysis of the Elands River it was found that the bifurcation ratio remained fairly constant for the first and second, second and third, third and fourth and fourth and fifth order streams (De Bruiyn, 1974).

Strahler (1969) pointed out that the consistency of the bifurcation ratio is dependent on the climate, rock-type and the geological development of an area. The inconsistency of the bifurcation ratio, when comparing the stream segments in the northern part of the area with those in the south, indicates that the underlying rock formations and the development of the area is not uniform. This can be traced to the relatively small number of stream segments in the more adult northern part of the area.

The low drainage density of this part of the area may also be linked to the high permeability of the underlying material, which causes infiltration of the precipitation, thus causing large areas to furnish the runoff necessary for the maintenance of a channel (Strahler, 1969). The latter is clearly indicated by the large number of influent streams on Pieterskraal 190 JR and on Leeuwfontein 188 JR.

2.3 GEOMORPHOLOGY

The geomorphological development of this area is, because of the relatively undulating terrain, difficult to determine. To the south of the study area, however, lies the Bankeveld (Wellington, 1937) which is an extremely well defined geomorphological unit. The geomorphological processes that gave rise to the landscape of the Bankeveld are also responsible for landscaping in the rest of the area.

2.3.1 Pre-Karoo Surface

The landscape of the Bankeveld is the result of two main cycles of erosion, namely pre-Karoo and post-Karoo (mid Tertiary) with a later subcycle. Very little is known about landscape development before Karoo times, but it seems that the ice-sheet which covered the land during the Carboniferous, planed down the ridges (Wellington, 1937). The effect of erosion by the ice-sheet was also noticed by Dixey (1942) who found that patches of tillite still survived in places in the Bankeveld.

Wellington (1937) was of the opinion that a high pre-Karoo peneplain occurred between the Magaliesberg and the Witwatersrand and that this peneplain formed part of the glaciated plain on the Waterberg surface north of the Premier Mine, Witbank and Middelburg. It can also be seen as a very prominent surface to the south of Verena.

2.3.2 Karoo Surface

The Ecca beds have been deposited on the pre-Karoo landscape (King, 1962) which possessed a low relief. Wellington (1937) also noted similar conditions and stated that the Karoo surface was a 'rolling plain in which comparatively few streams form generally wide open valleys, so that few outcrops of the harder sandstones are seen except in the large river valleys'. He is convinced that the drainage on the Karoo surface was an indecisive one, where pans were developed. He further notes that the 'new drainage was able to adapt itself to the general slope of the underlying surface, cutting through the underlying beds as they are discovered'.

The Karoo beds were seemingly preserved along the watersheds as can be seen in the Moloto area where Ecca shales and sandstones are present. The present situation indicates that the topographical depression in the Moloto area existed at the time of deposition and that it was gradually filled with sediments, of which the remains can still be seen as outliers.

2.3.3 Post-Karoo Surface

King (1962) regards the features of the landscape in the Pretoria area as being of Karoo age and that most of the ridges are resurrected pre-Karoo features. Kynaston (1929) also favours the idea that the present topography is partly a fossil pre-Karoo landscape. It exhibits the same direction and amount of dip as that of the old topography. This can be seen in the erosion relicts of Karoo sediments at higher elevations around Moloto and Enkeldoorn.

A very flat landscape after the removal of the Karoo cover is postulated by Wellington (1937). He also ascribes the diversified surface of the Bankeveld and the Witwatersrand to weathering and erosion after the removal of the Karoo beds. The post-Karoo period is marked by two cycles : a post-Karoo cycle and a subordinate Bushveld cycle (Dixey, 1942). The homoclinal ridges of the Bankeveld, which are the relicts of the pre-Karoo peneplain, have been affected to a small degree by the Bushveld cycle.

The large number of valleys present in the post-Karoo peneplain, are considered as being active since the end of the Tertiary, making them younger than the post-Karoo cycle, probably part of the Bushveld cycle (Dixey, 1942).

2.3.4 Recent Erosion Cycle

The absence of river capture and the extreme youthfulness of the gaps cut by the tributaries led Wellington (1926a) to deduce that the lateral valley streams eroded their headwaters during a relatively short period of time. The valleys in the Daspoort area are shallow on the secondary watersheds, an aspect which led Reynhardt (personal communication) to a similar conclusion.

An investigation of the secondary streams indicated a discontinuity in the erosion cycle between the post-Karoo and recent times (Wellington, 1926b). Reynhardt (personal communication) suggested that if the present landscape resulted from long-termed stream action, without interruption in the erosion cycle, the secondary streams would have incised over a longer distance than is the case at present. A non-interruption of the erosion cycle would also have caused river piracy. The absence of river capture and of prominent watersheds indicates that the present drainage pattern is not responsible for any escarpment development.

3 GENERAL STRATIGRAPHY

The wide variety of sedimentary, plutonic and volcanic rocks makes the study area extremely interesting for studying mutual interrelationships. The plutonic rocks not only belong to the Bushveld Complex, but younger alkaline intrusions, correlating with the Pilanesberg period of intrusion, are also present. The volcanic rocks belong both to the oldest and youngest formations in the area, namely the Rooiberg Group and the Karoo Sequence respectively. The sedimentary rocks belong to the Waterberg Group and the Karoo Sequence, while younger sediments occur along the river valleys. The surficial deposits and the sedimentary Karoo Sequence were, however, not investigated as part of this study.

The Rooiberg Group, which forms the roof-rocks in the study area, occurs as a synformal structure with a north-east, south-west striking axis. It is subdivided into the Kwaggasnek (lower) and Schrikkloof (upper) Formations. In the vicinity of the Rust de Winter Dam a number of pyroclastic beds are developed, which for the purpose of this study, are called the Rust de Winter member of the Schrikkloof Formation.

The Kwaggasnek and Schrikkloof Formations are separated from one another by a well developed volcanic breccia or agglomerate, while the base of the Rust de Winter member, is an ash-flow tuff similar to the one defined by Rhodes and Du Plessis (1976) at the top of the Schrikkloof Formation. In some places the development of the agglomerate marker is extremely lenticular in which cases an underlying zone, containing quartzite xenoliths, was used to define the position of the contact between the Kwaggasnek and Schrikkloof Formations.

The Kwaggasnek Formation, of 1 500 to 2 500 m, is characterized by seemingly homogeneous massive felsite containing phenocrysts of quartz and feldspar. An amygdaloidal felsite, described by Rhodes and Du Plessis (1976) near the top of the Kwaggasnek Formation, could not be positively identified.

The Schrikkloof Formation displays a complex eruptive history, consisting of the lenticular marker (agglomerate, breccia) at the base, followed by a vast amount of flow-banded and massive felsite with numerous tuff and agglomerate layers.

The Rust de Winter member, which is very thin and only locally developed in the study area, consists in ascending order of basal ash-flow tuff, rhyolite, black vitric tuff, agglomerate and quartzite at the top.

Granophyre forms a fairly thick succession between the granite and the felsite as well as between the basic portion and the granites. It can be subdivided into the Sterk River, the Stavoren and Blinkwater types. The first-mentioned is developed between the granite and the felsite, while the Stavoren granophyre formed between Transvaal sediments and Bushveld granite. The Blinkwater type occurs between the mafic portion of the Bushveld Complex and the Bushveld granite. Collectively these granophyre types form the Rashoop Granophyre Suite.

The granites, which form part of the Lebowa Granite Suite, are represented by the Nebo and Makhutso Granites. The Nebo Granite can be subdivided into the porphyritic Verena granite and the Sekhukhuni granite. The Klipvoor and Klipkloof granites, which were correlated with the Bobbejaankop granite, are also present in the area.

The overlying Waterberg Group is represented by the Wilgerivier Formation of the Nylstroom Subgroup in this area. The unit consists of reddish conglomerate, sandstone and shale, as well as an interbedded rhyolite, which has also been classified as a quartz porphyry.

The deposition of the Waterberg Group was followed by intrusive and extrusive cycles starting with the Franspoort alkaline bodies and the extrusion of the Pretoria Centrocline, also known as the Roodeplaat Complex.

An interesting post-Karoo feature in this area is the Pretoria salt pan which has been described as a crypto-volcanic or as an impact feature.

The lithological subdivision within the study area is given in Table 3.1.

TABLE 3.1 : STRATIGRAPHIC SUBDIVISION OF UNITS AS USED IN THIS STUDY.

SEDIMENTARY COLUMN				IGNEOUS COLUMN				
			Karoo sedimentary sequence, recent and surficial deposits					
				Syenite, foyaite and carbonatite				
				Trachyte, trachyandesite with sporadic occurrences of breccia and dykes of foyaite porphyry				Roodeplaat Complex
				Diabase/dolerite undifferentiated				
Waterberg Group	Wilgerivier Formation		Sandstone, pebble sandstone shale and conglomerate	Grey to light pink granite porphyry		Klipkloof Granite	Lebowa Granite Suite	Bushveld Complex
				Red medium-grained granite with pegmatite veins		Klipvoor Granite		
				Porphyritic biotite granite with fine-grained facies in places		Makhutso Granite		
				Porphyritic rhyolite				
				Pink porphyritic granite with aplite veins and dykes	Verena Granite	Nebo Granite		
				Pink coarse-grained granite with aplite veins and dykes	Sekhukhuni Granite			
				Granophyre, microgranophyre, porphyritic granophyre and leptite	Sterk River Granophyre, Stavoren Granophyre, Blinkwater Granophyre		Rashoop Granophyre Suite	
Rooiberg Group	Schrikkloof Formation	Rust de Winter member	Basal ash-flow tuff, black glassy tuff, agglomerate and quartzite					
			Impersistent volcanic breccia at base, lenticular tuff and agglomerate, sandstone lenses	Red, brown and pale coloured felsite with flow-banding and multicoloured flow-banded rhyolite locally near top				
	Kwaggasnek Formation		Scattered quartzite xenoliths	Red, dark brown and black felsite with locally developed contorted flow-banding near top				

4 ROOIBERG GROUP

4.1 INTRODUCTION

The Rooiberg Group occurs as remnants within the lobes of the Bushveld Complex (Fig. 4.1). The patchy appearance of the felsites seems to be structurally and erosionally controlled as the remnants coincide mainly with syn- and antiformal structures, thus surviving deep erosion in the area.

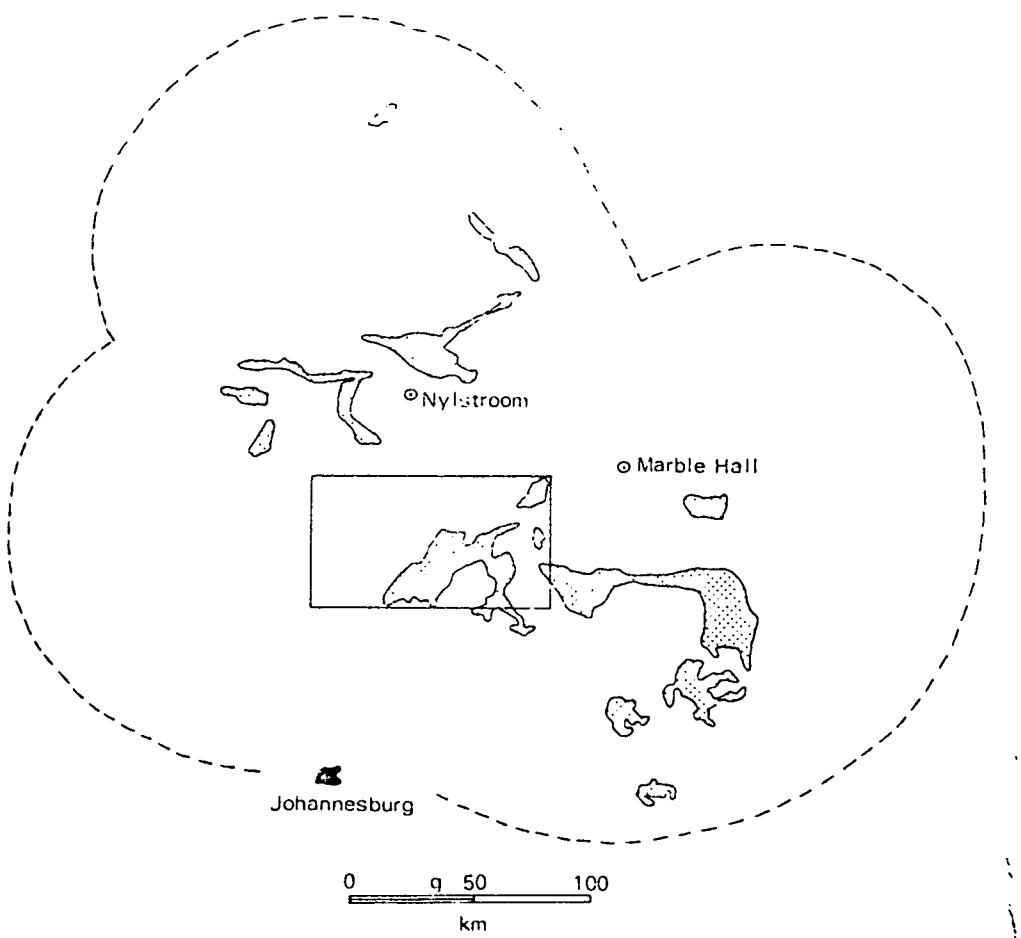

Fig. 4.1. Sketchmap of the distribution of the Rooiberg Group with the limits of the Bushveld Complex indicated by the dashed line. The position of the study area is blocked.

4.2 STRATIGRAPHY

Numerous attempts have been made in the past to subdivide the Rooiberg Group. In 1932 Lombaard proposed a classification for the Rooiberg felsites, which was adopted by other workers with only small modifications, for instance Wolhuter (1954) and Glatthaar (1956), while Menge (1963) proposed a threefold subdivision for these rocks in the Nylstroom area. Wilke (1963) and De Villiers (1963) both contributed to the stratigraphy of the Rooiberg Group when they reported the presence of quartzite xenoliths and agglomerate from the area west of Potgietersrust. Von Gruenewaldt (1966, 1968) confirmed a remarkable similarity between the succession as mapped by him and that described initially by Lombaard (1932). He subdivided the Rooiberg Goup into three main units, consisting of felsite at the base followed by amygdaloidal felsite with agglomerate, intercalated felsite, shale and conglomerate at the top (Table 4.1). Coetzee (1970) also proposed a threefold classification, which in general, corresponds with that of Von Gruenewaldt (1966, 1968).

A classification by Rhodes and Du Plessis (1976) was in part accepted by the South African Committee on Stratigraphy (SACS) for the rocks of this group. According to their classification only two distinct lithological units are developed in the Rooiberg Group, namely the Kwaggasnek (lower) and the Schrikkloof (upper) Formations.

Later work by Clubley-Armstrong (1977) in the Loskop Dam area indicates that the Rooiberg Group in the west differs from that in the east where the Damwal Formation forms an additional unit at the base of the succession. He also recognized the twofold classification, as described by Rhodes and Du Plessis (1976), but referred to it as the Doornkloof and Klipnek members of the Selonsrivier Formation (Table 4.1).

A study of the stratigraphy pointed out that the classification as proposed by Rhodes and Du Plessis (1976) is also applicable to the felsitic rocks in the study area (Table 4.1). The distribution of these formations, in the study area, are shown on Fig. 4.2. The lithostratigraphic sequence, emphasizing the top of the succession, is shown in Fig. 4.3.

TABLE 4.1 : STRATIGRAPHIC SUBDIVISION OF THE ROOIBERG GROUP ACCORDING TO VARIOUS AUTHORS AND THAT USED IN THIS STUDY.

1		2		3		4		5
								Quartzite, agglomerate, rhyolite, tuff
Quartz porphyry		Not mapped		Ignimbrite				Ignimbrite
Shale, conglomerate, chert	Upper felsite zone		Upper Formation				Schrikkloof Formation	
Non-porphyritic and porphyritic felsite		Porphyritic felsite		Fine-grained, flow-banded, porphyritic felsite		Red flow-banded felsite		Fine-grained, flow-banded, porphyritic felsite
Shale		Shale		Shale and tuffaceous beds	Selonsrivier Formation Doornkloof member	Mudstone, sandstone		Shale and tuffaceous beds
Non-porphyritic felsite						Black felsite, amygdaloidal felsite		
Agglomerate		Agglomerate and porphyritic felsite		Volcanic breccia and agglomerate		Volcanic breccia		Volcanic breccia and agglomerate
(VARIABLE FELSITE) Amygdaloidal and flow-banded felsite	Middle	Amygdaloidal, pseudo spherulitic felsite and microgranophyre	Lower Formation	Zone of quartzite xenoliths, amygdaloidal, flow-banded felsite	Klipnek member	Sandstone and tuff beds quartzite xenoliths	Kwaggasnek Formation	Zone of quartzite xenoliths Flow-banded felsite
Porphyritic and non-porphyritic felsite	Lower	Microgranophyre, granophyre and microgranite		Massive felsite, porphyritic and recrystallized in lower parts		Massive red, porphyritic felsite		Massive felsite, porphyritic and recrystallized in lower parts
Not described		Not described		Not described	Damwal Formation	Sandstone/quartzite Lithophysal, amygdaloidal felsite, agglomerate, volcanic breccia, tuff, sandstone		Not observed
						Granophyric red felsite Micrographic felsite Leptite		

1. Succession north of Nylstroom (Coetzee, 1970).
2. Succession north of Middelburg (Von Gruenewaldt, 1966, 1968).
3. Succession according to Rhodes and Du Plessis (1976).
4. Succession in the vicinity of Loskop Dam (Clubley-Armstrong, 1977).
5. Succession in the Rust de Winter area (this study).

Coertze *et al* (1977) subdivided the Rooiberg Group in the present study area into the Selonsrivier (top) and Damwal (bottom) Formations; this subdivision is also shown on the 1:250 000 Geological map (1978) of Pretoria. According to this classification, the stratigraphy of the study area belongs to the Doornkloof and Klipnek Members of the Selonsrivier Formation, as defined by Clubley-Armstrong (1977). The succession in the present study area, however, is very similar to that described by Du Plessis (1976) in the Warmbad area and it was therefore decided to use Du Plessis' (1976) subdivision in the present study. The chemical data presented by Du Plessis (1976), corresponds very well with that of the present study (see chapter 4.8) and serves as further corroboration for this correlation.

The presence of a sandstone/quartzite unit between the Damwal and the Selonsrivier Formations indicates a hiatus in the volcanic activity (Clubley-Armstrong, 1977). The breccia or agglomerate, which is present in the Selonsrivier Formation likewise indicates a break in the volcanic activity; the Klipnek Member (Clubley-Armstrong, 1977) thus contains most of the pyroclastic material and the Doornkloof Member mainly felsite. This agglomerate was used by Du Plessis (1976) and Rhodes and Du Plessis (1976) to subdivide the Rooiberg Group into a lower and an upper unit. The agglomerate is also present in the study area and as this is an indication of a change in the eruptive history of the Rooiberg Group, this unit is subdivided into the Kwaggasnek and Schrikkloof Formations, similar to the subdivision on the Warmbad area (Du Plessis, 1976; Coertze *et al*, 1977).

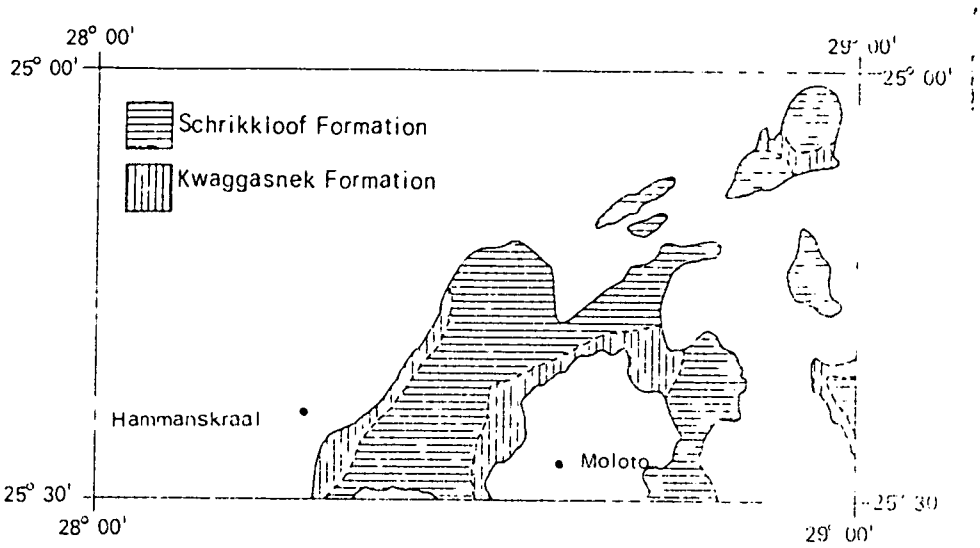

Fig. 4.2. *General distribution of the formations comprising the Rooiberg Group in the area north of Pretoria.*

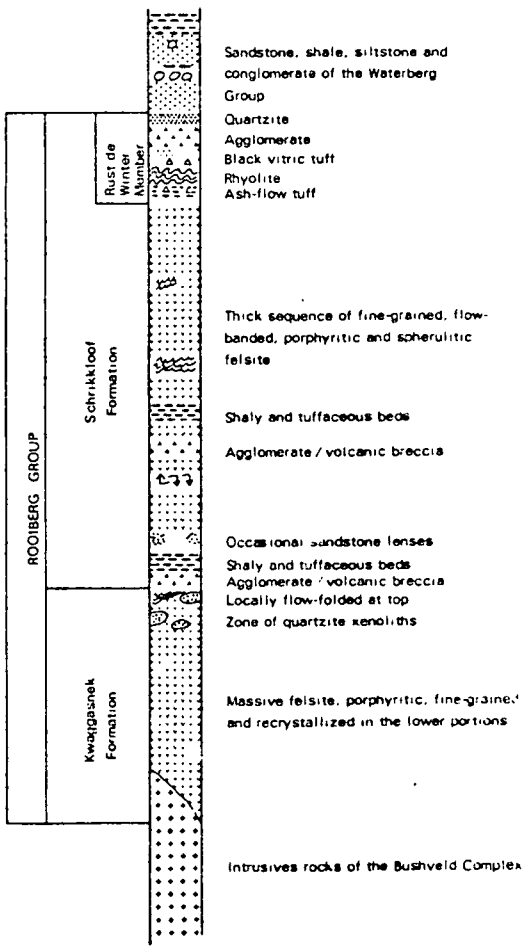

Fig. 4.3. *Column depicting the lithostratigraphy as used in the study area.*

4.3 KWAGGASNEK FORMATION

4.3.1 General Description

The Kwaggasnek Formation consists of dark red to dark brown massive felsite. According to the classification of IUGS (1976), the term 'felsite' refers to massive rhyolite; felsite, however, is used in the present study as this is a well-known rock term for the Rooiberg Group. The Kwaggasnek felsite lacks flow-banding, except near the top where it occasionally shows flow-folding. Another characteristic feature of this unit is the lack of interbedded tuff, agglomerate and sandstone. Devitrification textures are prominent in these rocks of which spherulites, assuming macroscopic proportions, are common (Fig. 4.4).

Fig. 4.4. Well developed spherulites in the Kwaggasnek Formation of the Rooiberg Group on Hartebeestfontein 240 JR.

The portion immediately below the agglomerate marker of the Schrikkloof Formation contains a large number of quartzite xenoliths. These xenoliths vary greatly in size, ranging from approximately one metre to three metres in diameter (Fig. 4.5). In contrast with the observation of Du Plessis (1976) that the xenoliths are highly recrystallized, some of the xenoliths in this area retained their original bedding and cross-bedding. The variable dips of the bedding within the xenoliths indicate disruption from their original positions. It is difficult to estimate the thickness of this quartzite xenolith bearing zone, but it may well be in the order of ten to twenty metres thick.

Fig. 4.6. *Photomicrograph of a typical euhedral quartz phenocryst in the felsite of the Kwaggasnek Formation (crossed nicols, x 20).*

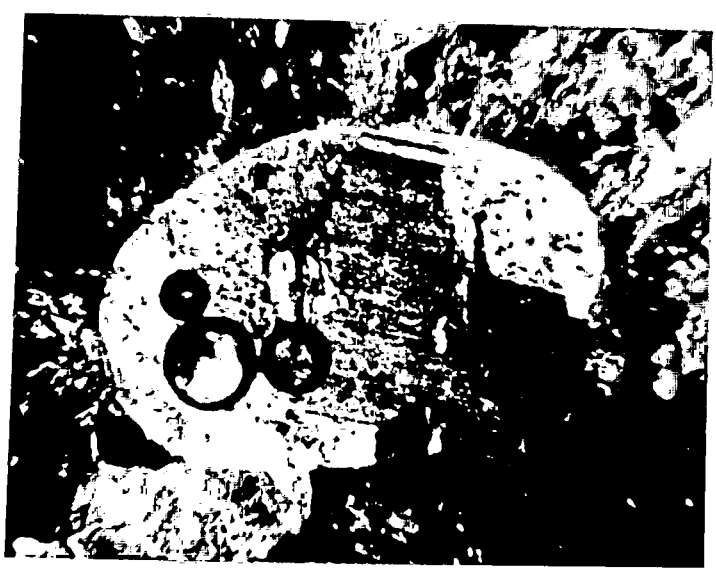

Fig. 4.7. *Photomicrograph of a rounded plagioclase phenocryst in the felsite of the Kwaggasnek Formation (crossed nicols, x 20).*

No phenocrysts of K-feldspar could be identified under the microscope. The individual crystals in the groundmass seldom exceed 0,22 mm, while 0,11 mm is more common for the granular types. Crystallites, which range between 0,44 and 0,11 mm in length, are well developed in some samples, while in other specimens they, however, form spherulites which have a diameter of between 0,50 and 0,13 mm. Not all crystallites are arranged in a radial pattern; some tend to have a quite random orientation. In some of the samples, spherulites, ranging from 2 to 1,4 mm in diameter, are surrounded by fine-grained granophyric textures (Fig. 4.8) giving rise to a 'bow-tie' arrangement. Some spherulites contain large crystals within their cores, but no attempt was made to determine the composition of these crystals.

Fig. 4.8. Photomicrograph of a spherulite displaying granophyric texture along its outer margins and a 'bow-tie' arrangement in the Kwaggasnek Formation (crossed nicols, x 20).

A sample close to the granophyre-felsite contact displays a plumose texture which formed by the concentration of scopulites (Fig. 4.9) in a groundmass which resembles a vitric tuff. Fragments of devitrified material in the tuff display axiolitic textures. The felsite, juxtaposed to a syenite plug on Groenfontein 120 JR, contains large crystals, giving rise to a trachytic texture.

Fig. 4.9. Photomicrograph of scopulites forming a plumose texture in the Kwaggasnek Formation (crossed nicols, x 20).

Sericitisation is present in a great deal of the samples investigated. Some of the phenocrysts are affected to such an extent that positive identification is not possible. Ore minerals also form as an alteration product replacing the groundmass around some phenocrysts (Fig. 4.10).

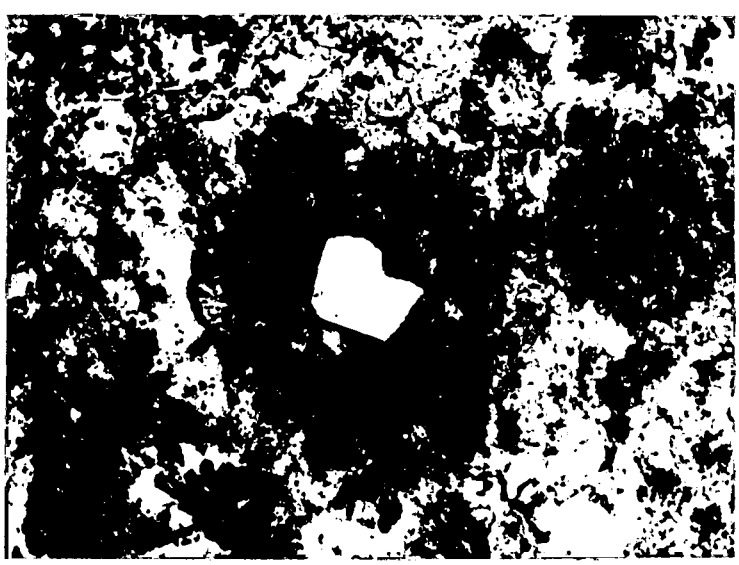

Fig. 4.10. Photomicrograph showing the concentration of ore minerals around a phenocryst in the Kwaggasnek Formation (crossed nicols, x 20).

Fine-grained pyroboles could be distinguished. Due to the small grain-size of these minerals, it is difficult to determine their composition, but it is thought, on the basis of refractive indices, that they constitute aegirine. The pyroboles most commonly form radial patterns while a streaky arrangement also occurs.

4.3.2.2 Quartzite Xenoliths

The quartzite xenoliths in the upper portion of the Kwaggasnek Formation display both rounded and recrystallized grains. The grains in some quartzites are well rounded (Fig. 4.11), while in others they are angular to sub-rounded. Very little cement and matrix could be observed while calcite and sericite are present as interstitial material. Quartz is the most dominant major component with subordinate plagioclase and K-feldspar.

Fig. 4.11. Photomicrograph of rounded quartz grains in a quartzite xenolith (crossed nicols, x 20).

Where the quartzite has been subjected to complete, or near complete alteration, no matrix or cement material could be observed. In these cases the quartz forms an interlocking mosaic of idioblastic grains (Fig. 4.12). No plagioclase or K-feldspar could be found in these samples.

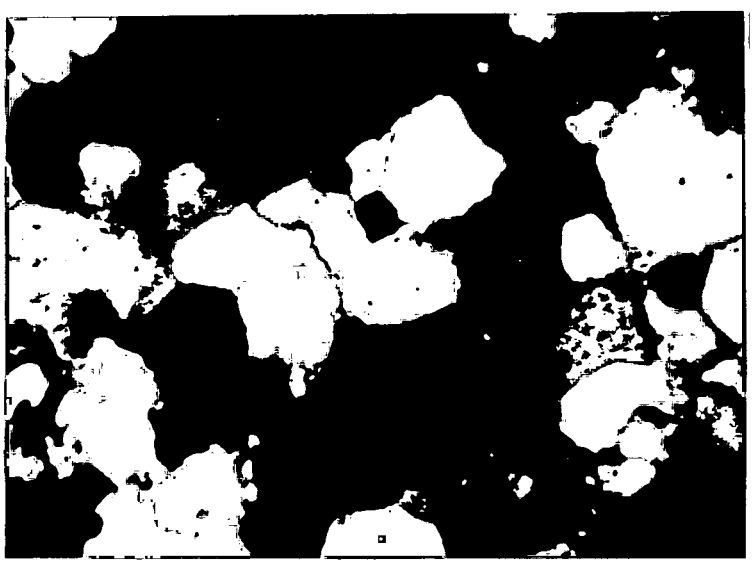

Fig. 4.12. Photomicrograph of interlocking mosaic of quartz grains in a quartzite xenolith (crossed nicols, x 20).

4.3.2.3 Flow-banded Felsite

The flow-banded felsite is a fine to very fine-grained rock, consisting of euhedral to subhedral quartz, K-feldspar, plagioclase and dust fine ore. The ore occurs interstitially, but is mostly concentrated on the flow planes. The flow-banding is approximately 2 to 2,5 mm thick and very often contorted.

The lamella are separated from one another by very fine-grained zones which also contain ore minerals. The felsite, which is composed of moderately fine-grained crystallites, show a prominent grading from the bottom of the lamella towards the centre.

4.4 SCHRIKKLOOF FORMATION

4.4.1 General Description

The Schrikkloof Formation consists of both massive and flow-banded felsite, the latter being the more dominant. An agglomerate/volcanic breccia, along the base of the Schrikkloof Formation, was used as a marker to separate the two formations.

The felsite is usually red to pale brown while black varieties can also be seen. The flow-banding in the felsite does not display contortion, except on Klipplaatdrift 239 JR, where it is well developed.

Tuff, agglomerate, lapilli tuff and sandstone lenses are interbedded with the felsite. The sandstone, which is not very well developed in this area, was reported by Rhodes (1972, personal communication) to form prominent lenses near Loskop Dam, to the east of the study area.

Lithic tuffs, which grade into lapilli tuffs, for example at Leeuwdraai 211 JR, occur sporadically, while on Fairfield 238 JR an ash-fall vitric tuff is developed. The tuffs, with the exception of the one on Fairfield 238 JR, which is light reddish, are marked by black colouration. On Groenfontein 125 JR the tuff lenses, which display a very fine-grained shaly texture, contain flattened bombs at the top, the latter indicating the end of a sedimentary cycle.

In the vicinity of Hammanskraal an agglomerate, containing blocks of 10 to 20 cm in diameter, is well developed. Stratigraphically it corresponds roughly with the tuff and basal agglomerate horizon, which indicates a widespread and virtually consistent pyroclastic event during that epoch in the development of the Rooiberg Group.

Two isolated breccia bodies also occur in this area. The one is located on Tweefontein 220 JR and the other on Roodekoppies 167 JR. Neither of these could be correlated with any other known occurrences of agglomerate or breccia. The lack of these rock types in the lower formation, however, justifies their classification with the Schrikkloof Formation.

The lithostratigraphic heterogeneity of the Schrikkloof Formation signifies a more complex eruptive history than that of the more homogeneous Kwaggasnek Formation.

The Schrikkloof Formation is marked locally by the presence of the Rust de Winter member at its top. The latter consists of a number of tuff flows, quartzite, agglomerate and rhyolite.

4.4.2 Macroscopic and Microscopic Description

4.4.2.1 Agglomerate

In handspecimen the agglomerate consists of large fragments of varying composition in a fine-grained felsitic groundmass. The fragments range in size from blocks of the order of 20 to 40 cm to fragments of 1 cm or less in diameter, while shards of variable shapes and sizes also occur.

Quartz is the dominant constituent of the felsitic groundmass while altered feldspar was also identified. Xenomorphic to hypideomorphic crystallites, ranging from 0,1 to 0,05 mm in size, form part of the groundmass.

The fragments are rounded to subrounded and consist mainly of microscopically unidentifiable material. These fragments have been highly altered and quartz is the only mineral that can be identified with certainty. Some of the fragments display structures resembling perlitic cracks (Fig. 4.13) which may indicate their volcanic origin.

The shards also exhibit alteration to a large extent and axiolites are the most prominent textures (Fig. 4.14). Ferruginisation, sericitisation and also chloritisation is often a prominent feature of these rocks. Sericitisation,

which is common throughout the rock, is especially well developed within some of the fragments. This causes a cloudy effect, making positive identification of any particular mineral an almost impossible task. Chloritisation also hampers the identification of minerals within these fragments. Some fragments are surrounded by ore minerals outlining their boundaries. The ore varies from crystals to earthy massive varieties of which magnetite forms the dominant constituent.

4.4.2.2 Massive Felsite

The felsite consists of large phenocrysts (2–1 mm in length) and smaller crystals (1–0, 1 mm in length) in a groundmass which consists mainly of volcanic dust. Spherulites and microlites of various shapes are also present.

The phenocrysts consist mainly of plagioclase (An_{10-25}) while quartz phenocrysts are also present. On the other hand no K-feldspar phenocrysts could be identified. A microscopic examination reveals that the rock consists of approximately 15 per cent phenocrysts in a fine-grained matrix.

The phenocrysts often occur in glomeroporphyritic concentrations (Fig. 4.15). The plagioclase phenocrysts are usually subhedral in shape while euhedral crystals can also be seen. Polysynthetic twinning is well developed, but due to secondary alteration the composition (An_{10-25}) could only be determined in a few cases. These An-values were corroborated by an X-ray method described in Appendix I (Table 4.2).

Very little alkali feldspar is present in the felsite. X-ray diffractometer examinations on the felsites (Appendix I) indicate that the alkali-feldspar composition lies between $Or_{90}Ab_{10}$ and $Or_{75}Ab_{25}$ (Table 4.2). The alkali feldspars normally form euhedral to subhedral crystallites of 0,05 mm in length.

Anhedral to subhedral quartz phenocrysts and euhedral crystallites are very prominent, the latter giving rise to typical spherulitic textures.

TABLE 4.2 : PLAGIOCLASE, ALKALI FELDSPAR AND FEMIC MINERAL FREE MODAL COMPOSITION OF THE FELSITES OF THE ROOIBERG GROUP, INDICATING TEXTURAL PARAMETERS WHERE DETERMINED

SAMPLE NUMBER	% An	% Ab	WEIGHT % QUARTZ	WEIGHT % ORTHOCLASE	WEIGHT % ALBITE	$\bar{s}$	C.I.	n
				1				
72/204	18	15	39	15	28	0,43	94	4
72/56	22	10	43	17	25	0,79	38	3
73/82	5	22	62	10	22	0,54	19	1
72/60	20	25	45	11	10	0,61	49	3
72/57	28	15	43	19	26	1,10	18	2
73/36	15	15	40	16	25	0,80	37	3
73/33	13	15	38	17	26	0,57	140	8
73/65	18	18	56	12	18	0,47	129	6
73/64	18	15	48	16	24	0,70	57	4
73/90	18	15	36	15	15	0,53	228	12
73/41	18	15	20	13	18	0,92	22	2
73/37	17	18	42	29	28	0,14	356	5
73/63	13	20	60	14	18	0,39	128	5
73/85	18	24	45	20	30	0,69	83	5
73/84	10	20	33	26	17	0,45	533	24
				2				
72/168	18	25	44	14	10	0,30	167	5
72/148	15	25	43	15	22	3,60	11	4
72/118	14	15	46	16	16	0,39	256	10
72/30	13	15	45	13	14	0,61	230	14
73/106	15	20	48	17	20	0,60	133	8
73/108	13	15	45	23	28	0,61	99	6
73/117	13	25	47	16	15	0,64	63	4
72/13	13	25	38	17	24	0,85	106	9
72/14	25	22	36	13	20	0,78	155	12
72/119	14	25	45	15	14	0,50	141	7
72/126	10	18	36	22	30	0,43	698	20
73/311	13	10	48	20	17	1,63	12	2
72/165	18	25	32	18	24			

1. = Samples from Kwaggasnek Formation.

2. = Samples from Schrikkloof Formation.

$\bar{s}$ = Mean calculated diameter of phenocryst in mm.

C.I. = Crystallinity Index calculated according to Appendix III.

n = Number of phenocrysts per cm^2.

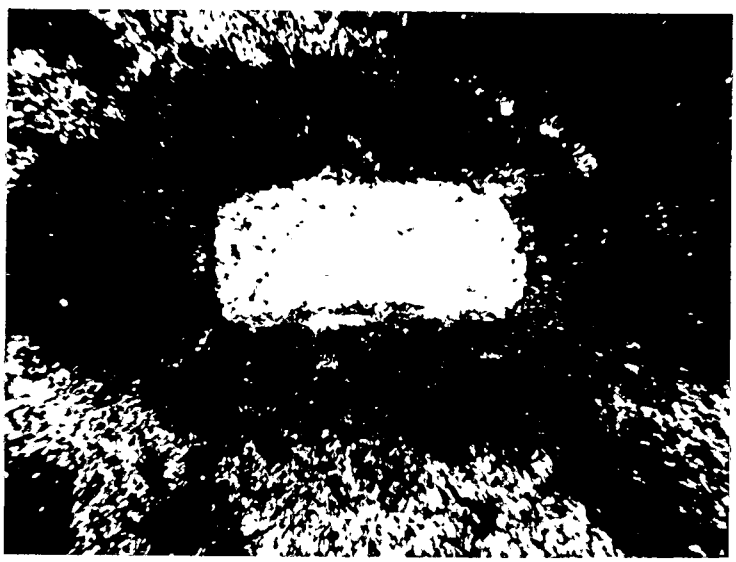

Fig. 4.16. Photomicrograph of a corona of ore surrounding a quartz phenocryst in the Schrikkloof Formation (crossed nicols, x 20).

ferruginous material. A characteristic feature of these rocks is the scarcity of phenocrysts.

Altered plagioclase, 0,1 – 0,6 mm in size, has a composition of An_{10} – An_{30} and displays very little polysynthetic twinning.

The alkali-feldspar (orthoclase), 0,2 – 0,4 mm in size, is highly altered and its presence is only revealed by a number of cloudy crystals.

Quartz, which is clear, forms a dominant constituent of the banded felsite and a large variation in grain size (from 0,1 to 0,7 mm) could be measured.

Small amounts of very fine-grained biotite (0,09 mm and smaller) are often closely associated with ore minerals which in some cases defines the flow-banding planes.

Sericite and chlorite forms as alteration products on orthoclase and biotite respectively.

4.4.2.4 Tuff

Two distinct types are developed in this area, namely a crystal tuff and a mixture of crystal and lithic tuff. The crystal tuff, which is very well defined in the ash-fall tuff on Fairfield 238 JR, consists of quartz, K-feldspar, some doubtful plagioclase and very little ore. The euhedral grains, ranging from 0,2 to 0,5 mm in diameter, display graded bedding under the miscroscope. The contorted bedding is emphasized by interbedded fine-grained crystalline material.

On Leeuwdraai 211 JR, a vitric tuff which can be recognized as an ash-flow tuff, crops out. It consists of small shards (Fig. 4.17) in a matrix of welded quartz and other subordinate minerals. The shards display alteration to axiolitic textures, while the groundmass is relatively unaltered. Magnetite forms the dominant ore mineral in these rocks.

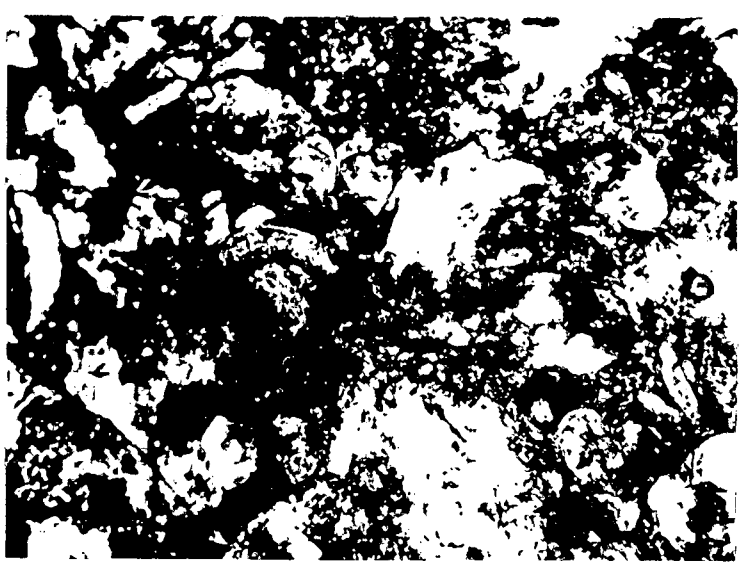

Fig. 4.17. Photomicrograph of a vitric tuff showing shard fragments in the Schrikkloof Formation (crossed nicols, x 20).

The tuffs, which can be classified as litho-vitric, are composed of fine- to medium-grained felsitic fragments, 1 to 2 mm in diameter, within a very fine-grained matrix. Shards within the finely fragmented matrix display axiolitic textures. The groundmass material, which ranges in size from 0,1 to 0,5 mm, consists, in order of abundance, of quartz, K-feldspar and small amounts of plagioclase.

Ore, of which magnetite is the dominant constituent, is generally euhedral and very fine-grained. Sericite formed as an alteration product in most of the samples investigated.

4.4.2.5 Agglomerate and Breccia

The agglomerate consists of felsite fragments in a fine-grained matrix of angular quartz, K-feldspar and plagioclase. The agglomerate on Groenfontein 125 JR is marked by the presence of schorl.

The fragments, which are mostly angular, are composed of fine-grained quartz, K-feldspar, plagioclase, small amounts of biotite and minor ore. The minerals are 0,1 to 0,4 mm in diameter showing euhedral to subhedral shapes. The feldspars are altered to sericite while the biotite is highly chloritised.

The fine-grained matrix also consists of quartz, K-feldspar, plagioclase and biotite. Ore minerals, of which magnetite is the dominant constituent, form as interstitial material.

4.5 RUST DE WINTER MEMBER

4.5.1 General Description

The Rust de Winter member crops out along the western rim of a basin-like structure (Folder I). The distribution of this unit, together with tilting of the layers and associated faulting, indicates that this may well represent a subsided caldera. Rhodes (1972, personal communication) was also in favour of such a structure based on his experience on the calderas in New Mexico.

This member consists of a basal ash-flow tuff, rhyolite, vitric tuff, agglomerate and quartzite, forming the top of the Rooiberg Group in part of the study area. This member was previously correlated with the Waterberg Group, which overlies this unit in the east (Geological Map of the Republic of South Africa, 1970). Boreholes in this area, however, confirm the overlying relationship of the Waterberg Group with the pyroclastic units of the Rust de Winter member.

4.5.2 Microscopic Description

4.5.2.1 Basal Ash-flow Tuff

These rocks consist of fine-grained shards (0,5 – 1,0 mm) in a very fine-grained hypohyaline matrix. The shards are mainly angular to fork-shaped (Fig. 4.18) and have been altered, displaying axiolitic textures. Perlitic cracks are also developed in some of the larger glass fragments.

The groundmass is highly altered, consisting of dust fine particles with occasional crystallites. The latter has a size ranging between 0,05 to 0,1 mm. The ore in the matrix is mainly euhedral magnetite.

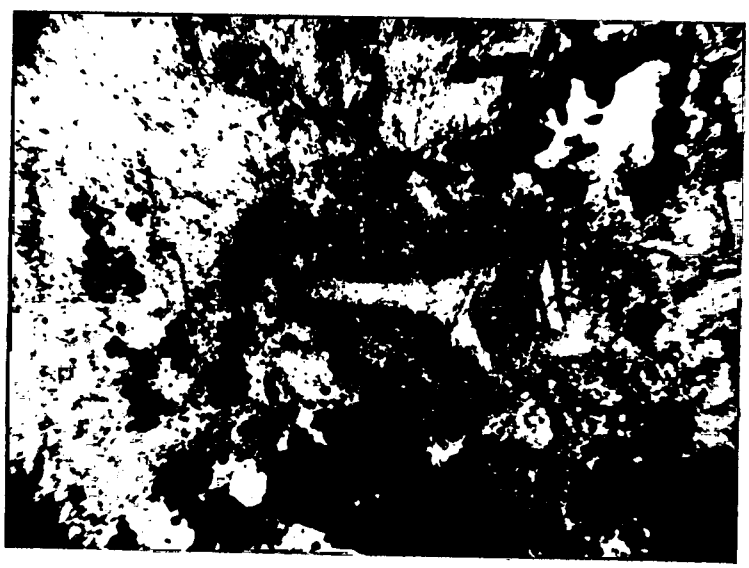

Fig. 4.18. Photomicrograph of a fork-shaped shard in the Rust de Winter member of the Schrikkloof Formation (crossed nicols, x 20).

4.5.2.2 Rhyolite

This rock type was previously classified and described by Glatthaar (1956) as a multicoloured tuff. The present investigation, however, reveals that the rock should be classified as a flow-banded rhyolite.

The rhyolite exhibits contorted flow-banding and consists of a very dense, fine-grained felsitic matrix in which small undefined axiolites are present. The rock displays light and dark coloured layers in hand-specimen, but no mineralogical differences could be determined under the microscope.

4.5.2.3 Black Vitric Tuff

The vitric tuff consists of angular fragments displaying perlitic cracks and axiolitic textures in a fine-grained groundmass of which quartz forms the dominant constituent. The angular to subrounded fragments in the tuff consist of pumice and glass.

4.5.2.4 Agglomerate

The agglomerate consists mainly of rounded to subrounded fragments (25 to 50 mm diameter) of felsitic composition in a fine-grained, iron-rich matrix. The ferruginisation of the matrix makes it extremely difficult to determine the mineralogical composition thereof.

The felsite fragments consist of quartz, K-feldspar, plagioclase and subordinate mafic minerals. The crystals are very fine-grained and display subhedral shapes. Sericitisation of the feldspars is a marked feature of the fragments, while magnetite is present as small ideomorphic crystals. Some of the fragments display a decolourised reaction rim, which can be seen as a light coloured halo. Colour differences range from red in the centre to light or pale pink on the outside.

4.5.2.5 Quartzite

Quartzite crops out in two localities (Folder I). The one in the west is a very pure quartzite, containing very little iron, with angular grains cemented by calcite and silica.

The eastern quartzite contains a large amount of impurities, mainly iron oxides and Glatthaar (1956) compared its formation to that of a banded ironstone. This quartzite consists of fine-grained rounded to angular quartz grains cemented by hematite or calcite with very little matrix material.

4.6 MODAL AND TEXTURAL ANALYSIS

Modal and textural analysis of the felsitic rocks of both the Kwaggasnek and Schrikkloof Formations were conducted in order to determine any significant differences.

4.6.1 Modal Composition

Modal analysis was carried out on 15 samples from the Kwaggasnek Formation and 13 from the Schrikkloof Formation, using an X-ray diffractometric technique, described by Tatlock (1966) (see Appendix II). These analyses indicate that the rocks, with the exception of a few very quartz-rich varieties, consist of quartz of the order of 50 per cent, K-feldspar around 20 per cent and plagioclase around 30 per cent (based on felsic minerals only) (Table 4.2).

The rocks group towards the quartz apex of a ternary diagram (Fig. 4.19). The plots of the two different formations overlap with one another and therefore cannot be separated modally.

4.6.2 Textural Properties

Textural analysis, based on the whole rock index (WRI) of Hawkes (1967), subsequently modified by Rhodes (1973) for use with volcanic rocks, was conducted according to the scheme in Appendix III. The WRI functions on the assumption that any magma is subjected to undercooling prior to and during intrusion. This phenomenon is then reflected in the number of phenocrysts contained per unit volume of the rock.

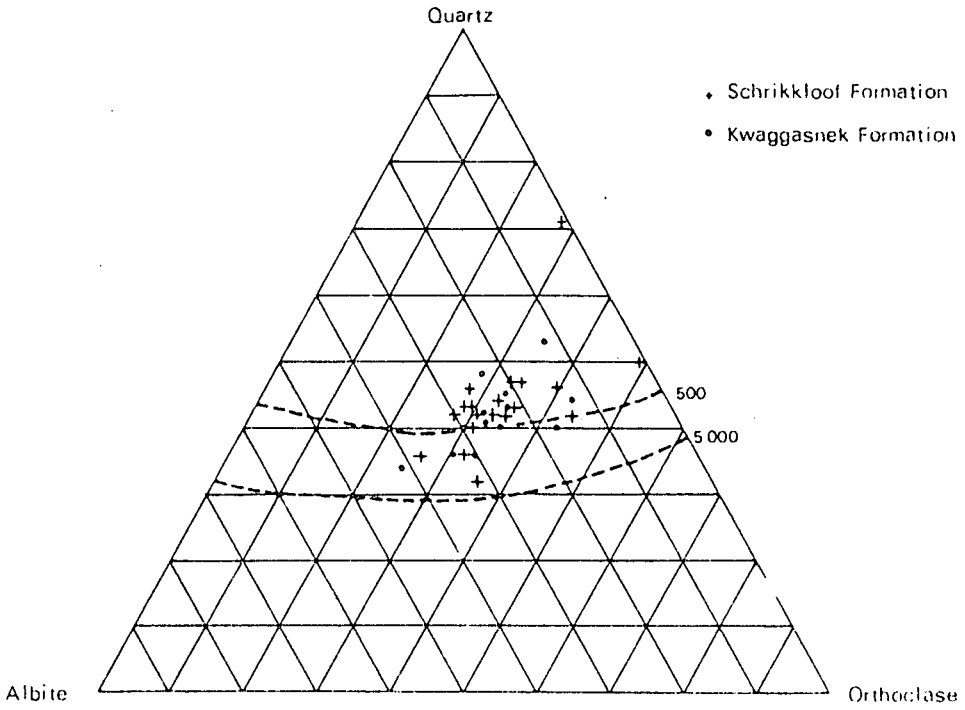

Fig. 4.19. Ternary diagram of the Rooiberg Group (isobars after Tuttle and Bowen, 1958).

The development of phenocrysts at a temperature within the metastable zone (Harker, 1909) will continue until it reaches the labile zone of Wager (1961), where rapid crystallization takes place. Hawkes (1930) explained the development of glass by means of this process (Fig. 4.20) where, if the cooling of the magma was very rapid, it would pass through both the metastable and labile zones with little or no crystallization.

De Bruiyn (1975) investigated the volcanic rocks and used the term crystallinity index (C.I.) in the place of the whole rock index (WRI) normally used for plutonic rocks. The C.I., which is temperature dependent, can be used to distinguish between various volcanic sequences.

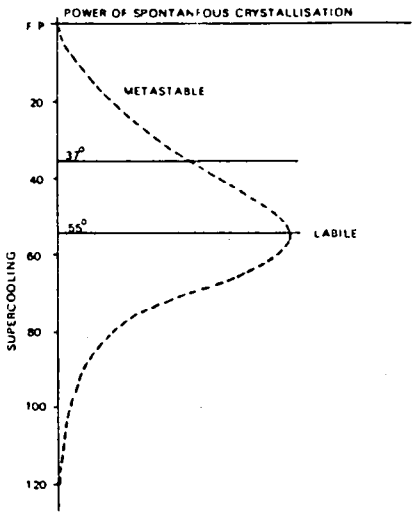

Fig. 4.20. Curve describing the undercooling of a magma showing different fields (after Tyrrel, 1956).

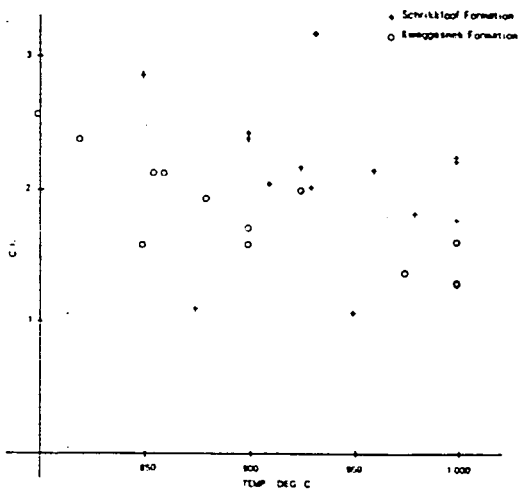

Fig. 4.21. Plot of crystallinity index (CI) against the formational temperatures of the Rooiberg Group in the study area.

A plot of C.I. versus formational temperatures (Fig. 4.21) indicates a marked difference in the cooling history of the two formations. From the figure it can be observed that the freezing temperatures are the same, but the major difference lies in the C.I.. This indicates that two fields are present with the lowermost Kwaggasnek Formation containing more phenocrysts for a given temperature than the overlying Schrikkloof Formation.

A comparison of the long and short axes of the plagioclase phenocrysts, based on the method used for zircons by Alper and Poldervaart (1957), Larsen and Poldervaart (1957) and Leith and Rhodes (1971), also stresses the differences in the cooling histories of the two formations (see Appendix IV). The results are given in Table 4.3 and reveal a major difference between the two formations : the Schrikkloof Formation contains larger sized phenocrysts, indicating that it remained at the metastable zone for a longer

period of time. This size difference of the phenocrysts is also amplified by the significant statistical differences which were encountered for the two formations : the long axis yields a t-value of 2,4076 and the short axis one of 3,2292; values greater than 2,33 are statistically significant (Spiegel, 1972).

TABLE 4.3. STATISTICAL PARAMETERS OF PHENOCRYSTS IN THE FELSITE OF THE ROOIBERG GROUP

	1	2
n	273	430
$\bar{x}$	0,6378	0,7258
Sx	0,4180	0,5019
$\bar{y}$	0,3762	0,4487
Sy	0,2361	0,3191
$\bar{s}$	0,4811	0,5629
$\bar{v}$	0,2208	0,4249
Ratio	1,6954	1,6174
R	0,7284	0,8678
Slope	0,5648	0,6358
Recip	1,7704	1,5727
Std error slope	0,02342	0,01524
D	47,78	35,84
Reg line	0,5648x + 0,01595	0,6358x – 0,01268
$\bar{e}$	1,8146	1,7393

1. Kwaggasnek Formation
2. Schrikkloof Formation

n = number of phenocrysts measured; $\bar{x}$ = mean length; Sx = standard deviation of length; $\bar{y}$ = mean breadth; Sy = standard deviation of breadth; $\bar{s}$ = mean calculated diameter; $\bar{v}$ = mean calculated volume; Ratio = $\bar{x}/\bar{y}$; R = correlation coefficient; Slope = slope of regression line; Recip = 1/Slope; Std error slope = standard error of the slope; D = 1/std error slope; Reg line = regression line; $\bar{e}$ = mean elongation

This variation in the phenocryst populations can also be illustrated diagrammatically (Fig. 4.22) where the frequency distribution of the various parameters are essentially similar, but the major differences appear in the areas of the maxima.

4.7 CHEMICAL ANALYSES

The chemical analyses were carried out by Bergström and Bakker using a Philips X-ray fluorescence spectrometer. The Fe_2O_3 and FeO were determined by means of gravimetric methods. An analytical accuracy of approximately 2 per cent was maintained throughout.

A total of 13 samples of the Kwaggasnek Formation and 19 samples of the Schrikkloof Formation were submitted for chemical analysis (Table 4.4).

Barth-Niggli molecular norms (Barth, 1962) were determined by means of a computer programme as described by Hutchison and Jeacocke (1971) and the data are given in Table 4.4. The data indicate that high normative quartz are present in certain cases, while other samples display high normative orthoclase. A number of specimens also contain considerable amounts of anorthite, along with low corundum values. The Differentiation Index spans a large field, but mostly straddles the lower 90 values.

The C.I.P.W. norms were calculated and these indicate that the felsites, when plotted on the QAPF-diagram, fall within the rhyolite field (Fig. 4.23) with only a very small number plotting within the field of alkali-rhyolite. These data indicate that a small amount of differentiation has taken place in the Rooiberg felsites. It also gives the root names for classification of the volcanic rocks as suggested by the IUGS Subcommission on the Systematics of Igneous Rocks (1976), which clearly shows that felsites fall within the liparite field.

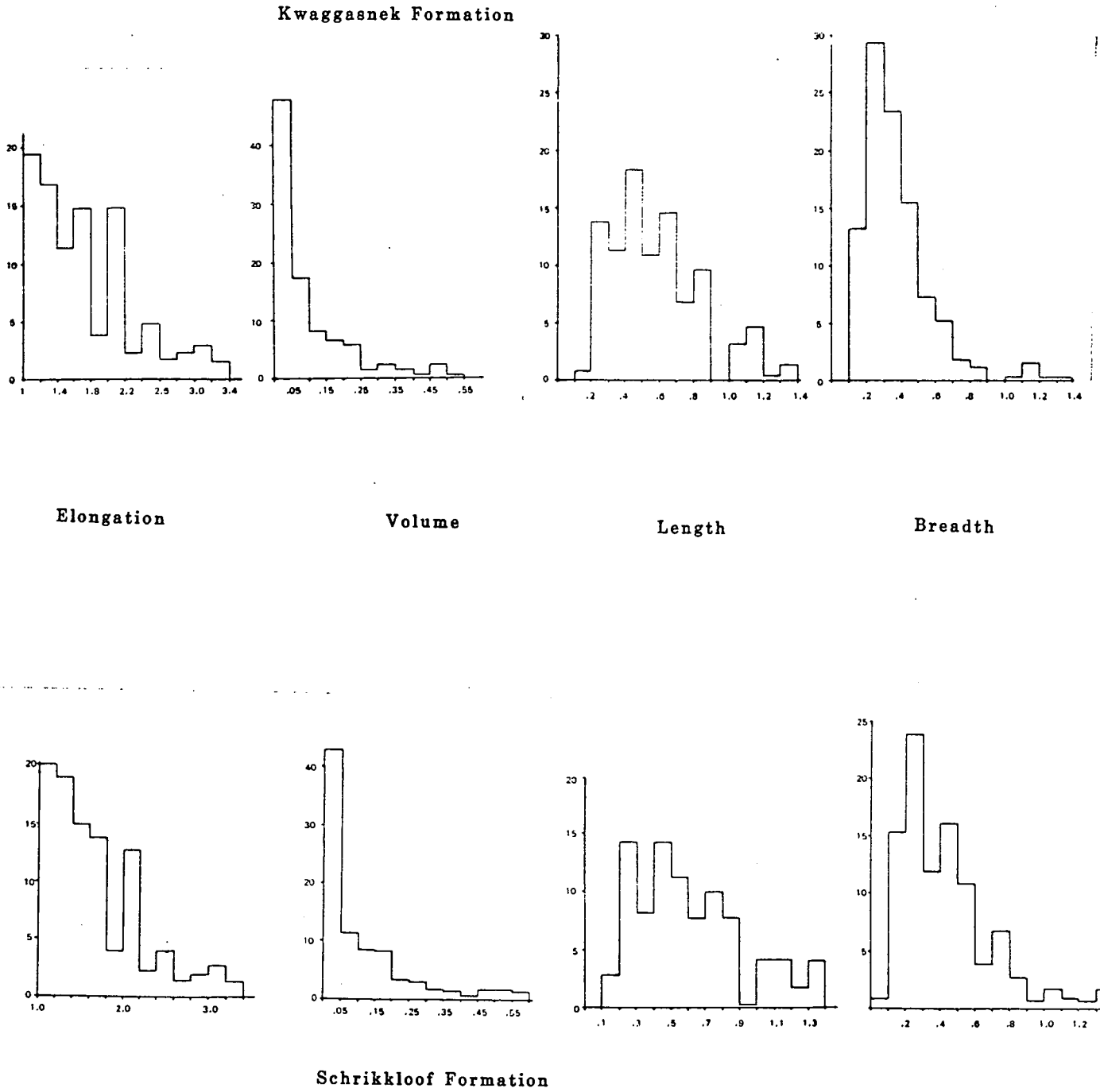

Fig. 4.22. Histograms of the various parameters of the phenocrysts in the Rooiberg Group.

TABLE 4.4 : CHEMICAL AND NORMATIVE COMPOSITIONS OF THE ROOIBERG GROUP

Sample No.	72/204	72/56	72/60	72/57	73/36	73/33	73/65	72/8
SiO_2	67,10	73,10	71,80	73,40	68,40	69,20	68,40	71,02
TiO_2	0,39	0,28	0,36	0,26	0,39	0,36	0,61	0,38
Al_2O_3	11,60	11,80	11,30	11,70	12,00	11,60	11,00	12,04
Fe_2O_3	2,86	2,44	6,19	1,94	3,99	3,48	6,45	2,24
FeO	6,10	2,80	0,60	2,90	4,60	3,50	3,00	1,69
MnO	0,13	0,40	0,56	0,08	0,14	0,08	0,25	0,11
MgO	0,10	0,20	0,20	0,20	0,30	0,20	0,20	0,76
CaO	2,33	0,62	0,17	0,85	0,68	1,78	0,13	1,14
Na_2O	2,90	2,30	1,30	2,50	2,50	2,60	1,10	2,78
K_2O	4,01	4,66	6,24	4,90	4,80	4,63	4,62	4,62
H_2O^+	1,30	0,70	1,30	0,40	1,40	2,00	2,10	0,62
H_2O^-	0,30	0,10	0,40	0,10	0,20	0,20	0,40	0,16
P_2O_5	0,10	0,05	0,06	0,05	0,10	0,09	0,10	0,04
CO_2	0,10	0,30	0,10	0,40	0,50	0,30	0,80	0,72
ZrO_2	390	370	410	380	380	400	420	450
Ni	16	14	10	18	10	14	38	10
BaO	900	950	1 050	1 150	1 100	950	970	1 190
SrO	67	70	33	60	55	84	75	55
Rb_2O	155	175	280	185	200	185	150	250
TOTAL	99,47	99,91	100,76	99,86	100,17	100,18	99,33	98,52
Qtz	30,03	40,19	39,46	38,02	34,51	32,98	44,71	35,70
Cor	-0,97	3,36	2,78	2,30	3,09	0,44	4,98	2,81
Zir	0,04	0,04	0,04	0,04	0,04	0,04	0,04	0,05
Or	18,06	25,37	38,44	26,65	25,54	25,60	29,23	25,69
Ab	27,54	21,52	12,33	23,22	23,58	24,60	10,76	26,06
An	9,60	0,06	–	0,70	–	5,56	–	–
Bi	11,19	5,30	0,78	5,27	6,79	5,16	0,80	4,49
Hm	–	–	3,17	–	–	–	0,33	–
Mt	3,16	2,66	2,08	2,10	4,38	3,83	6,85	2,45
Il	–	–	0,57	–	–	–	0,93	–
Tn	0,86	0,61	0,01	0,56	–	0,79	–	0,66
Cc	0,27	0,79	0,27	1,05	1,33	0,80	0,36	1,90
Ap	0,22	0,11	0,13	0,11	0,14	0,20	–	0,09
DI	74,69	90,47	93,04	90,22	86,76	83,66	89,73	90,31

Sample No.	72/115	72/118	72/30	73/106	73/111	73/108	73/114	72/117
SiO_2	74,30	71,40	71,10	73,20	72,90	74,00	73,20	72,60
TiO_2	0,29	0,30	0,34	0,28	0,27	0,28	0,25	0,28
Al_2O_3	11,70	11,60	11,90	11,20	11,40	11,50	11,20	11,50
Fe_2O_3	6,04	2,27	4,72	2,84	2,69	2,46	1,25	1,47
FeO	0,60	3,50	2,10	2,30	2,70	2,40	3,00	4,50
MnO	0,01	0,27	0,06	0,06	0,41	0,10	0,05	0,11
MgO	0,20	0,10	0,20	0,10	0,20	0,10	0,10	0,20
CaO	0,08	0,56	0,13	0,43	0,15	0,14	0,41	0,08
Na_2O	0,10	2,10	2,50	2,60	2,20	2,70	2,50	1,90
K_2O	3,78	5,16	4,70	4,50	5,00	4,47	4,24	5,04
H_2O^+	2,10	1,20	1,40	1,50	1,10	1,40	1,00	1,60
H_2O^-	0,50	0,30	0,10	0,20	0,10	0,20	0,10	0,20
P_2O_5	0,04	0,04	0,06	0,05	0,04	0,04	0,04	0,03
CO_2	0,10	0,50	0,10	0,05	0,40	0,30	1,10	0,10
ZrO_2	460	460	450	430	440	460	460	470
Ni	10	13	58	10	15	10	88	13
BaO	1 260	950	790	1 340	1 080	1 030	800	860
SrO	70	31	46	52	38	47	21	23
Rb_2O	340	220	210	170	175	145	180	210
TOTAL	99,95	99,47	99,51	99,96	99,74	100,26	99,59	99,77
Qtz	59,82	38,51	37,70	39,40	39,79	39,80	40,94	41,39
Cor	8,86	2,95	3,11	2,05	2,71	2,53	2,84	3,37
Zir	0,05	0,05	0,05	0,04	0,04	0,05	0,05	0,05
Or	23,85	28,53	28,83	26,34	28,25	25,78	22,82	25,96
Ab	0,98	19,89	23,70	24,64	20,72	25,30	23,40	18,05
An	–	–	–	0,79	–	–	–	–
Bi	0,80	5,80	0,78	2,75	4,37	2,85	5,26	8,86
Hm	4,00	–	0,44	–	–	–	–	–
Mt	0,89	2,50	4,55	3,13	2,95	2,68	1,36	1,63
Il	0,44	0,44	0,50	–	0,40	0,41	0,36	0,41
Tn	–	–	–	0,62	–	–	–	–
Cc	0,28	1,25	0,27	0,13	0,40	0,37	2,90	0,24
Ap	–	–	0,05	0,11	–	–	0,06	–
DI	93,56	89,93	93,38	92,46	91,52	93,45	90,05	88,82

Sample No.	73/64	73/90	73/91	73/37	73/85	72/168	72/165A	72/148
SiO_2	71,20	73,90	73,80	68,80	69,90	69,00	73,30	70,30
TiO_2	0,38	0,28	0,26	0,38	0,38	0,37	0,28	0,42
Al_2O_3	11,50	11,80	11,70	11,60	11,70	12,00	11,20	12,10
Fe_2O_3	5,76	1,64	2,29	3,29	4,98	6,18	3,67	3,64
FeO	1,10	2,20	2,10	4,50	3,00	1,70	1,90	3,50
MnO	0,25	0,08	0,08	0,07	0,12	0,04	0,02	0,12
MgO	0,20	0,30	0,10	0,20	0,10	0,30	0,10	0,20
CaO	0,23	0,27	0,14	1,36	0,86	0,16	0,06	0,45
Na_2O	2,10	2,50	2,10	2,40	2,90	1,30	0,10	2,50
K_2O	4,14	5,40	5,33	4,86	4,94	6,29	6,98	4,64
H_2O^+	2,00	1,40	1,20	1,50	0,80	1,90	1,70	1,40
H_2O^-	0,40	0,20	0,30	0,20	0,20	0,50	0,30	0,20
P_2O_5	0,12	0,04	0,04	0,10	0,10	0,09	0,04	0,13
CO_2	0,40	0,40	0,20	1,10	0,40	0,60	0,10	0,20
ZrO_2	410	530	510	380	390	400	420	390
Ni	17	10	13	44	68	17	10	17
BaO	1 180	1 290	1 270	910	990	1 480	1 200	1 190
SrO	57	66	33	91	59	60	13	65
Rb_2O	157	175	180	180	195	300	270	200
TOTAL	100,05	100,62	99,84	100,52	100,55	100,68	99,94	99,99
Qtz	42,65	37,08	40,01	33,43	32,53	36,74	45,70	36,94
Cor	4,15	2,08	2,84	0,94	1,79	3,54	4,08	3,41
Zir	0,04	0,04	0,05	0,04	0,04	0,04	0,04	0,04
Or	25,62	30,59	31,56	25,70	28,89	38,73	43,97	26,05
Ab	20,13	23,24	19,79	22,82	27,03	12,40	0,96	23,61
An	–	–	–	4,56	–	–	–	–
Bi	0,79	3,91	2,37	7,54	2,24	1,17	0,43	4,45
Hm	2,61	–	–	–	–	2,26	–	–
Mt	2,51	1,78	2,51	3,64	5,40	3,47	4,12	4,03
Il	0,57	0,40	0,38	–	0,02	0,55	0,42	0,47
Tn	–	–	–	0,84	0,79	–	–	0,21
Cc	0,58	0,65	0,39	0,27	1,05	0,45	0,22	0,53
Ap	–	–	–	0,22	0,22	–	–	0,29
DI	92,60	93,03	94,24	82,93	90,28	91,44	94,75	90,04

Sample No.	73/117	72/14	72/13	72/281	73/104	72/119	72/126	72/311
SiO_2	72,20	71,00	70,70	72,40	73,40	72,30	72,10	72,50
TiO_2	0,26	0,37	0,38	0,27	0,27	0,30	0,24	0,31
Al_2O_3	11,20	12,10	12,14	11,20	11,40	11,80	12,50	11,50
Fe_2O_3	4,34	5,13	2,65	1,74	2,38	2,04	1,78	2,58
FeO	2,00	1,50	1,87	2,40	2,40	3,50	1,90	2,90
MnO	0,25	0,12	0,16	0,11	0,06	0,12	0,04	0,09
MgO	0,10	0,10	1,22	0,10	0,10	0,20	0,10	0,20
CaO	0,25	0,35	0,50	1,81	1,02	0,30	0,84	0,44
Na_2O	1,30	2,80	2,73	3,10	3,00	1,80	3,10	2,30
K_2O	5,77	4,57	4,42	4,13	4,92	5,09	5,60	5,09
H_2O^+	1,60	0,60	0,80	0,80	0,70	1,90	0,70	1,40
H_2O^-	0,30	0,10	0,22	0,26	0,20	0,20	0,10	0,10
P_2O_5	0,04	0,08	0,05	0,06	0,04	0,06	0,04	0,05
CO_2	0,10	0,30	0,16	0,10	0,10	0,30	0,20	0,50
ZrO_2	430	420	460	430	440	490	460	450
Ni	27	16	15	42	24	13	10	11
BaO	1 250	1 200	1 280	910	1 060	1 190	1 010	1 310
SrO	12	93	120	60	100	23	54	44
Rb_2O	240	160	170	140	210	220	230	220
TOTAL	99,91	99,31	98,20	98,58	100,17	100,10	99,45	100,16
Qtz	41,88	36,09	36,63	35,42	33,91	41,45	30,20	38,37
Cor	3,28	2,91	3,27	0,56	-0,13	3,84	0,69	2,52
Zir	0,04	0,05	0,04	0,04	0,04	0,05	0,05	0,05
Or	35,79	28,03	23,38	22,97	27,95	27,98	32,41	28,87
Ab	12,44	26,33	25,79	29,20	27,84	17,09	28,73	21,59
An	–	–	0,06	4,68	3,54	–	2,05	–
Bi	0,87	0,39	6,55	4,21	3,35	6,09	2,81	4,12
Hm	–	1,65	–	–	–	–	–	–
Mt	4,84	3,14	2,92	1,91	2,57	2,25	1,92	2,82
Il	0,14	0,54	–	–	–	0,44	–	0,45
Tn	0,37	–	0,84	0,60	0,58	–	0,52	–
Cc	0,27	0,80	0,43	0,30	0,26	0,72	0,52	1,01
Ap	0,09	0,02	0,11	0,15	0,09	–	0,09	–
DI	93,42	93,41	89,11	87,59	89,61	90,40	92,09	91,40

72/204	Felsite from Kwaggasnek Formation on Kameelpoortnek 218 JR
72/56	Felsite from Kwaggasnek Formation on Klipplaatdrift 239 JR
72/60	Felsite from Kwaggasnek Formation on Springfontein 213 JR
72/57	Felsite from Kwaggasnek Formation on Groenfontein 125 JR
73/36	Felsite from Kwaggasnek Formation on Groenfontein 120 JR
73/33	Felsite from Kwaggasnek Formation on Haakdoornfontein
73/65	Felsite from Kwaggasnek Formation on Welgevonden 124 JR
72/8	Felsite from Kwaggasnek Formation on Leeuwfontein 212 JR
73/64	Felsite from Kwaggasnek Formation on Welgevonden 124 JR
73/90	Felsite from Kwaggasnek Formation on Klipdrift 80 JR
73/91	Felsite from Kwaggasnek Formation on Hartebeestfontein 123 JR
73/37	Felsite from Kwaggasnek Formation on Kaallaagte 122 JR
73/85	Felsite from Kwaggasnek Formation on Hartebeestfontein 123 JR
72/168	Felsite from the Schrikkloof Formation on Hartebeestfontein 93 JS
72/165A	Felsite from the Schrikkloof Formation on Rhenosterfontein 227 JR
72/148	Felsite from the Schrikkloof Formation on Vrischgewaagd 226 JR
72/115	Felsite from the Schrikkloof Formation on Hartebeestspruit 434 JR
72/118	Felsite from the Schrikkloof Formation on Zustershoek 246 JR
72/30	Felsite from the Schrikkloof Formation on Groenfontein 125 JR
73/106	Felsite from the Schrikkloof Formation on Boekenhoutkloof 129 JR
73/111	Felsite from the Schrikkloof Formation on Welgedacht 130 JR
73/108	Felsite from the Schrikkloof Formation on Kloppersbos 128 JR
73/114	Felsite from the Schrikkloof Formation on Boveneind Groenfontein 126 JR
72/117	Felsite from the Schrikkloof Formation on Zustershoek 246 JR
73/117	Felsite from the Schrikkloof Formation on Leeuwdrift 82 JR
72/14	Felsite from the Schrikkloof Formation on Leeuwfontein 212 JR
72/13	Felsite from the Schrikkloof Formation on Leeuwdraai 211 JR
72/281	Felsite from the Schrikkloof Formation on Melkhoutfontein 183 JR
73/104	Felsite from the Schrikkloof Formation on Hartebeestfontein 123 JR
72/119	Felsite from the Schrikkloof Formation on Tweefontein
72/126	Felsite from the Schrikkloof Formation on Brakfontein 200 JR
72/311	Felsite from the Schrikkloof Formation on Pieterskraal 190 JR

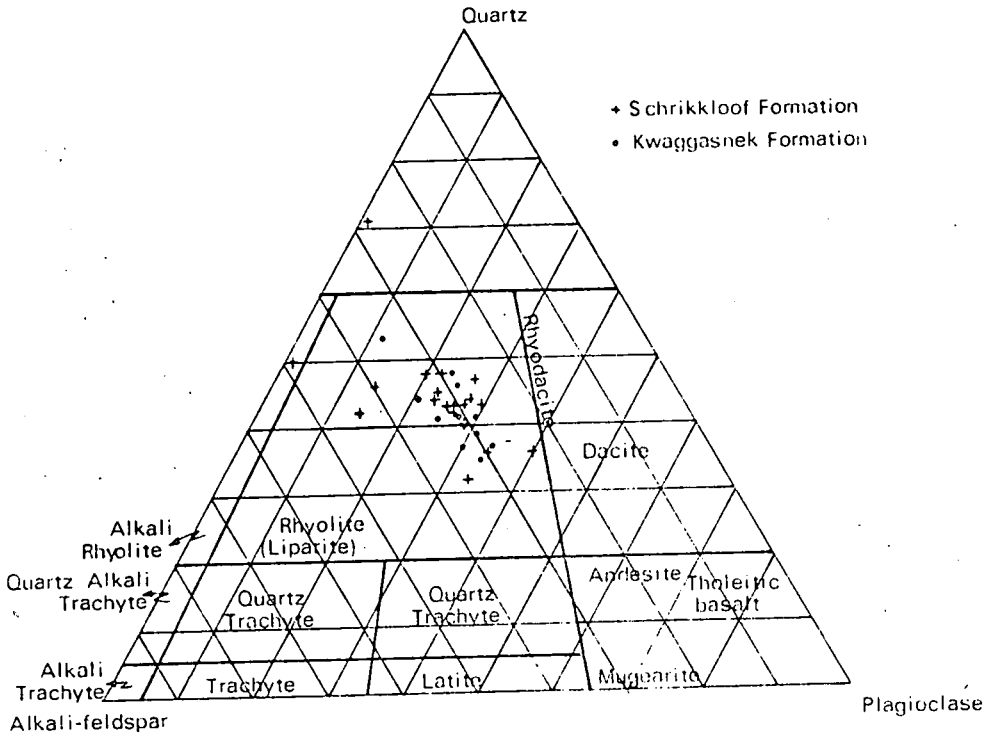

Fig. 4.23. QAP-diagram of the normative data of the Rooiberg Group (diagram after IUGS, 1976).

The measure of differentiation of a magma can best be described by using an AFM-diagram. Mac Donald and Katsura (1964) also used this plot to describe the differentiation of a basaltic magma into trachyte and rhyolite. In the case of the Rooiberg Group, a prominent trend along the AF-side can be observed (Fig. 4.24), which corresponds with the tholeiitic trend of Nockolds and Allen (1954, 1956).

The AFM-diagram also indicates a variation in the Alk and FeO (total) content within the felsitic rocks of both the Kwaggasnek and Schrikkloof Formations while MgO is relatively low and constant. The diagram, however, does not reveal a differentiation trend from the Schrikkloof to the Kwaggasnek Formation.

A clustering of points is revealed when the differentiation index (DI) is plotted against the SiO_2 and CaO contents of the rocks (Fig. 4.25). The Kwaggasnek Formation apparently contains less SiO_2 and more CaO than the Schrikkloof Formation, but the clustering of points is such that no definite differentiation trend can be deduced.

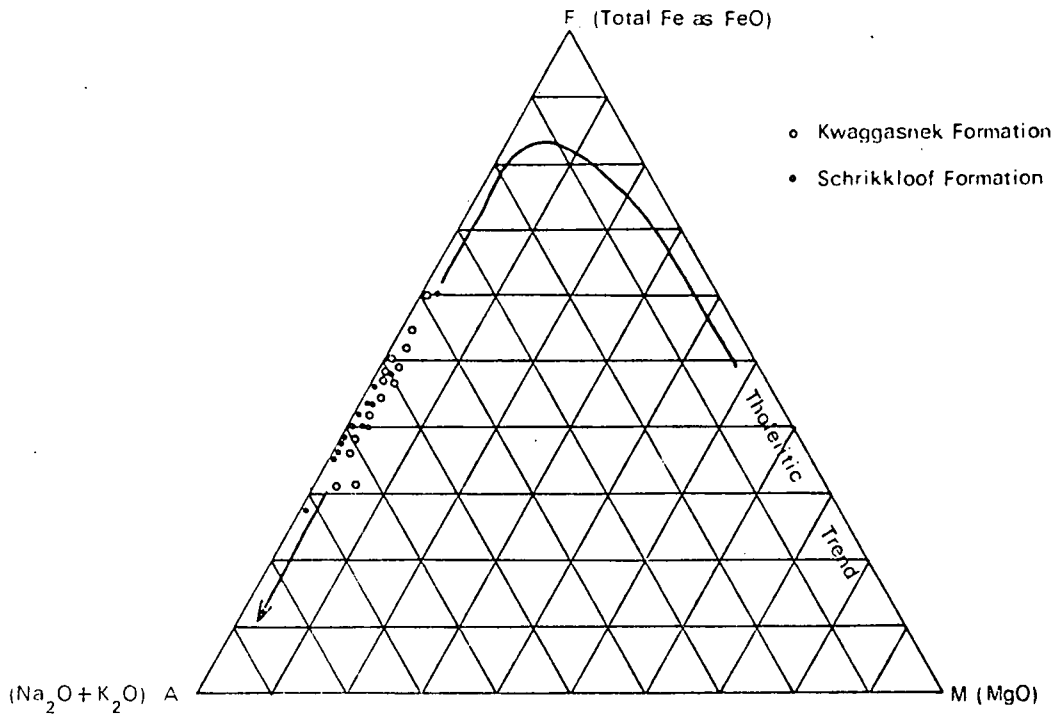

Fig. 4.24. AFM-diagram of the chemical data of the Rooiberg Group (tholeiitic trend after Nockolds and Allen, 1954, 1956).

When the trace element Rb_2O is plotted against SrO (Fig. 4.26), a definite trend is revealed for the Schrikkloof Formation; a clustering of points, however, is revealed for the Kwaggasnek Formation. In the plot of Rb_2O against BaO (Fig. 4.26) a clustering of points for both the Kwaggasnek and Schrikkloof Formations is observed. The conclusion is drawn that both the Kwaggasnek and Schrikkloof Formations crystallized from the same parental magma.

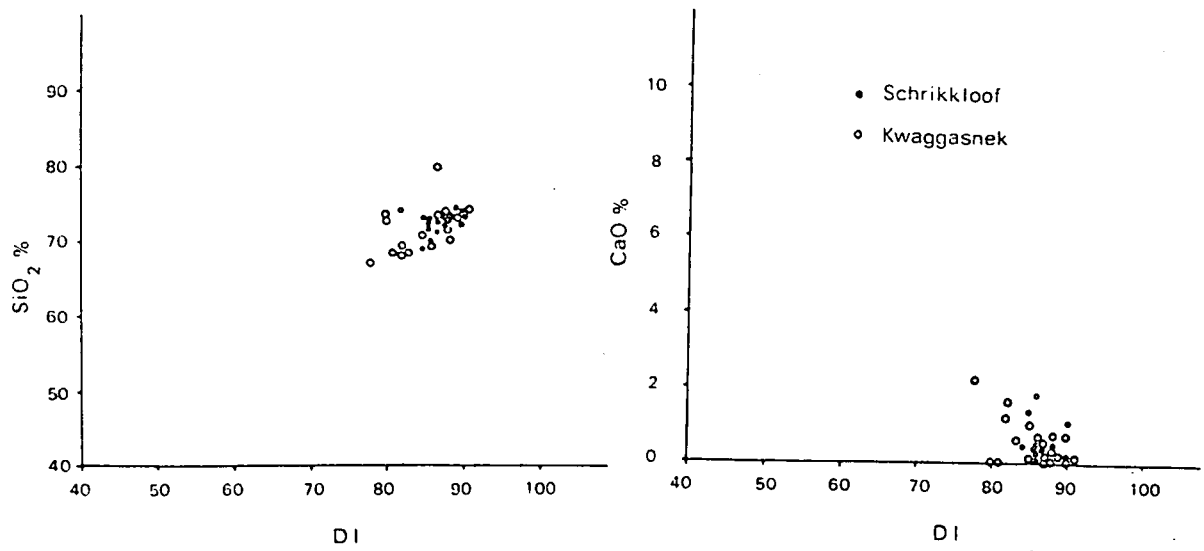

Fig. 4.25. Plot of SiO_2 and CaO against the differentiation index of the felsites.

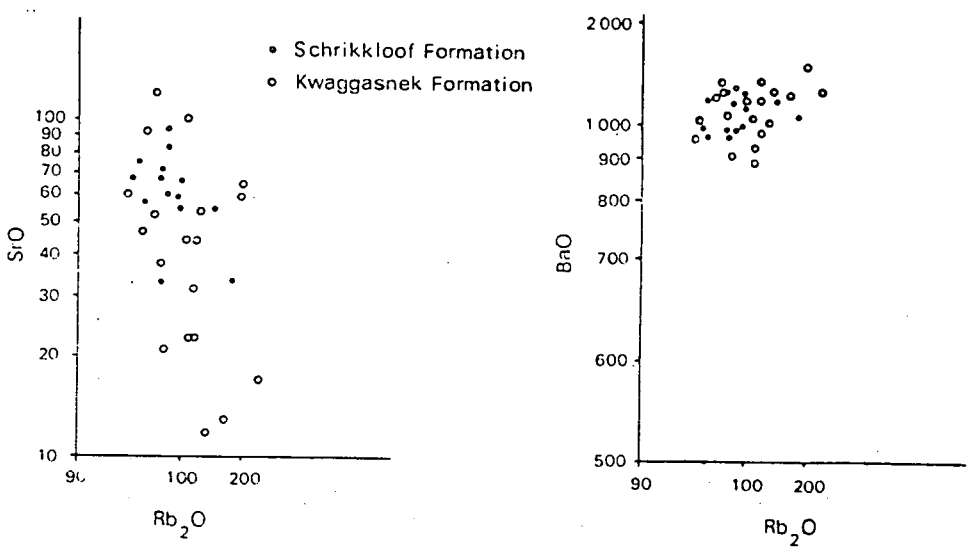

Fig. 4.26. Plot of trace elements in the felsites of the study area.

As the above chemical variation diagrams do not reveal a difference between the Kwaggasnek and Schrikkloof Formations, a statistical method, based on discriminant function analysis, was applied in order to accomplish this goal.

The principle of discriminant function analysis of multivariate data has been used in the field of petrology in a large number of cases. This was mainly

done to delineate differences in petrologic provinces. An example of this can be found in the work of Rhodes and Bornhorst (1975) who were able to differentiate between the granites and felsites of the Bushveld Complex on this basis.

Discriminant function analysis is a multivariate technique for the study and classification of data, as well as the degree of divergence between groups of data. This method has been described in great detail by Davis (1973), Li (1964), Harbaugh and Merriam (1968), Cooley and Lohnes (1962) and others. It was therefore unnecessary to enter into a description of the computational procedures.

A BMDP computer programme was used in the calculation of discriminant functions (BMDP.7M, biomed statistical programme developed at the University of California at Los Angeles). All data were recalculated to 100 per cent on a volatile-free basis and the discriminant functions determined for the analyses of which the stratigraphic positions are known (Table 4.5). In order to check the validity of the classification, analyses from Clubley-Armstrong's (1977) work (corresponding to his Doornkloof and Klipnek Members), as well as analyses from the Warmbad area (Du Plessis, 1976), were also considered. These data yielded a 78 per cent and a 100 per cent proportion of correspondence respectively, which corroborates the subdivision of the Rooiberg Group into a Kwaggasnek and Schrikkloof Formation as suggested by Du Plessis (1976). The number of samples analysed by both Du Plessis (1976) and Clubley-Armstrong (1977), however, is not sufficient to reach a definite conclusion.

The calculation of Canonical variables presents another method (Table 4.5) of determining the grouping. The Canonical variables are also submitted in Table 4.5. On a histogram, based on the calculated Canonical variables (Fig. 4.27), the cutting value for the two populations is at zero, the data from the Kwaggasnek Formation yield positive and the analyses from the Schrikkloof Formation negative values. Although an inadvertent overlap can be observed between the two groups, a clear cut divergence between the two groups is, however, demonstrated by this method.

TABLE 4.5 : DISCRIMINANT FUNCTIONS FOR THE KWAGGASNEK AND SCHRIKKLOOF FORMATIONS OF THE ROOIBERG GROUP

	D9		D8		D7		D6		D5		D4		D3		D2		
	A	B	A	B	A	B	A	B	A	B	A	B	A	B	A	B	Coefficients for canonical variables
SiO_2	140,06021	139,98594	109,74103	109,67017	100,81770	100,76985	88,34327	88,37701	66,97862	67,17841	64,33236	64,44325	47,55287	47,85243	25,62495	26,13157	0,05607
TiO_2	1895,17374	1888,29022	1420,56688	1413,73685	799,27717	794,04908	–	–	–	–	–	–	–	–	–	–	5,19601
Al_2O_3	338,32620	336,70181	256,58540	254,97023	186,36391	184,92979	174,78505	173,42667	–	–	–	–	–	–	–	–	1,22617
FeO	–	–	–	–	–	–	–	–	–	–	–	–	–	–	–	–	–
MnO	501,41540	494,41565	415,11974	408,12971	355,46377	348,62756	363,37725	356,48927	112,75210	107,81192	128,78051	124,37878	40,14680	36,74168	8,12834	5,02556	5,28376
MgO	-317,35480	-316,71622	-244,48199	-243,85161	–	–	–	–	–	–	–	–	–	–	–	–	-0,48204
CaO	218,31914	216,32784	146,00342	144,02027	130,88074	128,93658	106,31149	104,52804	57,74817	56,34214	74,62463	73,78554	–	–	–	–	1,50313
Na_2O	86,41313	87,02033	44,28663	44,89857	29,46094	30,11111	19,52658	20,24174	20,95739	21,66143	–	–	–	–	–	–	-0,45834
K_2O	102,82459	102,81301	–	–	–	–	–	–	–	–	–	–	–	–	–	–	0,00874
P_2O_5	335,87535	323,66714	716,29305	784,03296	1844,50275	1829,53993	3096,17056	3073,02057	2403,53076	2385,76376	2265,94412	2243,55511	1715,25046	1699,05353	–	–	9,21537
Cons	-7941,18463	-7912,17627	-5943,32477	-5914,76654	-5123,98682	-5099,64838	-4480,16467	-4464,22113	-2585,4328	-2598,2547	-2469,68484	-2475,17014	-1801,76976	-1822,19086	-932,84314	-969,59713	-21,81901
%	80,0	84,2	80,0	84,2	80,0	73,7	80,0	78,9	66,7	78,9	66,7	78,9	66,7	78,9	66,7	68,4	

A = Kwaggasnek Formation

B = Schrikkloof Formation

Cons = Constant to be added to sum of products of the oxide weight percentages and discriminant functions

% = Percentage of data correctly classified

In order to show which oxides show statistically significant differences between the two groups, the student's t-test was applied to the data from the study area. This test indicates that such differences do exist (Table 4.6). Although Rhodes and Bornhorst (1975) have expressed their misgivings about the validity of the t-test as a means to distinguish between two populations, Boneau (1960) found that if the number of degrees of freedom exceeds thirty and the distributions have approximately the same shape, the t-test may be used. The results obtained by the application of the t-test are corroborated by the Kolmogorov-Smirnov statistics as described by Miller and Kahn (1962) and Till (1974) (Table 4.6).

The use of discriminant function analysis, therefore, seems to yield a suitable method by which a distinction can be made between the different units in the Rooiberg Group.

4.8 GEOCHEMICAL CORRELATION

In order to facilitate a comparison between the various lithological units within the Rooiberg Group, discriminant function analysis was carried out. The BMDP stepwise discriminant function analysis programme was used for this purpose (BMDP.7M Biomed programme developed at the University of California at Los Angeles). The chemical analyses for the Doornkloof and Klipnek members, as well as those for the Damwal Formation were obtained from Clubley-Armstrong (1977).

A plot of Canonical variables (Fig. 4.28) indicates a marked chemical difference between the lower Damwal Formation in the Loskop Dam area and the upper Kwaggasnek and Schrikkloof Formations in the study area. A comparison between the Kwaggasnek and Schrikkloof Formations, however, reveals an overlapping field, while the Damwal Formation plots in a separate field (Fig. 4.28)

At this stage it should be mentioned that the degree of difference between the data of the Damwal Formation and those of the other units, which are chemically more similar, causes a clustering of the latter when the data of the Damwal Formation are included. This decrease in divergence, based on discriminant function analysis, can also be seen in Table 4.7.

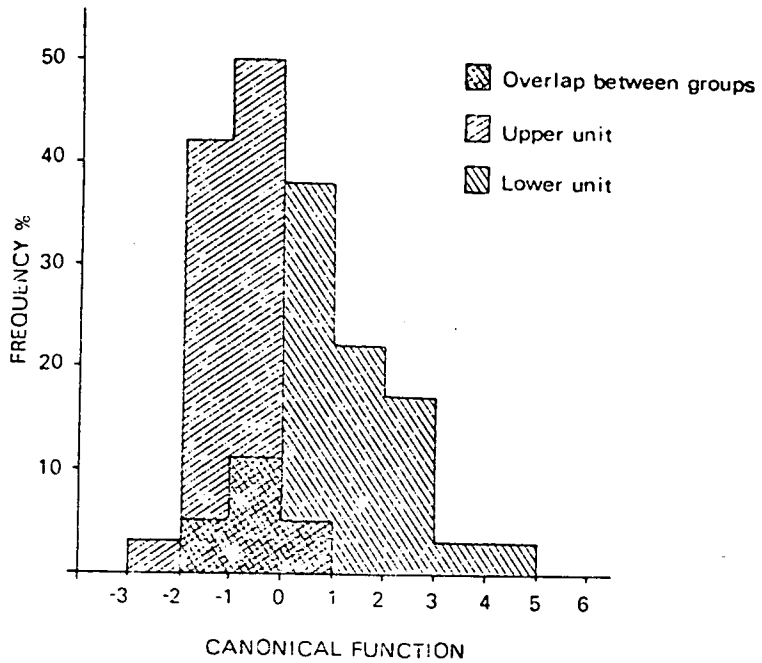

Fig. 4.27. Histogram of the Canonical variables of the Rooiberg Group in the study area.

TABLE 4.6. MEANS, STANDARD DEVIATIONS, T-VALUES AND VALUES FOR THE KOLMOGOROV-SMIRNOV STATISTIC FOR THE FELSITES OF THE ROOIBERG GROUP

	1		2			
	$\bar{x}$	s	$\bar{x}$	s	3	4
SiO_2	70,85077	3,20457	72,30684	1,54094	1,5223	0,40
T_1O_2	0,38000	0,11314	0,30526	0,05327	2,2194	0,50
$A1_2O_3$	11,65923	0,32407	11,65895	0,43290	0,0021	0,24
FeO	8,70538	3,27938	7,75526	1,28161	0,9940	0,27
MnO	0,17846	0,15410	0,11579	0,09912	1,2945	0,21
MgO	0,25154	0,16797	0,20789	0,25718	0,5806	0,50
CaO	0,75769	0,68685	0,48211	0,47911	1,2530	0,36
Na_2O	2,09308	0,76054	2,13789	0,88984	0,1527	0,11
K_2O	5,04846	0,90571	4,97579	0,77570	0,2361	0,08
P_2O_5	0,08231	0,04106	0,05421	0,02364	2,2278	0,45

1. Means and standard deviations for the oxides in the Kwaggasnek Formation.
2. Means and standard deviations for the oxides in the Schrikkloof Formation.
3. T-values of 1 compared with 2. Cutting value is 1,70 (95 per cent confidence level) for 30 degrees of freedom (Spiegel, 1971).
4. Kolmogorov-Smirnov statistic values for 1 compared with 2. Cutting value is 0,42 for degrees of freedom at the 95 per cent confidence level (Miller and Kahn, 1962).

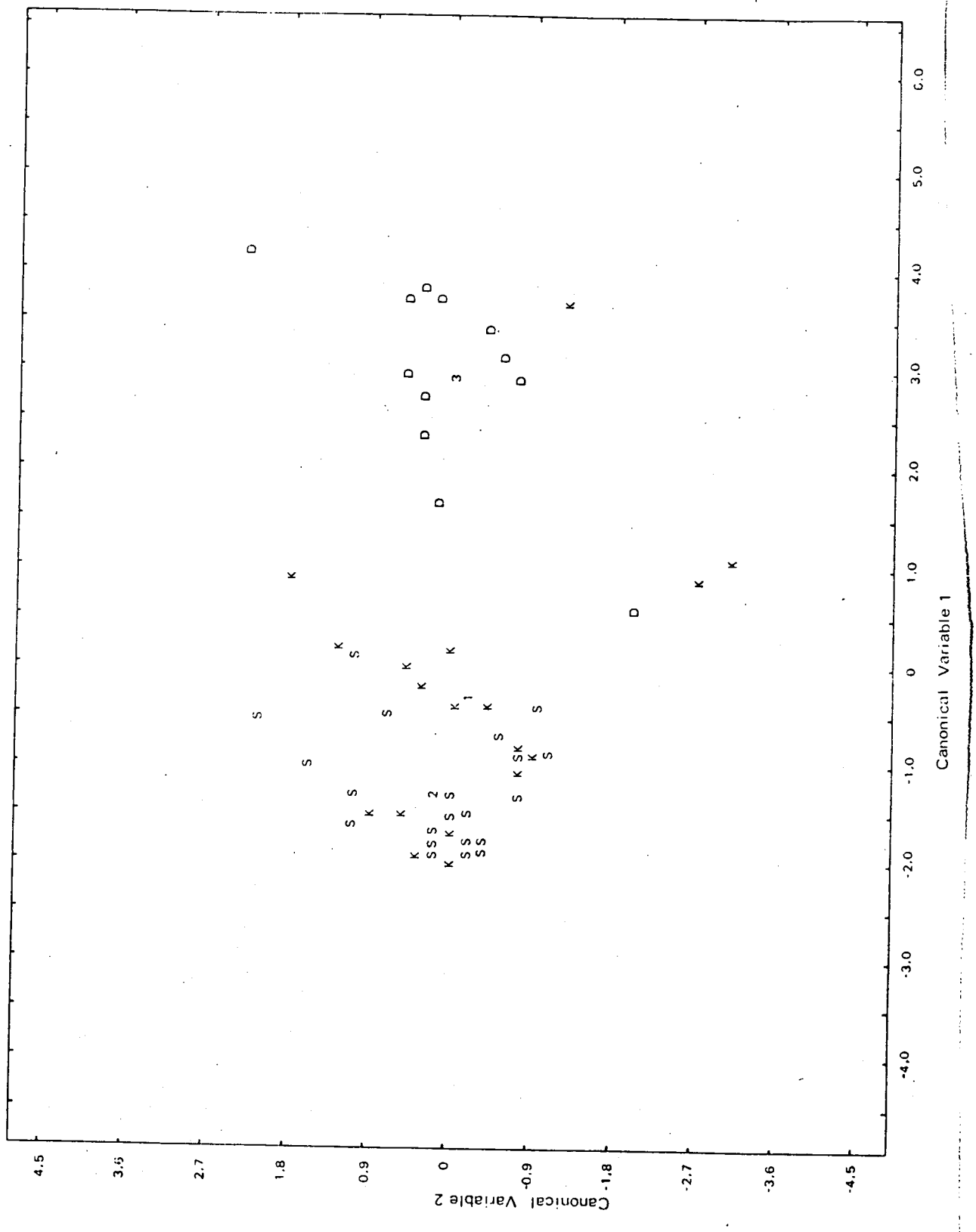

Fig. 4.28. Plot of Canonical variable one against Canonical variable two for the Damwal (D), Kwaggasnek (K), Schrikkloof (S) Formations. Means are indicated by 1, 2 and 3 respectively.

TABLE 4.7: PERCENTAGE OF DATA CORRECTLY CLASSIFIED

Discriminant Function	D9	D8	D7	D6	D5	D4	D3	D2
Damwal Formation	100,0	100,0	100,0	100,0	100,0	100,0	100,0	100,0
Kwaggasnek Formation	68,4	68,4	68,4	68,4	57,9	63,2	63,2	57,9
Schrikkloof Formation	79,2	75,0	70,8	79,2	50,0	66,7	75,0	70,8

The student's t-test on the chemical data of the Kwaggasnek Formation, which includes the data from the Doornkloof Member (Clubley-Armstrong, 1977) and the lower unit from the Warmbad area (Du Plessis, 1976), shows a significant difference with respect to SiO_2, TiO_2, Al_2O_3, MgO, CaO, K_2O and P_2O_5 contents (Table 4.8), between the Kwaggasnek and Damwal Formations. It is also apparent that the Damwal Formation differs from the Schrikkloof Formation (the data from the Klipnek member (Clubley-Armstrong, 1977) and from the upper unit from the Warmbad area (Du Plessis, 1976) being included), with regard to the same elements as well as FeO.

TABLE 4.8 : STATISTICAL DATA OF THE CHEMICAL COMPONENTS OF THE DAMWAL, KWAGGASNEK AND SCHRIKKLOOF FORMATIONS

	1		2		3		4	5	6
	$\bar{x}$	s	$\bar{x}$	s	$\bar{x}$	s			
SiO_2	68,77	1,47	72,34	2,10	73,99	1,42	5,5592	10,0874	2,9384
TiO_2	0,63	0,06	0,40	0,13	0,31	0,05	2,1809	16,6094	2,8091
Al_2O_3	13,43	0,68	12,26	0,60	12,07	0,51	4,8638	6,0701	1,0713
FeO	6,79	0,61	6,34	1,64	5,34	1,03	1,0681	5,2335	2,3233
MnO	0,14	0,08	0,17	0,14	0,12	0,09	0,8901	0,5866	1,4173
MgO	0,85	0,53	0,32	0,24	0,21	0,24	3,2542	3,9702	1,4505
CaO	2,50	0,89	0,84	0,70	0,56	0,53	5,4833	6,9317	1,4221
Na_2O	2,68	0,74	2,30	0,93	2,33	0,89	1,2471	1,2336	0,0970
K_2O	4,01	0,97	4,93	0,84	5,01	0,75	2,7189	3,1069	0,2849
P_2O_5	0,17	0,03	0,09	0,06	0,05	0,02	5,2418	12,4838	2,4358

1. Means and standard deviations of the Damwal Formation.
2. Means and standard deviations of the Kwaggasnek Formation.
3. Means and standard deviations of the Schrikkloof Formation.
4. Values of the t-test between the Damwal and Kwaggasnek Formations. Statistically significant data are underlined for the 95 per cent confidence level at 2,045 (Downie and Heath, 1970).
5. Values of the t-test between the Damwal and Schrikkloof Formations. Statistically significant data are underlined for the 95 per cent confidence level at 2,036 (Downie and Heath, 1970).
6. Values of the t-test between the Kwaggasnek and Schrikkloof Formations. Underlined data are 95 per cent significant at 2,021 (Downie and Heath, 1970).

The similarity between the Kwaggasnek and Schrikkloof Formations can be seen when the results in the table are compared. This similarity is also corroborated by a TiO_2 vs. SiO_2 plot (Fig. 4.29), in which it can also be seen that the Damwal Formation, which plots in a separate field, differs chemically from the other units. An AFM-diagram (Fig. 4.30), based on the same analyses, also indicates that a small overlap exists between the Damwal and Kwaggasnek Formations, while the latter overlaps largely with the Schrikkloof Formation.

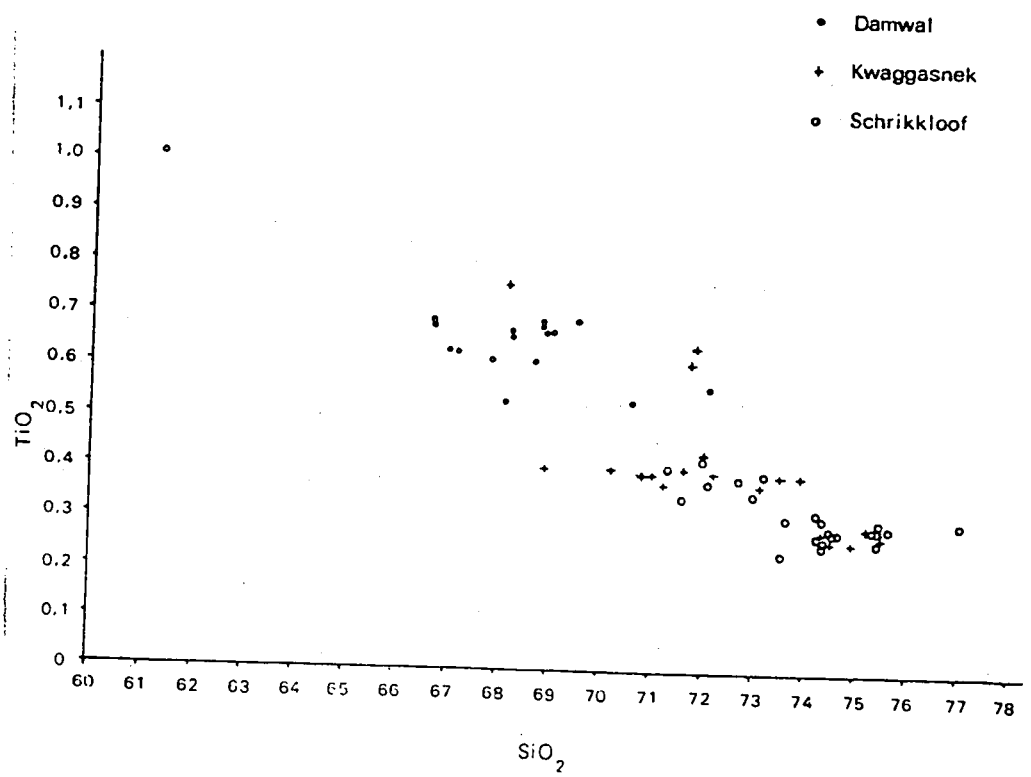

Fig. 4.29. Plot of TiO_2 against SiO_2 for the Damwal, Kwaggasnek and Schrikkloof Formations of the Rooiberg Group.

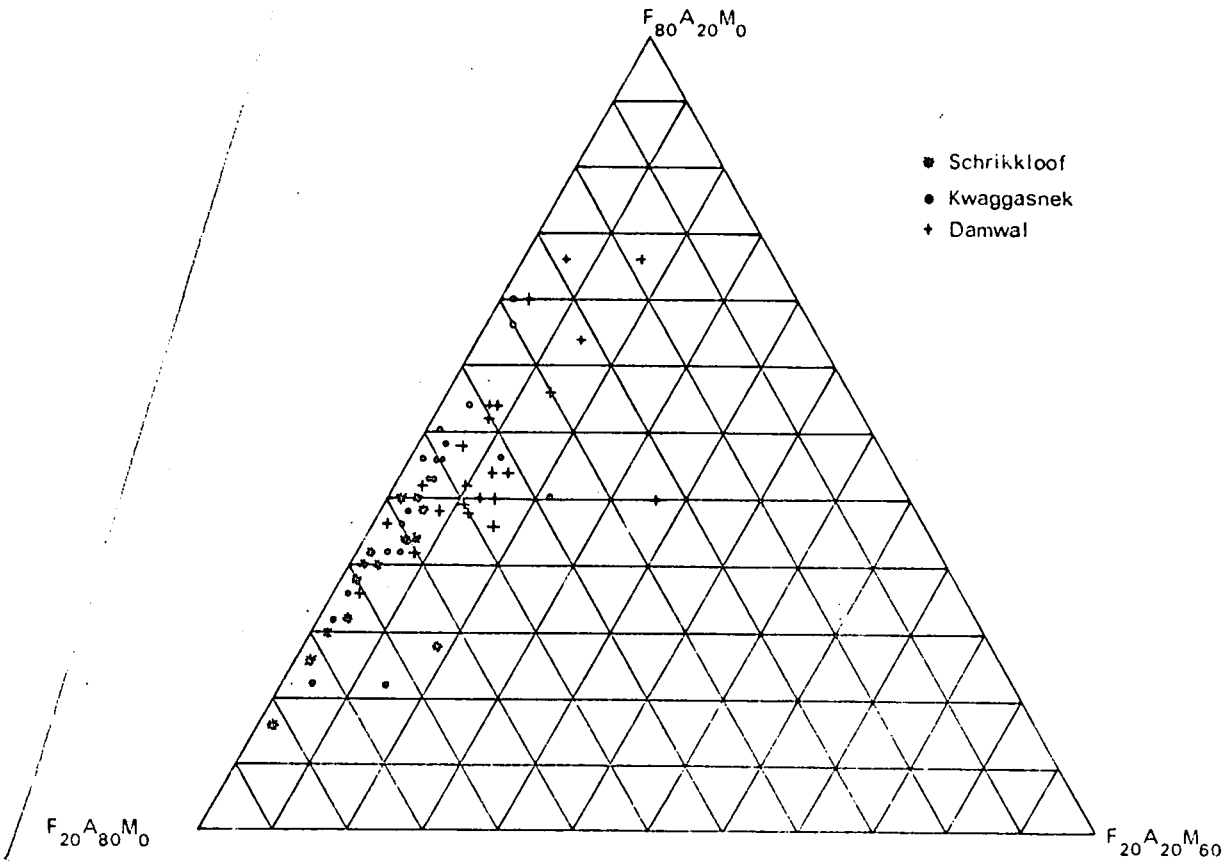

Fig. 4.30. AFM-diagram of the Damwal, Kwaggasnek and Schrikkloof Formations of the Rooiberg Group.

If the Kwaggasnek and Schrikkloof Formations are treated as a single unit and then compared with the Damwal Formation, a very high percentage of correctly classified analyses is obtained (Table 4.9). A test of statistical significance indicates that major differences in oxide concentrations are found in all elements except MnO and Na_2O (Table 4.10) between the Damwal and Kwaggasnek/ Schrikkloof Formations.

TABLE 4.9 : DISCRIMINANT FUNCTIONS AND CANONICAL CLASSIFICATION FUNCTIONS OF THE DAMWAL FORMATION AND THE COMBINATION KWAGGASNEK AND SCHRIKKLOOF FORMATIONS

	D9		D8		D7		D6		D5		D4		D3		D2		
	A	B	A	B	A	B	A	B	A	B	A	B	A	B	A	B	Coefficients for canonical variables
SiO_2	268,21077	266,19381	139,48400	137,31421	139,53807	137,36000	126,27404	124,30035	115,01960	113,27936	97,77338	96,38282	–	–	–	–	-0,49678
TiO_2	996,38344	964,50195	1420,04181	1388,66333	1407,40048	1377,95657	1352,16628	1323,57344	1167,14131	1142,38631	1000,97899	979,59309	-2,60517	-9,71779	–	–	-7,85254
Al_2O_3	360,09479	354,69681	206,28452	200,70392	206,12318	200,56727	189,86676	184,56134	152,25200	147,72680	128,21780	124,17991	36,06031	33,33312	35,94542	32,90454	-1,32954
FeO	177,60063	177,81149	–	–	–	–	–	–	–	–	–	–	–	–	–	–	0,05194
MnO	632,66363	627,29455	367,55370	361,86987	367,40544	361,74429	–	–	–	–	–	–	–	–	–	–	-1,32243
MgO	-30,27928	-26,90150	-155,20912	-151,97967	-154,26463	-151,17971	-132,72554	-129,97251	–	–	–	–	–	–	–	–	0,83196
CaO	384,33060	377,62547	226,74682	219,85459	226,22932	219,41629	188,01001	181,78588	154,72088	149,18724	91,24915	87,00246	-1,06790	-4,00163	-1,25888	-4,71402	-1,65150
Na_2O	–	–	–	–	–	–	–	–	–	–	–	–	–	–	–	–	
K_2O	147,23067	145,69366	81,71756	80,10276	81,56711	79,97534	69,19113	67,79005	73,13008	71,64730	–	–	–	–	–	–	-0,37857
P_2O_5	145,98413	152,43344	-40,69425	-34,46657	–	–	–	–	–	–	–	–	–	–	–	–	1,58849
Cons	-13373,00342	-13129,60779	-7033,83533	-6775,37811	-7033,47504	-6775,11963	-6361,67767	-6123,86548	-5689,71863	-5479,49329	-4657,89984	-4489,09259	-244,32269	-200,16505	-244,24189	-199,04078	59,18389
%	94,7	97,6	94,7	97,6	94,7	97,6	94,7	97,6	94,7	97,6	89,5	97,6	89,5	97,6	89,5	97,6	–

A = Values for Damwal Formation

B = Values for the combination Kwaggasnek and Schrikkloof Formations

Cons = Constant to be added to sum of the oxide weight percentages and discriminant functions

% = Percentage of data correctly classified

TABLE 4.10 : STATISTICAL ANALYSIS OF DATA FROM THE DAMWAL FORMATION AND THE COMBINED KWAGGASNEK AND SCHRIKKLOOF FORMATIONS

	1		2		3
	$\bar{x}$	s	$\bar{x}$	s	
SiO_2	68,77	1,47	73,24	1,93	9,94
TiO_2	0,63	0,06	0,36	0,11	12,36
Al_2O_3	13,43	0,68	12,15	0,55	7,21
FeO	6,79	0,61	5,79	1,42	3,85
MnO	0,14	0,08	0,14	0,12	0,00
MgO	0,85	0,53	0,26	0,24	4,64
CaO	2,50	0,89	0,69	0,62	8,03
Na_2O	2,68	0,74	2,12	0,90	2,55
K_2O	4,01	0,97	4,97	0,79	3,78
P_2O_5	0,17	0,03	0,07	0,04	10,82

1. Means and standard deviations of chemical components of the Damwal Formation.
2. Means and standard deviations of the chemical components of the combined Kwaggasnek and Schrikkloof Formations.
3. Values of the t-test between 1 and 2 with the underlined data being statistically significant at the 99 per cent confidence level.

The chemical correlation between the various units of the Rooiberg Group indicates a very strong resemblance between the Kwaggasnek and Schrikkloof Formations, whereas the Damwal Formation can easily be recognized as a chemically different entity. Since chemical data from the Rooiberg Group in the Warmbad area (data of Du Plessis, 1976) yield a 100 per cent correlation with that of the study area and a marked similarity exists between their respective lithologies, the succession of the study area was correlated with that of Du Plessis (1976), namely the Kwaggasnek and Schrikkloof Formations. For this reason the names Kwaggasnek and Schrikkloof were used instead of the Doornkloof and Klipnek members of the Selonsrivier Formation, as defined by Clubley-Armstrong (1977).

4.9 CONCLUSIONS

The dissimilarity between the size and the frequency distribution of the phenocryst populations within the Kwaggasnek and Schrikkloof Formations pointed out some of the very subtle differences between the rocks of these Formations. It also indicates differences between the physico-chemical conditions that prevailed in the magma chamber at the time of intrusion and extrusion.

Modal and textural analyses indicate that the mineralogy of the rocks change slightly in composition during crystallization, but give no substantive evidence that the rocks of the two formations display different mineralogical paragenesis. The chemical analyses also point towards certain chemical changes within the magma during crystallization, but no clear cut differences, based on this data alone, could be drawn. No distinct differentiation from the Kwaggasnek to the Schrikkloof can be observed from the various diagrams.

Discriminant function analysis yielding approximately 80 per cent classification (Table 4.5) and various other statistical methods, supply evidence to discriminate between rocks of the different formations. On this basis, it was possible to distinguish between the felsitic rocks of the Kwaggasnek and Schrikkloof Formations. Statistical analyses also facilitate the discrimination between the Damwal and Kwaggasnek/Schrikkloof Formations.

A statistical comparison between the felsitic rocks of the various formations of the Rooiberg Group reveals that a remarkable resemblance exists between the felsite of the Doornkloof and Klipnek members of the Selonsrivier Formation in the east and that of the Kwaggasnek and Schrikkloof Formations in the west and in the Warmbad area and that these formations differ chemically from the Damwal Formation in the Loskopdam area. The results of the present investigation indicate that the Kwaggasnek/Schrikkloof Formations formed from the same parental magma, while the Damwal Formation may represent a different magmatic entity.

5 RASHOOP GRANOPHYRE SUITE

5.1 INTRODUCTION

The origin of the granophyre of the Bushveld Complex, like most granophyre occurrences, constitutes a major petrogenetic problem. Another typical example of the controversial origin of the granophyre is found in the Rhum Inverness-shire Complex. This controversy was initiated by Vogt (1930) who regarded the formation of the granophyre as the product of cotectic crystallization, while Leighton (1954) proposed eutectic rather than cotectic crystallization. Black (1954), however, favoured a metasomatic origin, while Dunham (1965) and also Hughes (1960) regarded the formation of granophyre as the end result of cotectic crystallization.

Hall (1932) and Lombaard (1932) regarded the granophyre of the Bushveld Complex as the coarse crystalline phase of a felsite flow. Where it shows intrusive relationships, they regarded it as granophyre intruding its own roof or being related to a later felsite flow. In contrast with this hypothesis, Boshoff (1942) and Van der Westhuizen (1945) regarded the fine-grained acid rocks overlying the diorites of the Mafic Portion of the Bushveld Complex as the differentiation product of the basic magma. Strauss (1947, 1955) as well as Iannello (1971) proposed that the granophyre formed by a process of direct crystallization, by reconstruction of Rooiberg felsite and also from the recrystallization of quartzo-feldspathic sediments. These processes were also recognized by Von Gruenewaldt (1968, 1972) for the granophyre in the Tauteshoogte region, but he considered some of the granophyre to be of anatectic or palingenetic origin.

In the area around Stavoren, Strauss (1947) and Iannello (1971) described granophyre which represents metasomatically altered sediments of the Transvaal Sequence. This idea was opposed by Steyn (1962) on the results obtained from studies on zircon and he regarded the granophyre as the product of magmatic crystallization. Willemse (1964) on the other hand, found intrusive contacts between the granophyre and the underlying granite and hence considered it to be of metasomatic origin, while Rhodes (1975a) supported the magmatic origin for these rocks.

TABLE 5.1. NOMENCLATURE APPLIED TO THE GRANOPHYRES OF THE BUSHVELD COMPLEX (MODIFIED AFTER LENTHALL, 1973).

ORIGIN	Terminology as used by				
	Strauss (1947, 1955)	Von Gruenewaldt (1968, 1972)	Iannello (1971)	Lenthall (1973)	Rhodes (1975a)
Direct crystallization from a magma	Bushveld granophyre	–	–	–	Stavoren granophyre
Reconstruction of Rooiberg felsites	–	Rooiberg granophyre	Rooiberg granophyre	Waterval granophyre	–
Reconstruction of quartzo-feldspathic sediments	Pseudo-granophyre	–	Bushveld granophyre	–	–
Granophyre developed between Bushveld granite and its roof of quartzite	–	Stavoren granophyre	Bushveld granophyre	Stavoren granophyre	–

Clubley-Armstrong (1977) found that the granophyre in the Selonsrivier area formed by two processes:- in part magmatic and in part the product of recrystallization of felsite. In the Moloto area De Bruiyn (1975) also supported the latter.

The origin of the granophyre remains controversial and the possibility of different modes of origin has to be accepted.

In the past different names were given to the granophyre in different parts of the complex (Table 5.1). SACS (South African Committee on Stratigraphy), however, decided that the granophyre should collectively be called the Rashoop Granophyre Suite.

The subdivision of the Rashoop Granophyre Suite, based on interrelationships with the surrounding rock types, is given in Table 5.2.

TABLE 5.2. Subdivision of the Rashoop Granophyre Suite in the study area, based on the interrelationships with the surrounding country rocks (after Lenthall, 1973).

	Rashoop Granophyre Suite		
	Sterk River granophyre	Stavoren granophyre	Blinkwater granophyre
Overlying rock type	Rooiberg felsite	Transvaal sediments	Bushveld granite
Underlying rock type	Bushveld granite	Bushveld granite	Layered sequence

The Sterk River granophyre, which forms the dominant type in the study area, forms a sheet-like body between the felsite and the granites, while in the southern part of the region the Blinkwater granophyre is developed

along the contact between the Bushveld granites and the Mafic Phase. Stavoren granophyre, which is present between the Bushveld granite and the Transvaal sediments, only forms a very small portion of the granophyre present in the study area (Fig. 5.2). The association of granophyre with felsite and granite leads De Bruiyn (1975) to the conclusion that the first-mentioned formed as a result of the complete devitrification and recrystallization/metasomatism of the felsite, due to the intrusion of the granite.

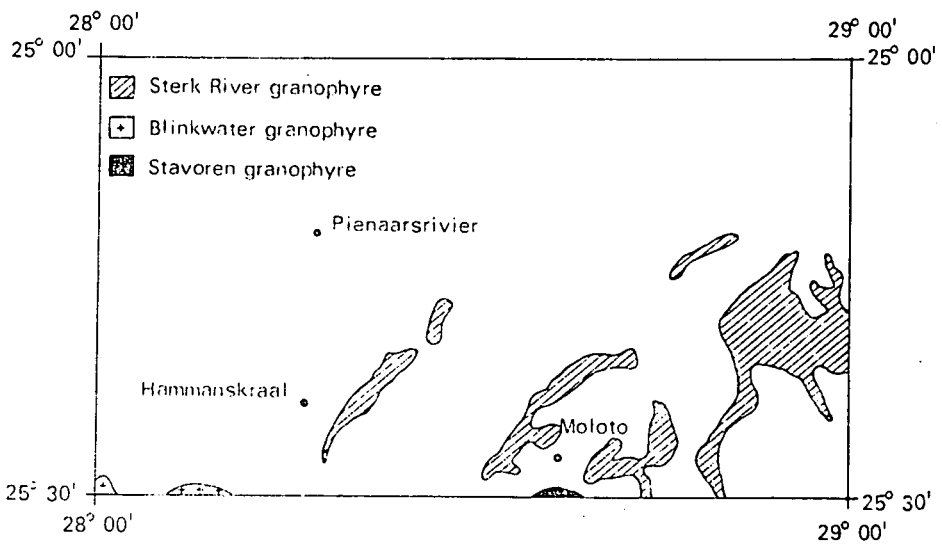

Fig. 5.1. Distribution of granophyre in the study area, with special reference to the different stratigraphic types.

Only a few intrusive contacts are present in the study area. Wagner (1927), however, described some *lit par lit* contacts between the granophyre and the Bushveld granite in the Zustershoek 246 JR region. Clubley-Armstrong

(1977) recognized three different types, namely granophyre, microgranophyre and porphyritic granophyre. According to this classification two types, namely microgranophyre and granophyre, form prominent outcrops in the study area, while the porphyritic type was observed in only a few localities.

The microgranophyre typically outcrops in the form of rounded boulders with a purplish colour, while the granophyre is reddish brown on smooth, dome-like outcrops. The contact relationships between these two types of granophyre, as well as between the felsite at the top and the underlying granite, are transitional. It was found that the granophyric texture becomes coarser and more prominent towards the base of the succession. This gradation is also apparent in the lower contact zone where the granophyre first grades into the granophyric granite and then into the granite proper. The gradational zone is characterized by the presence of larger quartz crystals in the lower portion, giving rise to the development of an almost graphic texture (Fig. 5.2). From this evidence alone, it is not certain whether the granophyre resulted from the reconstruction of the felsite or from the crystallization of the granitic magma or perhaps from both these mechanisms.

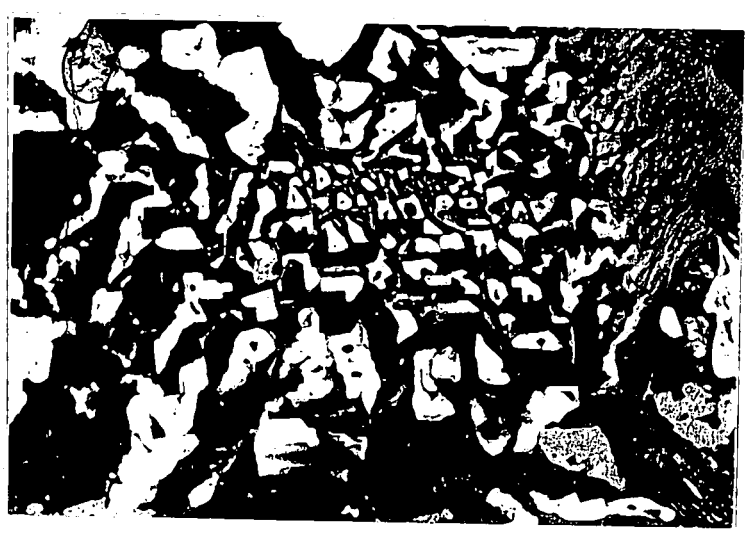

Fig. 5.2. Photomicrograph of very coarse-grained granophyric texture displayed by the granophyre close to the granite contact (crossed nicols, x 30).

5.2 PETROGRAPHY

The microgranophyre is a fine to very fine-grained rock with quartz, orthoclase, plagioclase, biotite and hornblende as major constituents and chlorite, zircon and fluorite as accessories.

The plagioclase, which forms large phenocrysts, acted as nuclei for the crystallization of the rest of the rock. This phenomenon was also reported by Hughes (1960), Von Gruenewaldt (1968) and Clubley-Armstrong (1977). The plagioclase (An_{10-20}) is usually euhedral and range between 0,2 – 0,8 in size. Optical continuity between the rims of the phenocrysts and the adjacent alkali feldspar of the granophyric intergrowths is often present (Fig. 5.3); the grain-size of the microgranophyric quartz likewise decreases towards the plagioclase. This feature was also noticed by Hughes (1960)

Fig. 5.3. Photomicrograph of a plagioclase phenocryst set in a matrix of granophyrically intergrown quartz and alkali feldspar. Notable is the increase in grain size from the centre (crossed nicols, x 20).

for the granophyre of the Southern Mountains Igneous Complex. Quartz constitutes approximately 38 volume per cent of Bushveld granophyres, although very few individual quartz phenocrysts are present. Where quartz phenocrysts do occur, the quartz of the intergrowth is in optical continuity with the phenocryst. Cuneiform textures are also present in the granophyre.

Orthoclase constitute about 30 per cent of the rock. Phenocrysts are occasionally present and are in optical continuity with the orthoclase of the intergrowths. The alkali feldspar is often sericitised.

Biotite and hornblende form the major femic constituents, with biotite being the most common. These minerals are fine-grained, euhedral in shape and frequently found in conjunction with fine-grained euhedral zircon and fluorite. Most of the biotite and hornblende show alteration to chlorite.

Euhedral, very fine-grained magnetite is also present and is normally associated with the femic minerals. Cassiterite forms a prominent constituent of the granophyre on Zustershoek 246 JR.

Phenocrysts of plagioclase are absent in the lower horizons of the granophyre; here microgranite develops interstitially between the granophyric texture. This phenomenon was also reported by Rhodes (1975a) in the Stavoren area, as well as by De Waal (1979) in the Zaaiplaats region.

The microgranophyre exhibits the same petrography as the granophyre, except that the latter is coarser grained.

5.3 MODAL AND TEXTURAL PROPERTIES

The modal analyses, conducted according to the method outlined in Appen-

dix II, are given in Table 5.3. The method described by Tuttle and Bowen (1958) was used to determine the usefulness of this data (Fig. 5.4). This method proved satisfactorily and reveals that most of the analyses fall within the field defined by Tuttle and Bowen (1958). The modal analyses gives a mean value of 39 per cent quartz, 30 per cent orthoclase and 32 per cent plagioclase, with minor mafic constituents.

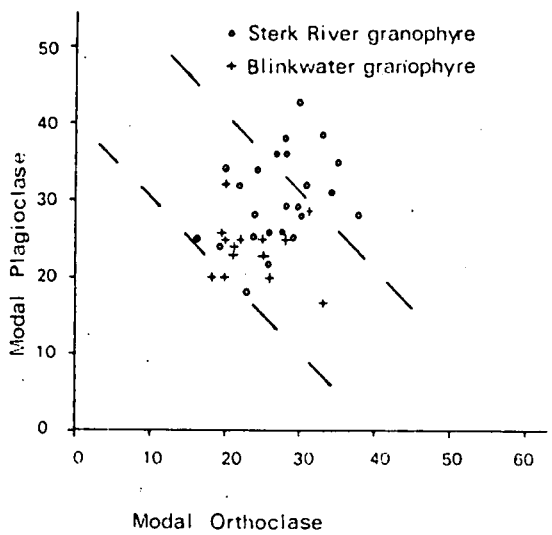

Fig. 5.4. Plot of modal plagioclase against modal orthoclase to determine the usefulness of the modal analysis (after the method of Tuttle and Bowen, 1958).

The phenocrysts in the granophyre are frequently idiomorphic, which makes measurement an easy operation using a graded ocular. A statistical analysis of this data is given in Table 5.4.

TABLE 5.3 : PLAGIOCLASE, ALKALI FELDSPAR AND MAFIC MINERAL FREE MODAL COMPOSITION AND TEXTURAL PARAMETERS OF THE RASHOOP GRANOPHYRE SUITE IN THE STUDY AREA

SAMPLE NUMBER	1	2	3	4	5	6	7	8
				Sterk River granophyre				
73/60	12	27	27	30	43	0,37	54	2
73/30	18	23	27	28	23	0,36	28	1
72/10	16	20	34	25	24	0,34	147	5
72/46	12	15	38	23	25	0,45	89	4
72/42	16	12	30	29	25	0,55	73	4
72/40	18	18	30	35	35	0,40	75	3
72/186	13	27	34	27	36	0,51	118	6
72/195	15	29	33	28	29	0,54	74	4
73/9	13	25	29	28	38	0,46	22	1
73/21	12	23	28	33	38	0,44	68	3
73/52	15	20	28	37	34	0,39	26	1
73/86	14	25	43	16	25	0,25	80	2
73/82	13	24	32	37	28	nd	nd	nd
72/36	10	20	35	22	32	0,34	265	9
73/59	15	25	45	20	34	0,14	143	2
72/74	7	25	30	25	25	0,56	71	4
72/73	15	30	32	20	25	0,57	88	5
72/72	14	25	34	34	31	0,68	44	3
72/75	15	30	34	30	29	0,59	102	6
72/67	18	20	46	28	25	0,36	56	2
72/65	14	20	37	30	29	0,36	28	1
72/91	15	25	33	28	36	0,68	129	2
72/89	13	30	30	24	34	0,35	29	1
72/96	18	25	27	25	23	0,57	70	4
72/87	13	20	36	23	18	0,28	136	1
72/25	13	25	35	24	28	nd	nd	nd
				Blinkwater granophyre				
73/8	8	23	35	33	17	nd	nd	nd
73/10	11	21	35	20	32	0,32	125	4
73/17	20	22	28	21	23	0,43	47	2
73/16	18	23	32	22	25	0,31	32	1
73/15	14	27	35	24	25	0,30	33	1
73/14	20	26	35	20	25	0,55	36	2
73/13	18	25	32	20	20	0,65	15	1
73/12	14	27	40	28	25	nd	nd	nd
73/4	13	20	46	26	20	0,25	80	2
73/3	15	21	40	21	24	0,31	32	1
73/2	10	30	32	20	25	nd	nd	nd
73/1	12	23	42	18	20	nd	nd	nd
73/31	15	20	38	25	23	0,31	161	5
73/28	15	32	38	31	29	0,45	22	1

1 = Weight percent anorthite in plagioclase
2 = Weight percent albite in alkali feldspar
3 = Weight percent quartz in sample
4 = Weight percent orthoclase in sample
5 = Weight percent plagioclase in sample
6 = Mean calculated phenocryst diameter
7 = Crystallinity Index
8 = Number of phenocrysts on one cm^2

TABLE 5.4. Statistical parameters of phenocrysts in the granophyres of the Rashoop Granophyre Suite, north of Pretoria.

n	444	Ratio	1,6225
$\bar{x}$	0,5984	R	0,8011
Sx	0,3282	Slope	0,6391
$\bar{y}$	0,3688	Recip	1,5646
Sy	0,2097	Std. error slope	0,0182
$\bar{s}$	0,4636	D	34,94
$\bar{v}$	0,1628	Reg. line	y = 0,6391 x – 0,0136

n = number of phenocrysts; $\bar{x}$ = mean of long axes; Sx = standard deviation of long axes; $\bar{y}$ = mean of short axes; Sy = standard deviation short axes; $\bar{s}$ = mean diameter; $\bar{v}$ = mean volume; Ratio = $\bar{x}/\bar{y}$; R = correlation coefficient; Slope = slope of regression line; Recip = 1/Slope; Std. error slope = standard error of the slope of the regression line; Reg. line = equation of the linear regression line.

It can be seen from Table 5.4 that a moderate correlation exists between the dimensions of the long and the short axes of the phenocrysts, as depicted by the correlation coefficient. A graphical representation of the various axes indicates that most of the phenocrysts have an elongation of approximately 1,5, while the statistical data yields a mean of 1,6225. This value also corresponds with the regression line in Figure 5.5. It can also be deduced from the graph that the majority of the phenocrysts fall in the range of 0,35–0,60 mm by 0,2–0,4 mm.

A study of the crystallinity index (C.I.) and the formational temperatures (the latter were determined by the two-feldspar method of Stormer, 1975) of the granophyres indicate that the Sterk River and Blinkwater granophyres formed at temperatures of 500°C – 650°C (Fig. 5.7). These temperatures are corroborated by a diagram of the mole fraction of albite in plagioclase against the mole fraction of albite in alkali feldspar, based on the two-feldspar geothermometer of Stormer (1975) (Fig. 5.7). The temperature of 500°C – 650°C is slightly lower than that suggested for granitic melts by Von Platen (1965), Winkler (1976) and Von Gruenewaldt (1972). This difference is attributed to an increase in the oxygen fugacity after intrusion (Whitney and Stormer, 1976).

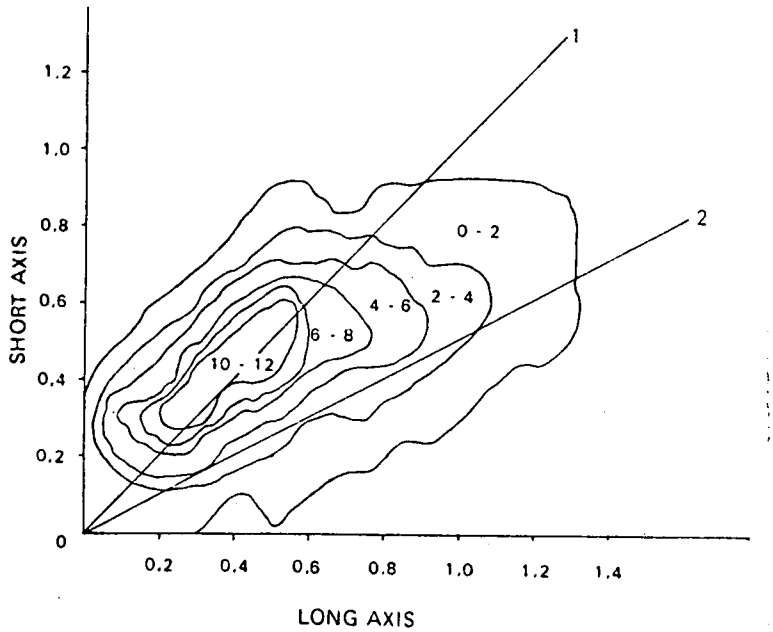

Fig. 5.5. *Plot of short axes against long axes of phenocrysts in the granophyre of the Rashoop Granophyre Suite, north of Pretoria.*

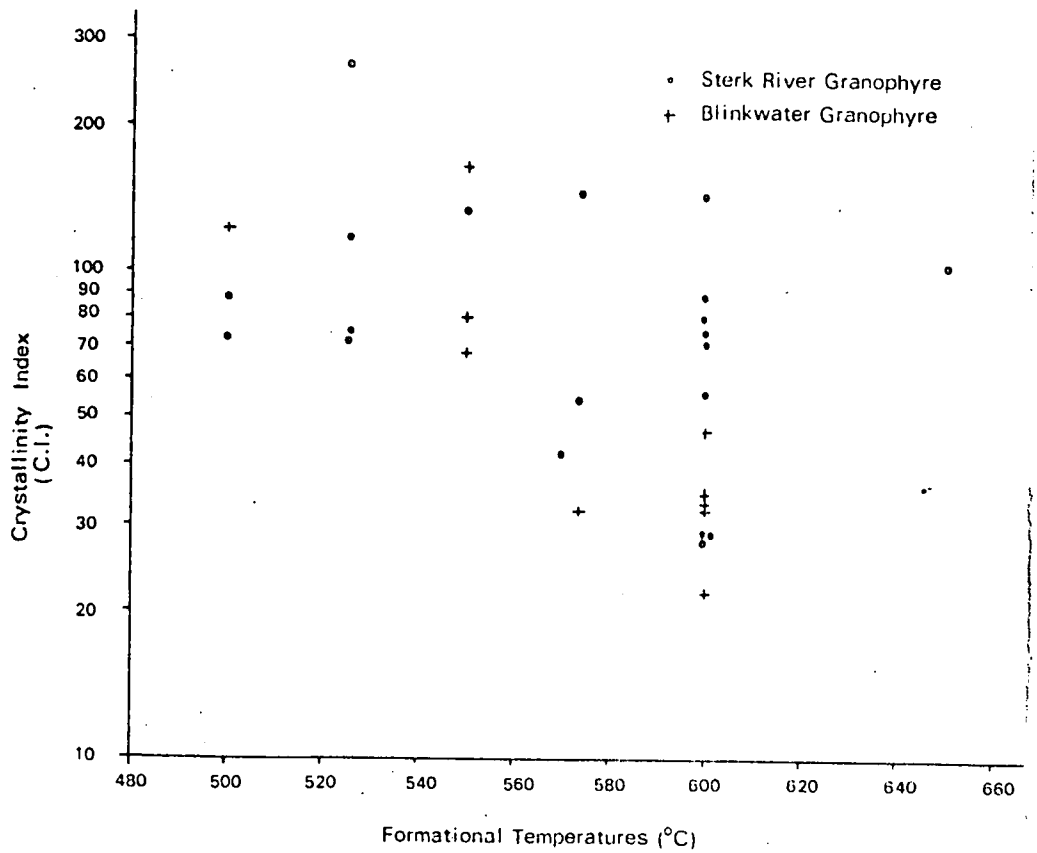

Fig. 5.6. *Temperature-phenocryst relationships in the Rashoop Granophyre Suite, north of Pretoria.*

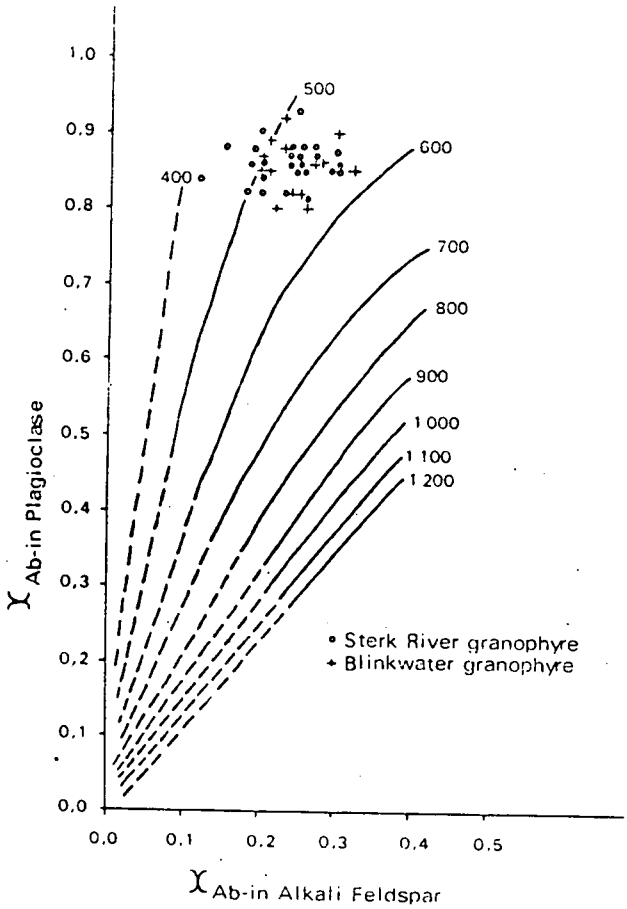

Fig. 5.7. *Mole fraction albite in plagioclase against mole fraction albite in alkali feldspar of the granophyres of the Rashoop Granophyre Suite, north of Pretoria (isotherms after Stormer, 1975).*

The above methods were also utilised to differentiate between the Blinkwater, the Sterk River and the Stavoren granophyre, but proved unsatisfactory.

5.4 GEOCHEMISTRY

To determine chemical similarities, 16 samples of the Sterk River granophyre and 10 of the Blinkwater granophyre (Table 5.5) were treated statistically. No samples of the Stavoren granophyre were analysed, due to small and weathered outcrops.

TABLE 5.5 : CHEMICAL AND NORMATIVE COMPOSITION OF THE RASHOOP GRANOPHYRE SUITE

Sample No.	72/20	72/12	72/9	73/60	73/30	72/10	72/46	72/42
SiO_2	74,18	74,12	74,02	73,00	72,00	74,00	75,70	74,60
TiO_2	0,29	0,27	0,26	0,28	0,30	0,26	0,24	0,26
Al_2O_3	12,33	12,16	11,75	11,80	11,90	11,60	11,60	11,50
Fe_2O_3	1,52	1,93	2,41	2,74	2,33	1,75	2,30	3,29
FeO	1,58	1,14	1,28	1,40	2,10	1,80	0,90	0,60
MnO	0,06	0,08	0,09	0,04	0,09	0,01	0,02	0,11
MgO	0,71	0,80	0,90	0,01	0,01	0,01	0,01	0,02
CaO	0,69	0,52	0,63	0,61	0,97	0,45	0,28	0,29
Na_2O	3,07	3,00	3,07	3,10	3,00	2,70	3,00	3,00
K_2O	5,01	5,19	5,02	5,11	5,46	5,40	5,19	5,52
H_2O^+	0,27	0,60	0,33	1,00	0,80	0,80	1,20	0,50
H_2O^-	0,19	0,14	0,15	0,30	0,20	0,20	0,10	0,30
P_2O_5	0,02	0,02	0,03	0,15	0,03	0,04	0,04	0,03
CO_2	0,20	0,22	0,11	0,10	0,10	0,40	0,10	0,60
ZrO_2	540	490	450	660	740	520	480	550
Ni	20	15	15	120	125	250	210	260
BaO	1 370	1 320	1 280	1 280	1 090	1 020	810	990
SrO	65	45	75	57	69	46	34	50
Rb_2O	210	200	200	200	195	210	210	200
TOTAL	100,34	100,40	100,25	99,87	99,51	99,62	100,85	100,82
Qtz	34,32	34,46	34,13	33,56	30,84	36,17	36,39	34,11
Cor	1,55	1,65	0,77	1,05	-0,11	1,49	1,18	0,66
Zir	0,05	0,05	0,05	0,07	0,07	0,05	0,05	0,06
Or	27,24	28,97	27,81	31,06	31,96	32,01	31,49	33,31
Ab	28,09	27,51	28,17	28,91	27,99	25,17	27,68	27,55
An	1,30	0,36	1,60	0,70	3,26	–	–	–
Bi	4,68	3,75	3,99	0,48	2,49	1,79	0,04	0,08
Hm	–	–	–	–	–	–	0,23	1,56
Mt	1,62	2,06	2,58	2,98	2,53	1,90	2,12	1,18
Il	–	–	–	–	–	0,38	0,08	0,37
Tn	0,62	0,58	0,56	0,61	0,65	–	0,40	–
Cc	0,52	0,57	0,28	0,26	0,26	1,00	0,26	0,66
Ap	0,04	0,04	0,06	0,33	0,07	–	0,09	–
DI	91,23	92,64	90,93	94,64	90,74	94,87	96,79	95,68

Sample No.	72/40	73/28	73/21	73/52	73/86	72/36	72/186	72/195	73/9
SiO_2	74,20	72,50	76,00	71,30	73,60	73,90	72,00	73,90	73,60
TiO_2	0,25	0,28	0,27	0,36	0,30	0,25	0,32	0,27	0,30
Al_2O_3	11,50	12,20	11,70	11,90	11,70	11,50	11,90	11,90	11,80
Fe_2O_3	2,05	1,72	2,06	3,86	2,03	1,91	2,85	2,04	2,16
FeO	1,60	2,00	0,40	1,60	2,30	2,00	2,00	1,70	1,60
MnO	0,03	0,06	0,02	0,08	0,06	0,06	0,10	0,05	0,09
MgO	0,01	0,01	0,10	0,10	0,10	0,10	0,01	0,01	0,20
CaO	0,56	0,76	0,71	0,71	0,90	0,67	0,75	0,43	0,49
Na_2O	3,20	2,80	3,10	3,00	2,80	3,40	3,40	3,20	4,20
K_2O	5,58	5,68	4,68	5,41	5,24	5,10	4,96	5,22	4,37
H_2O^+	0,40	0,70	0,50	0,70	0,80	0,60	0,60	0,60	0,50
H_2O^-	0,10	0,10	0,20	0,20	0,20	0,20	0,20	0,20	0,20
P_2O_5	0,04	0,04	0,03	0,03	0,05	0,04	0,04	0,05	0,03
CO_2	0,20	0,04	0,10	0,40	0,20	0,30	0,40	0,10	0,20
ZrO_2	500	680	340	820	580	520	790	630	640
Ni	250	135	130	175	100	280	115	120	130
BaO	1 040	1 130	770	900	1 040	1 130	940	1 220	940
SrO	38	60	12	60	37	57	40	49	49
Rb_2O	240	200	400	210	210	175	200	210	130
TOTAL	99,93	99,20	99,97	100,77	100,48	100,25	99,74	99,89	99,93
Qtz	32,12	31,95	37,21	31,62	34,55	32,50	31,53	33,31	30,43
Cor	-0,01	0,61	0,94	1,26	0,77	0,23	1,06	0,92	0,14
Zir	0,05	0,07	0,03	0,08	0,06	0,05	0,08	0,06	0,06
Or	32,84	33,14	28,44	33,14	29,99	29,28	29,13	30,65	24,94
Ab	29,49	26,15	28,66	27,95	25,95	31,34	31,52	29,62	38,52
An	0,58	2,58	1,96	–	2,08	0,51	–	0,47	0,09
Bi	1,60	2,82	0,04	0,04	3,14	2,65	1,79	1,83	2,29
Hm	–	–	0,79	0,18	–	–	–	–	–
Mt	2,20	1,87	1,03	3,92	2,19	2,05	3,08	2,20	2,31
Il	–	–	–	0,12	–	–	–	–	–
Tn	0,54	0,61	0,58	0,60	0,65	0,54	0,68	0,58	0,64
Cc	0,52	0,11	0,26	1,05	0,52	0,78	1,04	0,26	0,52
Ap	0,09	0,09	0,07	0,07	0,11	0,09	0,09	0,11	0,06
DI	94,48	91,92	95,28	94,03	91,31	93,40	93,31	94,55	94,09

Sample No.	73/10	73/17	73/16	73/15	73/14	73/13	73/4	73/3	73/31
SiO_2	73,50	72,00	73,60	73,50	72,40	72,30	74,90	74,70	73,30
TiO_2	0,37	0,33	0,29	0,30	0,31	0,35	0,33	0,31	0,32
Al_2O_3	11,70	11,70	11,60	11,70	11,60	11,40	11,30	11,80	11,30
Fe_2O_3	2,85	1,56	1,77	2,49	2,07	2,70	3,23	1,57	2,54
FeO	1,50	3,30	2,30	2,10	2,40	2,50	1,00	1,60	2,00
MnO	0,03	0,05	0,05	0,04	0,02	0,09	0,04	0,01	0,08
MgO	0,10	0,10	0,10	0,10	0,10	0,10	0,10	0,10	0,10
CaO	0,13	1,52	1,03	0,46	1,07	0,14	0,29	0,27	0,64
Na_2O	4,10	2,90	3,00	2,70	2,90	2,70	3,20	3,20	2,90
K_2O	3,77	5,15	5,18	5,23	5,37	5,50	4,51	4,93	5,27
H_2O^+	0,80	0,80	0,60	0,90	0,80	0,90	0,80	0,50	0,70
H_2O^-	0,30	0,20	0,10	0,10	0,20	0,20	0,30	0,20	0,10
P_2O_5	0,02	0,05	0,04	0,03	0,04	0,05	0,04	0,03	0,03
CO_2	0,40	0,40	0,20	0,20	0,20	0,30	0,20	0,10	0,10
ZrO_2	650	600	560	600	540	620	610	590	860
Ni	270	120	10	110	100	135	110	110	58
BaO	880	1 110	1 080	1 050	1 490	1 400	1 020	1 070	1 090
SrO	34	64	65	45	66	52	63	62	67
Rb_2O	182	185	175	200	195	200	165	175	185
TOTAL	99,76	100,27	100,05	100,05	99,72	100,27	100,44	99,52	99,61
Qtz	33,62	32,05	33,27	36,05	31,94	32,76	37,28	35,43	34,02
Cor	0,99	-0,02	0,05	1,81	-0,32	0,11	1,30	1,35	0,34
Zir	0,07	0,06	0,06	0,06	0,05	0,06	0,06	0,06	0,08
Or	22,73	27,60	29,21	30,43	27,66	31,52	27,27	28,75	30,84
Ab	37,96	26,86	27,74	25,14	26,96	25,08	29,67	29,67	27,05
An	–	3,86	2,86	–	3,77	2,55	–	–	1,49
Bi	0,38	6,04	3,69	2,58	8,31	3,34	0,38	2,12	2,40
Hm	0,09	–	–	–	–	–	1,08	–	–
Mt	2,94	1,68	1,91	2,70	0,78	2,92	1,87	1,70	2,76
Il	0,50	–	–	0,10	–	–	0,44	0,15	–
Tn	–	0,71	0,62	0,64	0,26	0,76	0,06	0,44	0,70
Cc	0,33	1,04	0,52	0,53	0,52	0,79	0,52	0,26	0,26
Ap	–	0,11	0,09	0,07	0,87	0,11	0,09	0,07	0,07
DI	95,36	86,56	90,32	93,49	86,28	89,54	95,57	95,26	92,34

72/20	Sterk River granophyre from Prins Anna 234 JR
72/12	Sterk River granophyre from Enkeldoornoog 219 JR
72/9	Sterk River granophyre from Varkfontein 241 JR
73/60	Sterk River granophyre from Welgevonden 124 JR
72/10	Sterk River granophyre from Fairfield 238 JR
72/46	Sterk River granophyre from Zustershoek 246 JR
72/42	Sterk River granophyre from Zandspruit 189 JR
72/40	Sterk River granophyre from Boekenhoutfontein 198 JR
73/28	Blinkwater granophyre from Vastfontein 271 JR
73/21	Sterk River granophyre from Uitvlugt 79 JR
73/52	Sterk River granophyre from Rooibank 89 JR
73/86	Sterk River granophyre from Klipdrift 121 JR
72/36	Sterk River granophyre from Prins Anna 234 JR
72/186	Sterk River granophyre from Leeuwfontein 248 JR
72/195	Sterk River granophyre from Gemsbokfontein 199 JR
73/9	Sterk River granophyre from Rondefontein 84 JR
73/10	Blinkwater granophyre from Bultfontein 107 JR
73/17	Blinkwater granophyre from Nooitgedacht 256 JR
73/16	Blinkwater granophyre from Tyne 250 JQ
73/15	Blinkwater granophyre from Klipgat 249 JQ
73/14	Blinkwater granophyre from Rietgat 105 JR
73/13	Blinkwater granophyre from Rietgat 105 JR
73/4	Blinkwater granophyre from Boekenhoutfontein 261 JR
73/3	Blinkwater granophyre from Boekenhoutfontein 261 JR
73/31	Blinkwater granophyre from Bultfontein 107 JR

The chemical data in Table 5.5 do not reveal any major differences between the various granophyres. Variation diagrams were therefore utilised to discriminate between these rocks. A normative quartz-albite-orthoclase ternary diagram (Fig. 5.8) reveals no significant difference in the normative composition of the two types of granophyre. It does, however, show a concentration of points around the ternary minimum (m), suggesting that the $P_{(H_2O)}$ was between 500 and 5 000 bars at the time of crystallization of the granophyre.

An AFM-diagram indicates a spread along the Alk-FeO axis with very low MgO values (Fig. 5.9). From this diagram it is evident that the magma, from which the granophyre originated, changed composition along the well established tholeiitic trend. The samples from the different granophyre types, however, overlap to a large extent and no differentiation between the various granophyre types can be observed. The diagram also illustrates the relative position of the granophyre along the tholeiitic trend. It can be seen that the granophyre plots further along the line and may represent the late stage magmatic products of the magma that formed the extrusives of the Rooiberg Group.

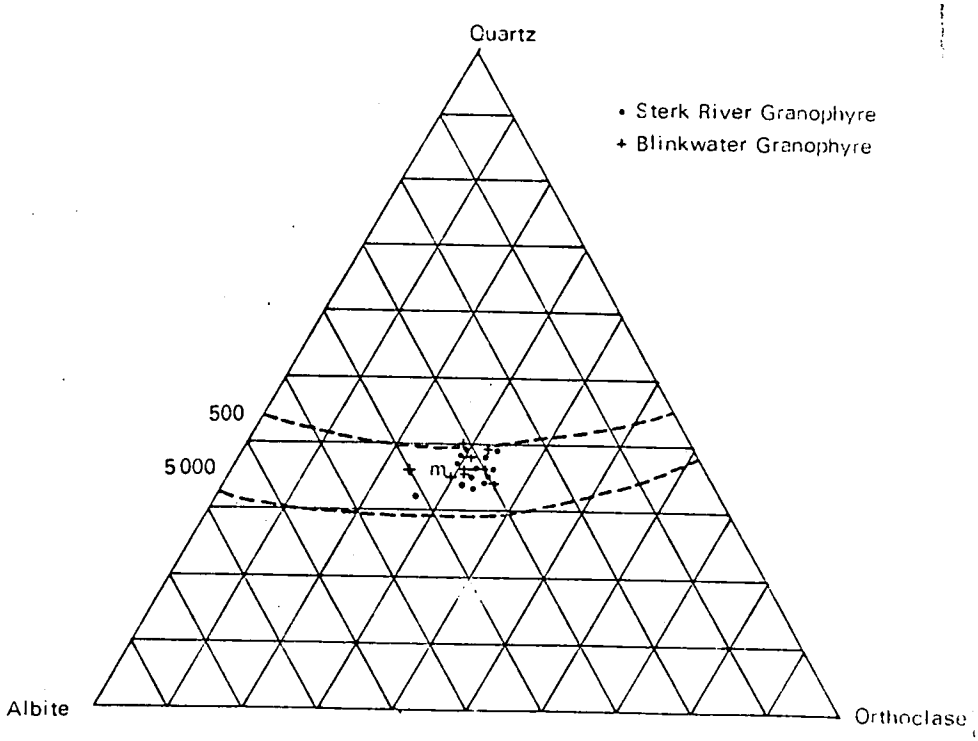

Fig. 5.8. Normative ternary diagram of the granophyres of the Rashoop Granophyre Suite, north of Pretoria (isobars after Tuttle and Bowen, 1958).

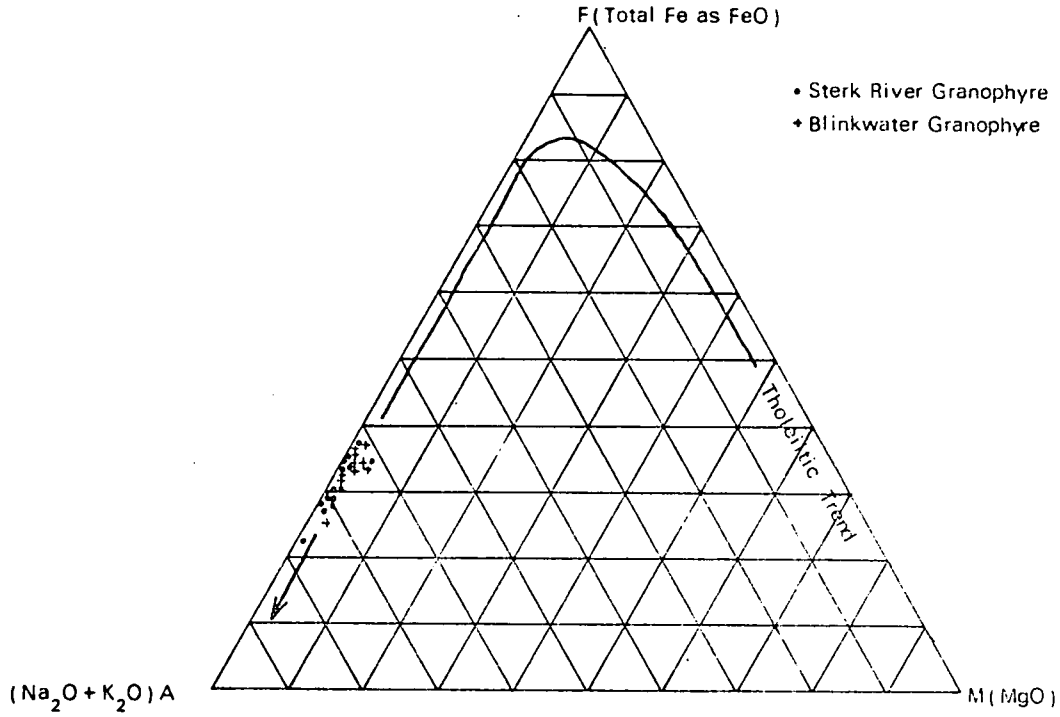

Fig. 5.9. *AFM-diagram of the granophyres of the Rashoop Granophyre Suite and the felsites of the Rooiberg Group, north of Pretoria (tholeiitic trend after Nockolds and Allen, 1954, 1956).*

The change in the chemical composition during the formation of the granophyre is further illustrated when the differentiation index (DI) is plotted against SiO_2 (Fig. 5.10). This diagram illustrates the general differentiation trend that prevailed during the formation of the granophyres. The positive correlation between SiO_2 content and DI indicates a normal differentiation trend.

A plot of DI against formational temperatures (Fig. 5.11), shows that the granophyre crystallized at temperatures between 500°C and 600°C, which is in agreement with the temperature minimum in the quartz-albite-orthoclase diagram (Fig. 5.8) and the temperature of eutectic crystallization.

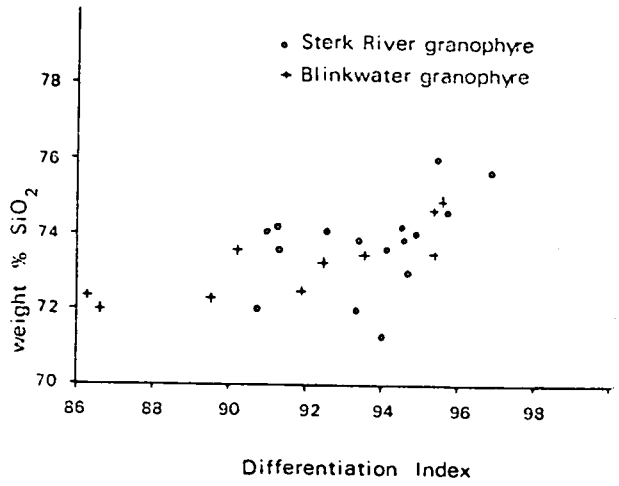

Fig. 5.10. Plot of SiO_2 against differentiation index of the granophyres of the Rashoop Granophyre Suite, north of Pretoria.

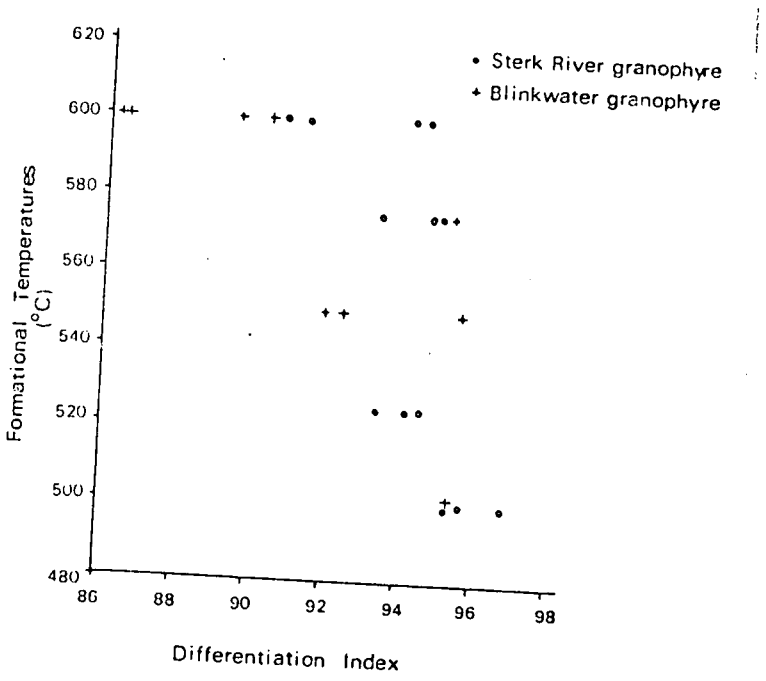

Fig. 5.11. Plot of formational temperatures against the differentiation indices of the granophyres of the Rashoop Granophyre Suite, north of Pretoria.

The similarity in the chemical composition between the Sterk River and the Blinkwater granophyre, as illustrated by the chemical data and the various diagrams used in this investigation, suggests that the two types formed at different stratigraphic positions, but had a common source and origin.

The chemical variation diagrams, as well as the size distribution of the plagioclase phenocrysts, are indicative of physiochemical changes in the parental magma during the formation of the granophyre; all the granophyres have the same source magma as no differentiation from the one to the other can be observed. The granophyre probably represents the microcrystalline product of a fast crystallizing granitic magma against cooler roof-rocks of Rooiberg felsite or Transvaal sediments. Walraven (1979), however, regards the granophyre and the Rooiberg felsite as being co-magmatic. The granophyre most probably formed as a product of eutectic crystallization; this is indicated by the clustering of points around m, which is the ternary minimum (Fig. 5.8).

5.5 CONCLUSIONS

Although three different types of granophyre, based on their field relationships with the underlying and overlying rock types, can be distinguished in the study area, modal, textural and chemical methods failed to produce any reliable method to distinguish between these granophyres.

The chemical variation diagrams, as well as the size distribution of the plagioclase phenocrysts, indicate a chemical change of the parental magma during the formation of the granophyre, but no differentiation from the one into the other can be observed and thus have the same source magma. The granophyre probably represents the microcrystalline product of a fast crystallizing granitic magma against cooler roof-rocks of Rooiberg felsite or Transvaal sediments. The correspondence between the chemical position of the granophyre and that of the ternary minimum on the QAO-diagram (Fig. 5.8) indicate that the granophyre most probably formed as products of eutectic crystallization.

6 LEBOWA GRANITE SUITE

6.1 INTRODUCTION

The granites of the Bushveld Complex have been investigated by many workers, but it was Molengraaff(1901) who first identified and described the 'Red Bushveld' granite and introduced the term 'Plutonic Series of the Bushveld' which he regarded as an event subsequent to the development of the Pretoria Series, but predating the Karoo. Molengraaff (1905) also described the structure of the Bushveld as a deroofed laccolith in which a large number of zones can be recognized.

Hall (1906), for the first time, used the term Bushveld Granite, but later he also reverted to the older and probably more widely accepted term of Red Granite (Hall, 1909). This name was adapted and used by many investigators such as Baring-Horwood (1909), Hatch and Corstorphine (1909), Mellor (1906), Merensky (1909), Kynaston and Mellor (1905) and Lombaard (1931), until Strauss and Truter (1944) and Strauss (1955) called it the Main Granite. These authors also recognized and described the Bobbejaankop Granite and the Foothills Granite in the Potgietersrust area for the first time (Strauss, 1955).

The difference between the Main Granite in the eastern and western parts of the Bushveld Complex led authors like Lenthall (1972a, 1972b), Hunter (1972) and De Waal (1972b) and others to rename the granites of the eastern part to the Sekhukhuni granite, while De Waal (1972b) used the term Veekraal granite for the occurrences in the west. Walraven (1977) found that the Veekraal granite occurs in the same stratigraphic position as the Sekhukhuni granite in the east, thus making it the possible equivalent of the Sekhukhuni granite defined by Lenthall (1972a).

As geochronological data on the various granites became available, the age relationships between the granites became known, enabling Coertze *et al* (1978) to subdivide the acid portion of the complex into three major types (Table 6.1). He referred to the granites collectively as the Lebowa Granite Suite, consisting of the Nebo Granite, including the Veekraal, Sekhukhuni

and Steelpoort Park granites, a number of younger granites of which the Makhutso Granite is formally recognized as a separate entity and the even younger Klipkloof and Bobbejaankop granites. The Bobbejaankop granite, which was recognized as such in the Zaaiplaats area (Strauss and Truter, 1944; Strauss, 1955) is now referred to as the Klipvoor granite in other parts of the complex, while the name Bobbejaankop granite is reserved for the Potgietersrust area only. Strauss (1947) correlated various granites, for instance the occurrences at Mutue Fides, with the Bobbejaankop granite, but the name Klipvoor is now also used for those localities.

TABLE 6.1. SUBDIVISION OF THE LEBOWA GRANITE SUITE (after Coertze *et al*, 1978).

LEBOWA GRANITE SUITE

NEBO GRANITE

Veekraal granite*
Sekhukhuni granite*
Steelpoort Park granite*

MAKHUTSO GRANITE

(including Magnet Heights granite)
Klipkloof granite*
Bobbejaankop granite*
(including the Klipvoor granite* and other granites resembling the Bobbejaankop granite*). An asterisk indicates an informal name.

Uranium/lead isotope studies point out that the Nebo Granite is the oldest member of the granite suite, with an age of 1 920 m.y., while the Klipkloof granite yields ages of approximately 1 400 m.y. (Coertze *et al*, 1978).

6.2 GEOGRAPHICAL DISTRIBUTION AND GENERAL DESCRIPTION

The geographical distribution of the various granite types within the study area are shown on Figure 6.1. From the map it can be seen that the Nebo Granite forms the dominant type, while smaller plugs, sheets and dykes of Makhutso Granite, Klipvoor- and Klipkloof granite intrude the older Nebo Granite.

6.2.1 Nebo Granite

The Nebo Granite Suite (Table 6.1) includes a number of granites, based on their general character and geographical distribution. The Nebo Granite in the study area comprises of the Sekhukhuni granite and its marginal roof facies, the Verena granite.

6.2.1.1 Sekhukhuni granite

The Sekhukhuni granite has a wide distribution in the study area, as illustrated in Folder I and Figure 6.1. The granites occur as undulating, sheet-like bodies with regional cross-cutting relationships with the overlying rock units as can be seen on the map. Wagner (1921) described non-intrusive relationships with the overlying granophyre, while Lombaard (1931) reported intrusive contacts of this granite with the overlying rocks in the area to the east of the study area.

(a) Contact relationships

A transition from granite to granophyric granite into granophyre marks the upper contact of the Sekhukhuni granite. A similar relationship was noticed by Wagner (1921) in the Mutue Fides area. Lombaard (1931) reported a transition from granite to granite porphyry to granophyre in the Moos River area. He also pointed out that the granite porphyry forms part of the granite, rather than the granophyre. Lenthall (1975) mentioned the presence of an aplitic granite between the granophyre and the granophyric

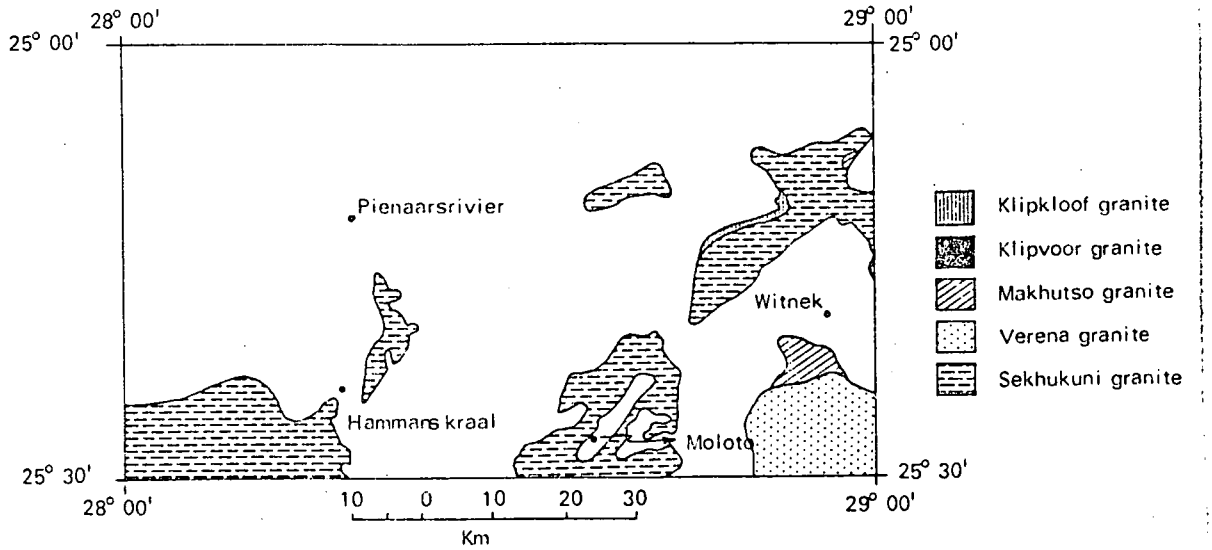

Fig. 6.1. Geographical distribution of the different granite types in the study area.

granite, a feature also noticed by Kynaston (1909). The presence of the aplitic granite was interpreted as an indication of the intrusive nature of the granite by Kynaston (1909). Lombaard (1931) described the aplitic granite as a granite porphyry, representing a marginal phase of the Sekhukhuni granite. The interpretation given by Lombaard (1931) also seems to be valid for the granites in the study area and, therefore, the granite porphyry was not mapped as a separate entity.

Porphyritic granite, similar in general appearance to the Verena granite, occurs along the felsite/granite contact, especially where the granophyre is not developed. Lombaard (1931) initially described these contact relationships in the present study area, while Hall (1932) described similar features in the area around Warmbad.

Where granophyre does occur between the Rooiberg felsite and the underlying Sekhukhuni granite the contact is gradational, with the granophyre gradually becoming coarser grained, while the granite contains micropegmatite textures. The latter becomes more pronounced until the rock becomes predominantly granophyric. Due to the transitional nature, the

exact position of the granite/granophyre-contact is difficult to establish in the field. It was, therefore, decided to use the first appearance of coarse-grained feldspar and quartz, not in the form of micropegmatite, as the contact between the granophyre and the granophyric granite. For practical reasons the granite and the granophyric granite are considered as part of the same unit in this study.

(b) Macroscopic description

The Sekhukhuni granite in the study area forms large, smooth, flat, domal, often well jointed outcrops, while large boulders, showing well developed exfoliation, are also frequently present. Similar outcrops can also be seen in the Potgietersrus area where the Main Granite (Strauss, 1955) crops out. Tors are developed on the farm Enkeldoorn 217 JR in the study area.

The colour of the Sekhukhuni granite varies from red to pale red to grey. The colour is the result of the colouration of the feldspar and the relative scarcity of ferromagnesian minerals. Certain patches, where the rock is extremely dark red, are scattered throughout the region. A good example of such a colour change can be seen on the farm Enkeldoorn 217 JR and also at Hammanskraal. The Sekhukhuni granite in the Dennilton area, as well as in the vicinity of the Albert Silver Mine, is usually grey; the porphyritic varieties are usually pinkish.

Lenthall (1975) found that the red colouration in the granite increases where mineralization has taken place and where aplite intersects the granite. Aplite, which represents the aplitic phase of the Sekhukhuni granite, also intrudes the granites in the study area. They frequently appear as deeply coloured red veins and dykes and often exhibit mairolitic textures. The width ranges between a few centimetres to almost a metre and due to positive weathering they often form small ridges on weathered surfaces (Fig. 6.2).

Fig. 6.2. Aplite dyke intersecting the Sekhukhuni granite on Klipplaat-drift 193 JR. Note the positive weathering of the aplite dyke.

(c) Petrographic description

The Sekhukhuni granite consists of orthoclase, plagioclase and quartz in order of abundance, with subordinate biotite and hornblende and accessory zircon, fluorite and ore.

The orthoclase is anhedral to euhedral and ranges from fine to coarse-grained (1–3 mm). Compositionally it falls within the region $Or_{75}Ab_{25}$ to $Or_{60}Ab_{40}$, corresponding to the maximum microcline-low albite series (Wright, 1968). The pink colour of the K-feldspar is due mainly to the concentration along crystal planes of iron in the form of hematite, as well as the fact that iron is incorporated into the original feldspar molecule (Strauss, 1955).

Subhedral to euhedral plagioclase, which does not display the same amount of alteration as the orthoclase, ranges from An_5 to An_{20}, thus corresponding

to albite or sodic oligoclase. Plagioclase also occurs as perthitic intergrowths with orthoclase. Strauss (1955) noted that orthoclase and plagioclase are usually intimately intergrown. This is clearly illustrated by the high albite content of the orthoclase, which was recorded in feldspar studies before homogenization by heat treatment (Appendix I).

Quartz generally displays an anhedral character, although a few euhedral crystals do occur. The anhedral quartz indicates that it crystallized after the feldspar, thus filling the voids between the latter.

Biotite, which is often altered to green chlorite, forms the dominant mafic constituent, while hornblende is also present in a few samples. According to Hall (1932), however, hornblende is the dominant femic mineral of the Main Bushveld Granite. Strauss (1955) stated that the mafic constituents change from hornblende to biotite from the bottom upwards. It can thus be inferred that the granite of the study area represents rocks near the top of the succession. MacCaskie (personal communication) subdivided the Sekhukhuni granite into hornblende and biotite-bearing types, but this classification was never accepted officially. Euhedral, fine-grained zircon is often poikilitically enclosed by biotite. The zircon content of the granite varies considerably and at Enkeldoorn 217 JR is markedly higher. The zircons are cracked, with the result that they could not be recovered intact for a length/breadth correlation as conducted by Leith and Rhodes (1971) on the granites in the Mapomulo area in Natal. Fluorite occurs with zircon in the granite at Enkeldoorn 217 JR, but is not common in the rest of the mapped area.

(d) Textural and modal analysis

The granite varies from fine to coarse-grained, while porphyritic varieties are locally developed near the upper contact. A plot of whole rock index (WRI) against the porphyritic index (PI) (Appendix III), indicates that the PI increases with a corresponding increase in WRI (Fig. 6:3). Since the mean grain size and the WRI are inversely related (Appendix III), it can be deducted that during crystallization the grain size of the matrix rapidly reduced with increase in phenocryst dimensions in the rock.

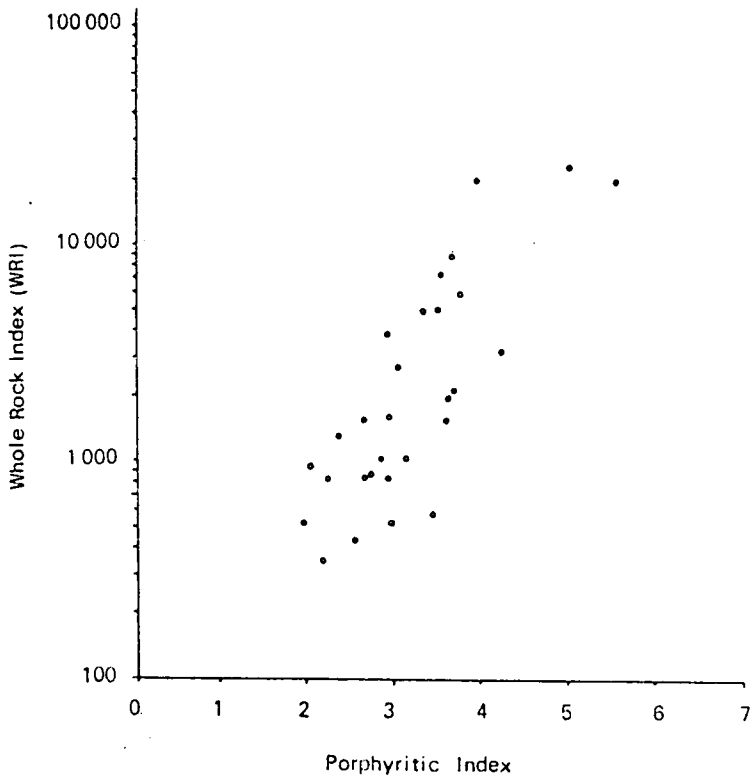

Fig. 6.3. Plot of whole rock index against porphyritic index of the Sekhukhuni granite.

Modal analysis of the granite was conducted according to the method described in Appendix II. These analyses indicate that the granite, on average, consists of 27 per cent quartz, 28 per cent K-feldspar, 30 per cent plagioclase (An_{5-20}), 10 per cent biotite and 2 per cent hornblende. Mafic-free mineral compositions are given in Table 6.2. A quartz-alkali feldspar-plagioclase diagram indicates that the Sekhukhuni granite falls within the 3b-granite field of Streckeisen (Fig. 6.4).

TABLE 6.2 : PLAGIOCLASE, ALKALI FELDSPAR AND MAFIC-FREE MODAL COMPOSITION OF THE SEKHUKHUNI GRANITE AND THE TEXTURAL PARAMETERS

Sample Number	1	2	3	4	5	6	7	8	9
72/7	13	28	28	27	30	0,87	3,14	1516	3,60
72/28	12	29	28	33	31	0,55	2,07	5913	3,74
72/29	12	33	28	33	31	0,36	1,78	22291	5,01
72/31	14	25	23	33	25	0,80	2,90	1985	3,64
72/33	12	25	27	28	31	0,49	1,79	8731	3,68
72/38a	7	25	26	30	32	1,41	3,07	354	2,17
72/89	14	29	28	24	28	1,23	3,68	536	2,99
72/51	13	29	26	29	29	1,04	2,84	882	2,73
72/52	10	15	20	27	24	1,01	2,05	970	2,03
72/53	14	38	29	28	31	0,79	2,90	2062	3,69
72/85	11	37	26	28	30	0,98	2,79	1075	2,86
72/83	12	20	26	28	34	1,31	3,34	442	2,55
72/144	8	15	30	31	35	0,91	2,18	1314	2,38
72/138	7	15	31	29	33	0,59	1,94	4913	3,30
72/134	11	22	28	31	32	0,72	2,19	2723	3,06
72/105	10	15	27	24	35	0,52	1,83	7175	3,53
72/104	14	30	26	27	30	0,64	1,86	3835	2,92
72/103	10	29	28	25	30	0,37	2,08	19360	5,58
72/101	12	30	27	23	25	0,37	1,46	19805	3,96
72/155	10	30	31	30	30	1,05	3,06	854	2,90
72/280	12	25	24	28	26	0,86	2,29	1568	2,66
72/146	8	16	29	30	36	1,05	2,83	854	2,68
72/82	9	17	29	28	32	0,68	2,89	3152	4,24
72/128	7	32	28	30	32	0,86	2,55	1586	2,97
72/107	13	25	26	25	25	1,05	2,37	854	2,24
72/104	12	22	23	24	27	1,20	4,06	586	3,40
72/107a	10	15	30	33	35	0,99	3,07	1045	3,12
72/126	8	29	27	20	35				
72/164	13	29	26	20	33				
72/145	8	29	29	23	27				

Sample Number	1	2	3	4	5	6	7	8	9
72/281	10	32	31	18	27				
72/127	12	29	27	27	27				
73/49	11	32	34	25	30				
73/40	10	32	30	23	36				
72/100	12	25	23	25	20				
72/115	8	26	24	20	28				
73/48	5	29	31	29	29				
73/11	10	17	28	34	35				
73/50	20	29	30	28	32				
72/131	9	15	25	24	29				
72/32	15	20	31	25	25				
72/217	10	15	31	35	32				
72/51	13	29	26	29	29				
72/112	13	37	24	29	17				
73/18	10	27	23	29	31				
73/48	7	37	27	32	34				
72/84	11	37	26	28	30				
72/114	10	29	34	29	35				
72/39	14	29	30	32	33				
72/53	14	38	29	28	31				
73/20	10	29	30	33	30				
73/51	15	38	27	30	32				
72/30	12	29	28	33	31				

1 = Weight percent anorthite in plagioclase

2 = Weight percent albite in alkali feldspar

3 = Weight percent quartz in sample

4 = Weight percent orthoclase in sample

5 = Weight percent plagioclase in sample

6 = Mean calculated diameter of grains in sample

7 = Mean diameter of ten largest grains in sample

8 = Whole Rock Index

9 = Porphyritic Index

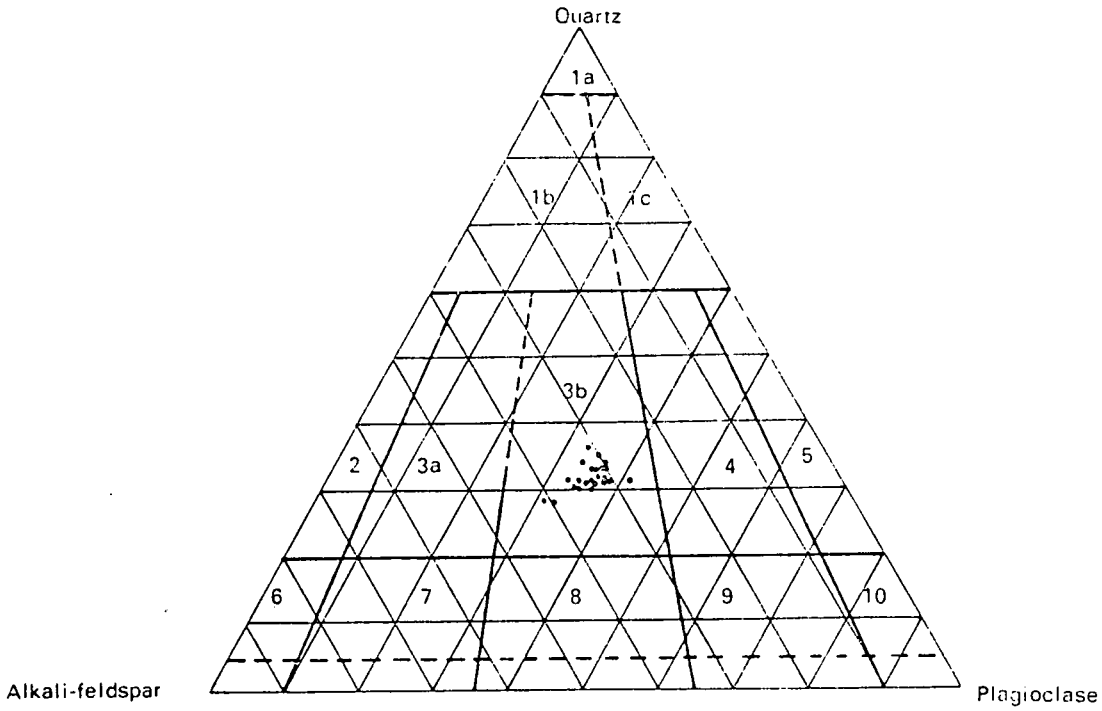

Fig. 6.4. QAP-diagram of the Sekhukhuni granite (diagram after Streckeisen, 1967).

It is also clear that the Sekhukhuni granite falls within the thermal trough between 500 and 5 000 bar, as defined by Tuttle and Bowen (1958), and that crystallization on this granite took place near the eutectic point (Fig. 6.5, diagram after Tuttle and Bowen, 1958).

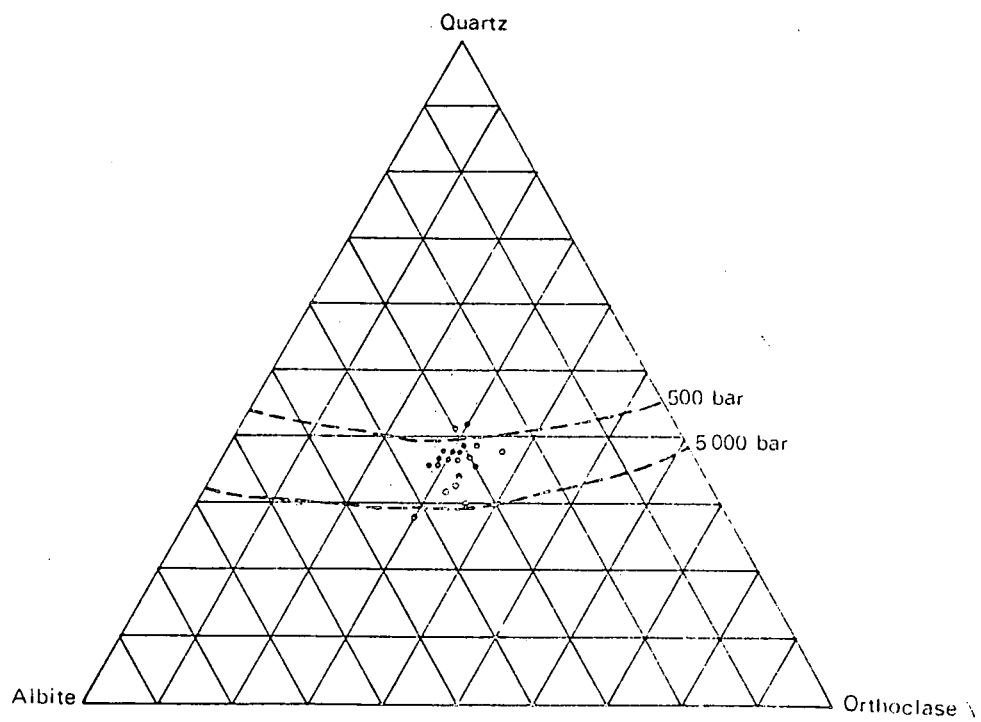

Fig. 6.5. Ternary diagram indicating the possible formational pressures of the Sekhukhuni granite (isobars after Tuttle and Bowen, 1958).

6.2.1.2 Verena granite

(a) General description

The Verena granite is well developed in the area west of the Verena hamlet, between Groblersdal and Bronkhorstspruit (Fig. 6.1). It is a porphyritic granite with large phenocrysts of K-feldspar in an equigranular groundmass.

Walraven (1977) reported the presence of a porphyritic granite between the Veekraal granite and the upper contact with the roof-rocks in the western part of the complex. A similar granite was described by Lombaard (1931), while Van Zijl (1965) recognized a porphyritic granite grading into coarse-grained varieties near the Albert Silver mine in the Bronkhorstspruit district. This may indicate that the Verena granite represents the roof facies of the Sekhukhuni granite in this area.

The intrusive relationship of this granite with the roof-rocks is revealed by the occurrence of a large number of leptitic xenoliths in the granite (Fig. 6.6), thus indicating magmatic stoping of the roof-rocks during the emplacement of the granitic magma.

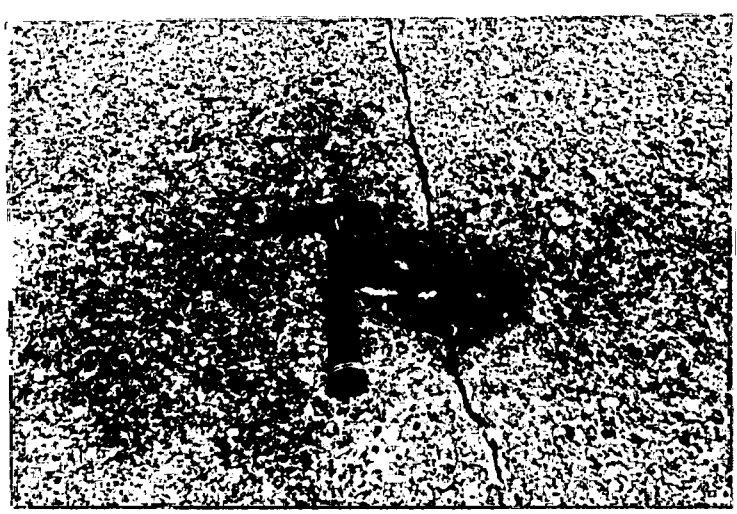

Fig. 6.6. Rounded leptite xenolith in the Verena granite on Wolvengaaten 255 JR.

(b) Macroscopic description

The outcrops of Verena granite are marked by numerous boulders displaying rough weathered surfaces. It also displays a very prominent jointing pattern which gives rise to tor-like outcrops which formed according to the process, described by Linton (1955) and Small (1972).

Aplite veins and dykes, ranging from a few centimetres to a metre in width, show cross-cutting relationships with the granite. The aplitic dykes frequently display miarolitic textures, very similar to the dykes in the Sekhukhuni granite.

The granite reveals no directional fabric, as determined by an aerial plot of the long axis directions of the phenocrysts possessing a 3 to 1 axial ratio. Van Zijl (1965) also mentioned the lack of structural features in this granite.

(c) Microscopic description

The Verena granite consists of K-feldspar phenocrysts in a groundmass of plagioclase, K-feldspar, quartz, biotite and hornblende with apatite, zircon and ore as accessory minerals. The K-feldspar phenocrysts are usually euhedral and very coarse-grained and are highly altered to sericite, making microscopic identification and investigation extremely difficult. Occasionally relatively fresh cores, surrounded by highly altered rims, can be seen under the microscope.

The plagioclase (An_{8-15}) normally occurs as medium-grained crystals in the groundmass. Alteration makes identification very difficult and often only remnants of plagioclase crystals can be seen in thin section.

Quartz forms interstitial material between the feldspar crystals. It is fine- to medium-grained, and usually anhedral.

Biotite is the dominant femic mineral, occurring as euhedral to subhedral crystals poikilitically enclosing small idiomorphic zircon. Hornblende,

showing considerable alteration to chlorite, is present as a subordinate mafic component. Apatite occurs as euhedral inclusions in the other minerals.

(d) Textural and modal analysis

The Verena granite is a very coarse-grained, porphyritic variety, with large K-feldspar phenocrysts. Due to the size of the phenocrysts, it was not possible to determine the whole rock and porphyritic indices. In hand-specimen, however, the phenocrysts vary between 3 to 5 cm in length and 1 to 1,5 cm in width.

The modal analyses were conducted according to the scheme described in Appendix II and the results are given in Table 6.3. The modal plagioclase were plotted against the modal orthoclase (Fig. 6.7) in order to test the validity of these analyses. It was found that the data correspond very well with that of Tuttle and Bowen (1958), indicating that the data fall within the expected range of accuracy.

TABLE 6.3. MAFIC-FREE MINERAL MODAL DATA OF THE VERENA GRANITE

Sample number	Qtz percentage	Or percentage	Ab percentage
72/227	31	35	33
72/228	29	25	32
72/242	32	31	32
72/251	31	34	33
72/252	33	31	34
72/234	32	31	34
72/220	35	29	34

All modal data are given in weight per cent of the component.

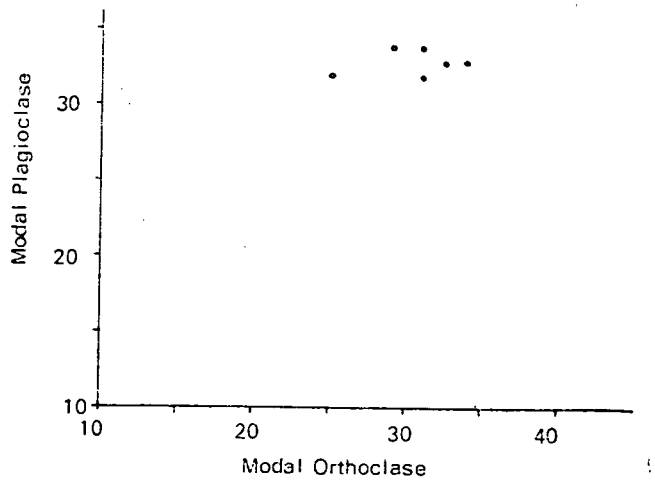

Fig. 6.7. Plot of modal plagioclase against modal orthoclase of the Verena granite.

A quartz-alkali feldspar-plagioclase diagram (Fig. 6.8) indicates that the Verena granite belongs to the 3b-granite of Streckeisen (1967).

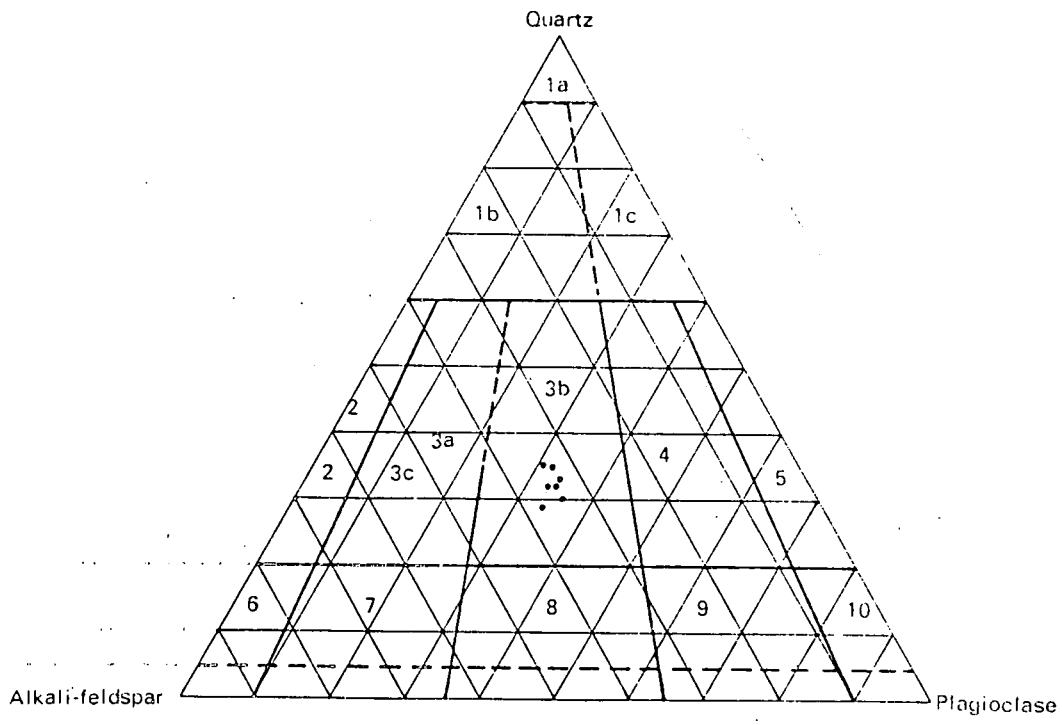

Fig. 6.8. QAP-diagram of the Verena granite (diagram after Streckeisen, 1967).

The same values also indicate that the Verena granite crystallized near the temperature minimum for pressures varying between 500 to 5 000 bars (Tuttle and Bowen, 1958) (Fig. 6.9).

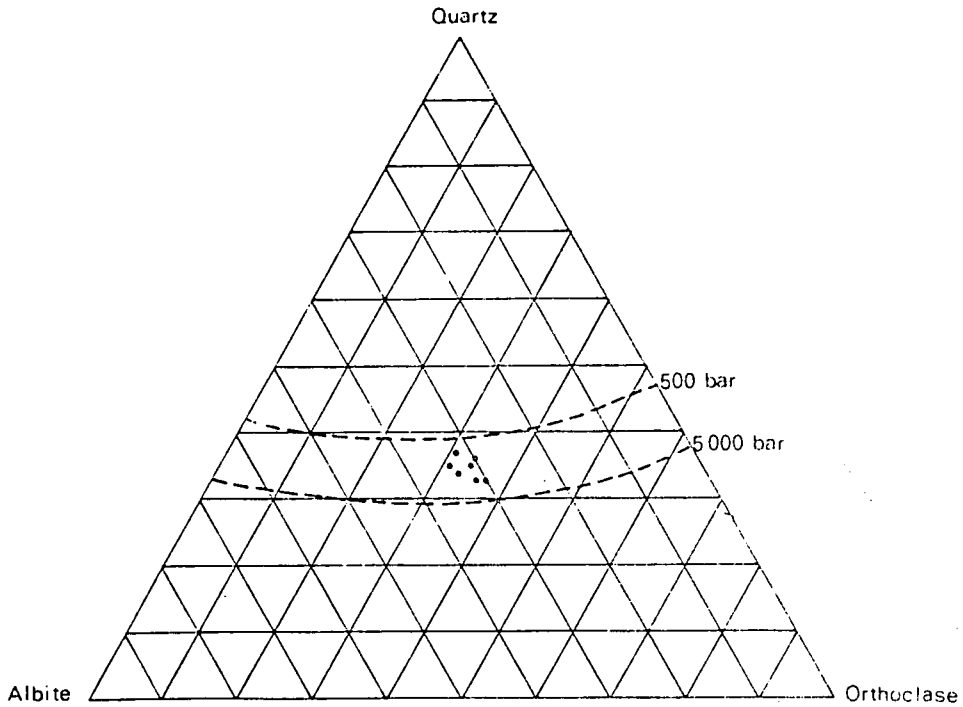

Fig. 6.9. Ternary diagram indicating the possible formational pressures of the Verena granite (isobars after Tuttle and Bowen, 1958).

A plot of Ab in plagioclase against Ab in alkali feldspar (Fig. 6.10) indicates that the possible formational temperatures fluctuated between 500°C and 580°C.

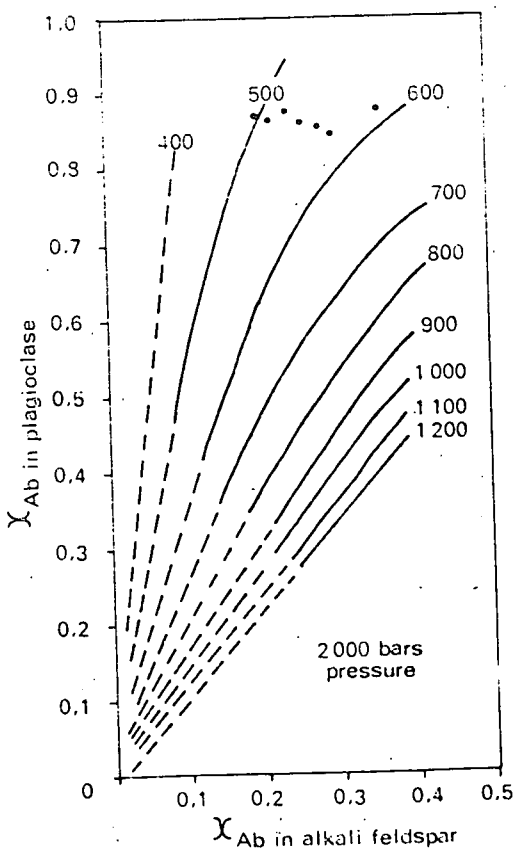

Fig. 6.10. Mole fraction albite in plagioclase against mole fraction albite in alkali feldspar of the Verena granite (isotherms after Stormer, 1975).

These temperatures are lower than those described for granite bodies by Von Platen (1965), Von Gruenewaldt (1972), Winkler (1976) and Whitney and Stormer (1976). Stormer (1975), however, calculates that an error of 30°C is possible when using a defocussed electron beam microprope. This error may be enhanced by the use of diffractometric methods. The presence of biotite may also indicate a greater oxygen fugacity (Whitney and Stormer, 1976), which would also lower the temperatures. The data are, however, comparable with that in section 5.3.

6.2.2 Makhutso Granite

(a) General description

This granite is named after the trading store on the farm Kameelrivier 160 JR and outcrops at two localities within this area (Fig. 6.1). It was first investigated and described by De Bruiyn and Rhodes (1975). The northern occurrence is partly covered by overlying Karoo sediments, while the southern one is better exposed. During the present investigation, only the latter was studied in detail.

The Makhutso Granite is characterized by the formation of tors. The granite is occasionally weathered, often displaying spheroidal structures, while sheet-like, domal outcrops are also present.

The southern occurrence of Makhutso Granite can be described as a boss-shaped body, a feature also commented on by Truter (1943), who mentioned its dome-shaped structure. Coertze *et al* (1978) also found a few dykes in the Sekhukhuni Plateau, which they describe as Makhutso Granite. This indicates that the mode of occurrence is not restricted to plutons only.

(b) Macroscopic description

The granite is a white to very light coloured, sometimes pinkish, rock and contains approximately 10 to 15 per cent femic minerals. The dominant femic mineral is biotite, which has been altered to chlorite. The granite becomes porphyritic towards the centre of the pluton; thus part of the pluton is also characterized by greenish-grey plagioclase.

The southern pluton has a marginal facies of white, fine-grained leucogranite. No contact between the marginal facies and the surrounding country rocks could be found. In one locality, on the farm Leeuwkop 228 JR, the Verena granite and the fine-grained Makhutso Granite outcrop within a few metres from one another, but the contact is obscured by alluvial deposits. Coertze *et al* (1978), however, describe intrusive relationships between the Makhutso Granite and the Sekhukhuni granite on the Sekhukhuni Plateau, indicating that the former is younger.

Inclusions of leptite are abundant in the granite of the southern pluton and on Hartebeestfontein 224 JR a large inclusion of leptite exhibits a mottled appearance. At the same locality the Makhutso Granite displays very sharp cross-cutting contact relationships with the leptite (Fig. 6.11). In other areas the granite does not contain large leptite inclusions, but smaller rounded xenoliths, similar to those in the Verena granite, are frequently present.

(c) Microscopic description

The Makhutso Granite consists of quartz, plagioclase, orthoclase, biotite and hornblende, with accessory minerals such as zircon, ore and sphene.

Orthoclase, which has the composition of $Or_{85}Ab_{15}$, shows perthitic intergrowths. The mineral is euhedral to subhedral and range between 1 and 2 mm in size. In contrast to the red K-feldspar in the Bobbejaankop granite, only white orthoclase is present in the Makhutso Granite.

Plagioclase, with a composition of An_{14}, forms fairly large euhedral crystals. Intergrowths with orthoclase are common.

Quartz generally occurs as interstitial anhedral to subhedral crystals.

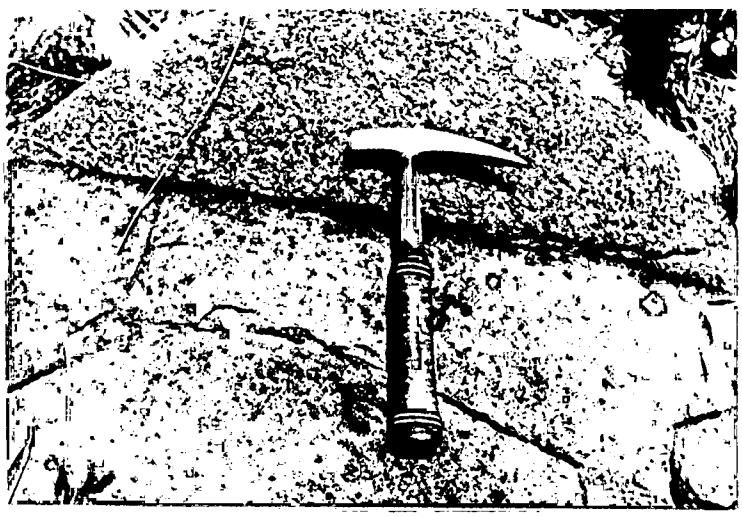

Fig. 6.11. Part of a lenticular body of leptite in the Makhutso Granite on Hartebeestfontein 224 JR.

(d) Textural and modal analysis

A textural analysis of this granite indicates that the whole rock index (WRI) varies between 600 and 3 000 and the porphyritic index (PI) between 1,14 and 3,19 (Table 6.4). This indicates that the grain size and phenocryst size distribution vary within reasonable limits within a single body of this granite. The relationship between the grain size and phenocryst size distribution is shown graphically on Figure 6.12. From the regression lines on this diagram it is evident that a general decrease in grain size (increase in WRI) is accompanied by a decrease in the value of PI, thus indicating an equigranular grain size distribution for the fine-grained facies of this rock.

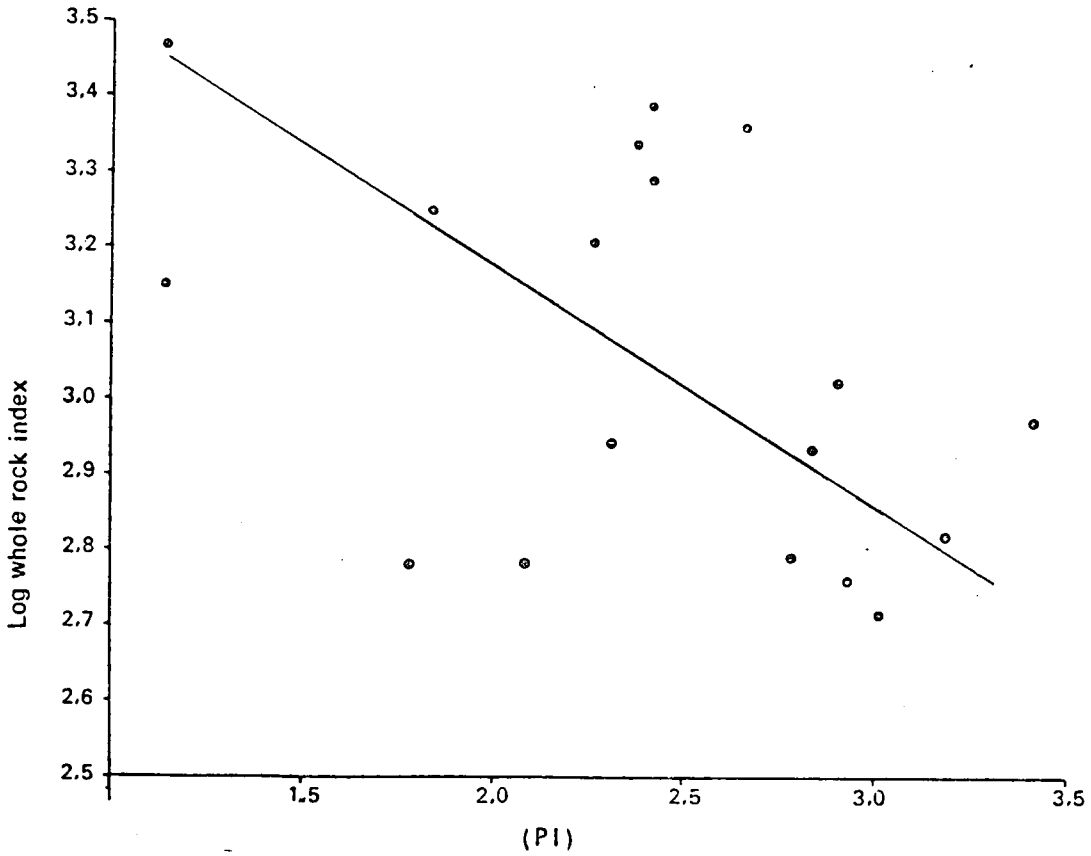

Fig. 6.12. Plot of log whole rock index against porphyritic index of the Makhutso Granite.

The average modal composition of this granite is 29 per cent quartz, 26 per cent orthoclase, 16 per cent plagioclase and 15 per cent mafic constituents (Table 6.4). When the modal felsic components of this granite (quartz-orthoclase-plagioclase) are plotted on the ternary diagram of Streckeisen (1967), it falls well within the 3b-field (Fig. 6.13).

This granite crystallized under P-T conditions (Fig. 6.14) very similar to those of the other granites.

TABLE 6.4 : PLAGIOCLASE, ALKALI FELDSPAR AND MAFIC-FREE MODAL COMPOSITIONS OF THE MAKHUTSO GRANITE, INDICATING TEXTURAL PARAMETERS

Sample Number	1	2	3	4	5	6	7	8	9
72/240	13	15	31	22	26	0,89	1,02	1414	1,14
72/238	10	15	32	26	28	0,82	1,51	1837	1,84
72/209	11	15	31	24	30	0,76	2,08	2315	2,67
72/208	13	15	32	26	31	1,19	2,13	598	1,79
72/212	13	15	29	24	28	0,97	2,82	1091	2,91
72/207	14	15	27	32	35	1,02	3,48	924	3,41
72/237	10	17	25	20	25	0,69	0,79	3043	1,14
72/1	15	15	32	27	27	1,13	3,61	699	3,19
72/236	16	15	22	22	27	1,19	2,48	598	2,09
72/257	15	15	22	22	30	1,20	3,52	573	2,93
72/216	12	15	28	28	36	0,85	1,94	1604	2,27
72/211	10	15	32	32	30	1,05	2,43	868	2,32
72/223	15	15	26	21	25	0,74	1,79	2455	2,42
72/1	12	14	29	23	28	0,77	1,83	2178	2,38
72/255	15	15	25	25	34	0,80	2,02	2967	2,52
72/256	12	15	34	31	30	1,03	2,93	911	2,84
72/241	8	15	35	30	31	1,23	3,71	536	3,02
72/189	14	15	30	28	29	1,17	3,26	624	2,79

1 = Weight per cent anorthite in plagioclase
2 = Weight per cent albite in alkali feldspar
3 = Weight per cent quartz in sample
4 = Weight per cent orthoclase in sample
5 = Weight per cent plagioclase in sample
6 = Mean calculated grain diameter
7 = Mean grain diameter of the ten largest grains
8 = Whole Rock Index
9 = Porphyritic Index

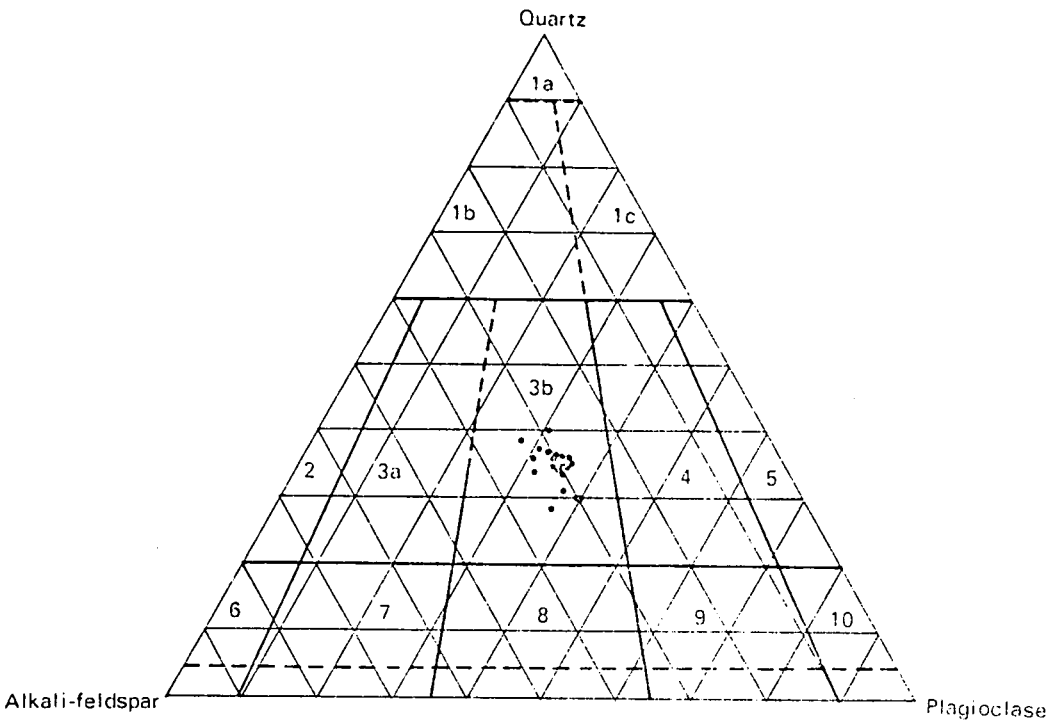

Fig. 6.13. QAP-diagram of the Makhutso Granite (diagram after Streckeisen, 1967).

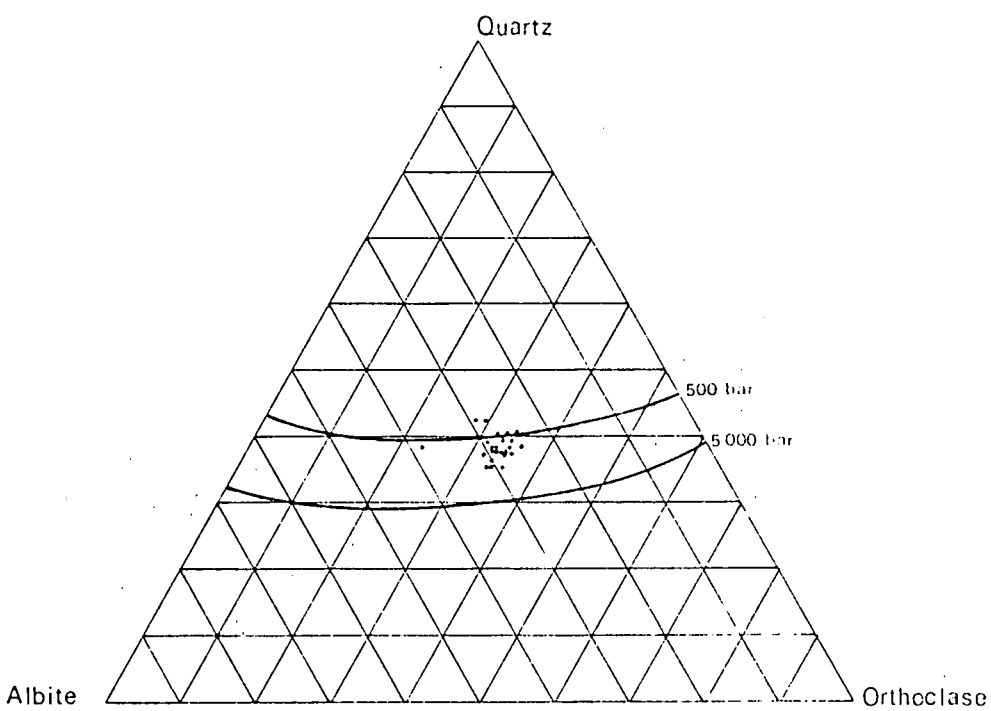

Fig. 6.14. Ternary diagram indicating possible formational pressures of the Makhutso Granite (isobars after Tuttle and Bowen, 1958).

6.2.3 Younger Granites

6.2.3.1 Klipvoor granite

(a) General description

This granite is correlated with the Bobbejaankop granite of the Zaaiplaats-Potgietersrus area, which was first described by Strauss and Truter (1944) and Strauss (1955). According to SACS the name 'Bobbejaankop granite' should be reserved for the younger granite of the Potgietersrus area and the name 'Klipvoor granite' is consequently introduced for similar granite in the present study area. Crocker (1976) used the names 'Paalkraal and Kenkelbos granite' for equivalents of the Bobbejaankop granite in the Rooiberg area, but these names were, however, not given recognition by Coertze *et al* (1978).

The pluton of Klipvoor granite within the study area (Fig. 6.1) is small compared to that at the type locality at Potgietersrus and Mutue Fides-Stavoren. It is surrounded on the north and west by a fine-grained, aplitic, sometimes porphyritic granite which is correlated with the still younger Klipkloof granite.

The Klipvoor granite in the study area displays the characteristic outcrop pattern of bald domes of the Bobbejaankop granite in the Zaaiplaats area, but the bald patches are often obscured by vegetation. According to Strauss and Truter (1944), the Bobbejaankop granite may be recognized by quartz grains which are coalesced to form chains on weathered surfaces. This is also a marked feature of the Klipvoor granite in the study area.

The megascopical characteristics of this granite correspond well with those of the Bobbejaankop granite in the Potgietersrust area, as defined by Strauss and Truter (1944) and Strauss (1955). The main difference, however, can be found in the feldspars, which, in the case of Bobbejaankop granite, reflect light poorly, while those in the Klipvoor granite reflect it rather well. Lenthall (personal communication) is of the opinion that the outlines of the feldspar in the Bobbejaankop granite are always vague, which is not the case in the Klipvoor granite.

(b) Macroscopic description

The Klipvoor granite is marked by its bright red colour, mainly caused by the deep red colouration of the K-feldspars. Weathered surfaces show miarolitic textures, while the biotite content increases and the hornblende content decreases towards the top of the intrusion. Fluorite is one of the accessory minerals in the rock, while tourmaline, together with quartz, form inclusions in the granite on Houtenbek 194 JR. This limited tourmalinisation of the granite may indicate the presence of a pneumatolytic phase during the late stage of crystallization, as schorl is often associated with late magmatic events (Deer *et al*, 1974). The biotite in the Klipvoor granite is almost completely altered and replaced by chlorite.

A large number of pegmatite veins, which were in the past exploited for scheelite and molybdenite, intersect the Klipvoor granite near its top (Fig. 6.15). Yttrian fluorite ($(Ca,RE)F_2$), a rare earth mineral, is present in the pegmatite (Berry, 1974).

Fig. 6.15. Small pegmatite in the Klipvoor granite on Houtenbek 194 JR.

Two samples, recovered from old mine dumps, displays interesting hydrothermal alteration effects. The one, which contains no mafic minerals, shows a high degree of decolouration and extraction of iron, while the other displays a marked green colouration due to intensive chloritisation. This chlorite is of the Thuringite-Chamosite series (Deer *et al*, 1974) and actually consists of a combination of clinochlore, grochaute and daphnite. Reaction rims with orthoclase are also evident, indicating some hydrothermal alteration of the hostrock.

(c) Microscopic description

This granite consists of orthoclase and plagioclase which are often perthitically intergrown, quartz and chloritised biotite, with accessory zircon, fluorite, tourmaline and ore. In the pegmatite, however, the major components are quartz, fluorite, microcline, chlorite and minerals such as scheelite, molybdenite and small amounts of cassiterite.

The quartz in the granite is mostly coarse-grained, equigranular and xenomorphic, filling the spaces between the feldspar crystals. This gives rise to a panidiomorphic texture.

Orthoclase ($Or_{72}Ab_{28}$) forms subhedral to anhedral, medium to coarse-grained crystals.

Medium to coarse-grained plagioclase (An_{10}) forms relatively unaltered, euhedral to anhedral crystals.

(d) Modal analysis

The modal analysis of this granite type is given in Table 6.5. The average rock composition is 30 per cent quartz, 20 per cent plagioclase, 20 per cent orthoclase and 20–25 per cent biotite and hornblende.

TABLE 6.5. MAFIC-FREE MODAL COMPOSITION OF THE KLIPVOOR GRANITE IN THE AREA NORTH OF PRETORIA

Sample number	Weight percentage Quartz	Weight percentage Orthoclase	Weight percentage Albite
72/199	26	19	17
72/198	36	14	17
72/139	27	18	18
72/137	34	24	22
72/133	27	21	26
72/124	30	24	20

The mafic-free mineral composition of this granite is 42 per cent quartz, 29 per cent plagioclase and 29 per cent orthoclase. When the mafic-free values are plotted on a quartz-alkali feldspar-plagioclase diagram (Fig. 6.16), it falls within the 3b-field of Streckeisen, 1967. This composition does not correspond with the cotectic trough as defined by Tuttle and Bowen (1958) (Fig. 6.17).

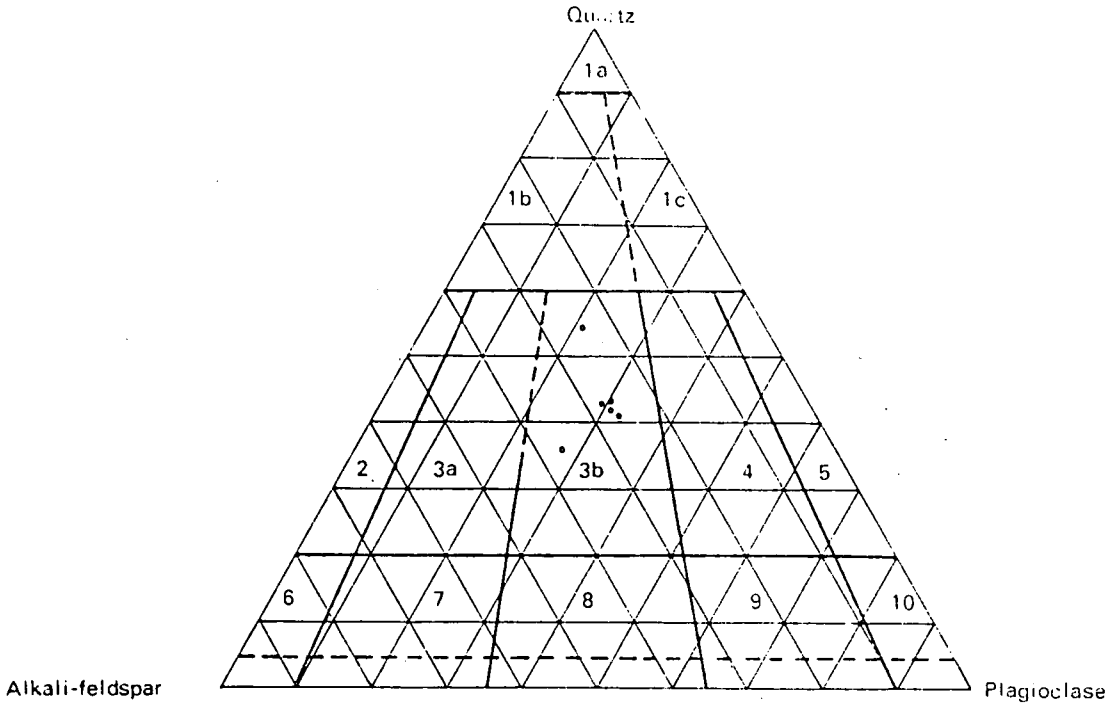

Fig. 6.16. QAP-diagram of the Klipvoor granite (diagram after Streckeisen, 1967).

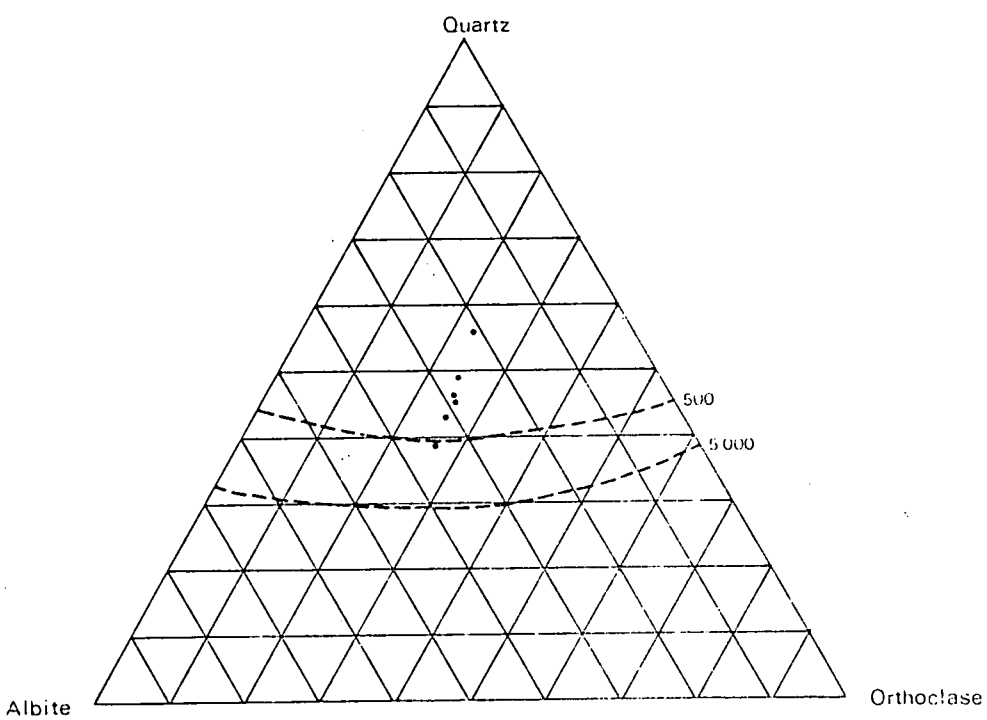

Fig. 6.17. Ternary diagram indicating possible formation pressures of the Klipvoor granite (isobars after Tuttle and Bowen, 1958).

6.2.3.2 Klipkloof granite

(a) General description

This granite surrounds the Klipvoor granite in the Houtenbek 194 JR area, as well as the Sekhukhuni granite on the farm Zandspruit 189 JR (Fig. 6.1). The granite was previously regarded as a marginal phase of the Klipvoor granite (De Bruiyn, 1974), but contact relationships indicate that it is younger than the Klipvoor granite.

The granite occurs as sheets and dykes between the Klipvoor granite and the Sterk River granophyre on the western margin of the Klipvoor granite on Houtenbek 194 JR, while to the north of this locality it forms thin sills within Sekhukhuni granite. On Zandspruit 189 JR, the granite seems to occur as a sill between the Sekhukhuni granite and the Rashoop Granophyre Suite. The contact relationships with the Sekhukhuni granite in the study area are usually sharp, displaying cross-cutting relationships with the older Sekhukhuni granite. Similar features were also described by Coertze *et al* (1978) between the Klipkloof and Sekhukhuni granites in the area north-east of Marble Hall.

(b) Macroscopic description

The Klipkloof granite is a fine-grained to aplitic granite which becomes porphyritic in places. It usually crops out as smooth domal koppies in the Zandspruit 189 JR area, while in the Houtenbek 194 JR region it can be distinguished by its prominent light grey colour, which contrasts sharply with the reddish colour of the surrounding rocks. The outcrops of this granite appears fresh compared to that of the granites which it intrudes. Spheroidal weathering characterizes the granite in the Zandspruit area, where it forms exfoliated domes and boulders.

(c) Microscopic description

The granite consists of quartz, orthoclase with perthitic intergrowths, plagioclase and minor amounts of biotite. The quartz usually occurs as

usually occurs as fine-grained subhedral crystals, although some samples contain euhedral phenocrysts. The orthoclase frequently forms euhedral phenocrysts ranging from medium to coarse-grained. Perthite is in both the groundmass orthoclase and in the phenocrysts. The granite contains plagioclase (An_{15-10}) in the groundmass, but no plagioclase phenocrysts were observed in the samples investigated.

Biotite is a subordinate constituent of this granite and is relatively unaltered. Opaque minerals and zircon constitute a very small percentage of the rock.

Modal mineral determinations indicate that this granite consists of 40 per cent quartz, 26 per cent plagioclase, 30 per cent orthoclase and 4 per cent biotite (Table 6.6).

The mafic-free modal composition, plotted onto the quartz-alkali feldspar-plagioclase ternary diagram, indicates that the Klipkloof granite falls within the 3b-granite field (Fig. 6.18).

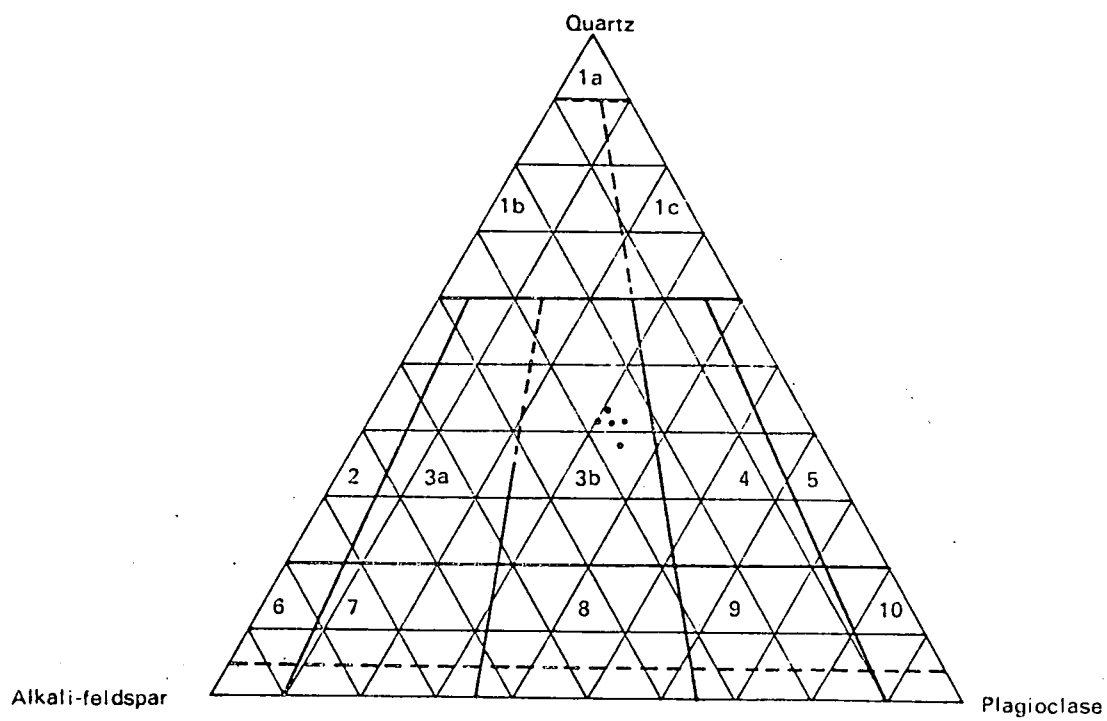

Fig. 6.18. QAP-diagram of the Klipkloof granite (diagram after Streckeisen, 1967).

TABLE 6.6 : PLAGIOCLASE, ALKALI FELDSPAR AND MAFIC-FREE MODAL COMPOSITION OF THE KLIPKLOOF GRANITE WITH TEXTURAL DATA INDICATED

Sample Number	1	2	3	4	5	6	7	8	9
72/199B	8	22	38	26	24	0,63	2,51	3953	3,98
72/198	12	26	41	30	27	0,62	1,62	4192	2,61
72/196	12	25	40	32	26	0,58	1,89	5172	3,25
72/192	10	28	40	29	27	0,69	2,04	3043	2,95
72/194	14	23	36	33	26	0,65	1,66	3692	2,55

1 = Weight percent anorthite in plagioclase

2 = Weight percent albite in alkali feldspar

3 = Weight percent quartz in sample

4 = Weight percent orthoclase in sample

5 = Weight percent plagioclase in sample

6 = Mean calculated grain diameter

7 = Mean grain diameter of the ten largest grains

8 = Whole Rock Index

9 = Porphyritic Index

TABLE 6.7 : CHEMICAL AND NORMATIVE COMPOSITION OF THE BUSHVELD GRANITES AND LEPTITE IN THE STUDY AREA

Sample No.	72/114	72/22	72/7	72/29	72/31	72/38A	72/89	72/51	72/52
SiO_2	74,15	75,63	73,00	73,60	72,90	76,50	73,60	72,10	75,90
TiO_2	0,17	0,15	0,28	0,20	0,21	0,12	0,26	0,22	0,24
Al_2O_3	12,53	12,04	12,10	11,60	12,70	11,20	11,70	12,10	11,50
Fe_2O_3	0,56	0,94	1,23	2,14	1,53	1,70	1,77	1,00	0,52
FeO	1,37	0,92	2,30	2,10	1,60	1,00	2,30	2,20	1,40
MnO	0,02	0,02	0,08	0,07	0,04	0,02	0,06	0,06	0,04
MgO	0,70	0,59	0,20	0,10	0,10	0,10	0,10	0,10	0,30
CaO	0,88	0,54	0,94	0,11	0,82	0,29	0,85	0,98	0,57
Na_2O	3,22	2,69	2,80	2,00	3,30	2,70	2,90	3,40	3,10
K_2O	5,12	5,44	5,36	5,69	5,67	5,14	5,07	4,78	4,87
H_2O^+	0,59	0,61	1,00	1,70	0,80	0,80	0,50	0,60	0,86
H_2O^-	0,12	0,14	0,30	0,30	0,30	0,20	0,10	0,20	0,20
P_2O_5	0,03	0,02	0,06	0,03	0,06	0,02	0,02	0,05	0,05
CO_2	0,27	0,14	0,50	0,10	0,20	0,20	0,10	0,20	0,10
ZrO_2	210	160	470	470	330	280	480	380	470
Ni	20	20	145	26	240	155	260	230	360
BaO	410	670	680	790	910	480	1 100	560	820
SrO	35	50	43	58	81	46	83	76	75
Rb_2O	330	290	240	200	180	290	210	210	190
TOTAL	99,83	99,99	100,31	99,89	100,40	100,09	99,54	100,14	99,78
Qtz	32,94	36,40	34,23	39,20	29,40	38,07	34,45	32,93	36,76
Cor	1,09	1,42	1,80	2,47	0,51	1,32	0,49	0,42	0,78
Zir	0,02	0,02	0,05	0,05	0,03	0,03	0,05	0,04	0,05
Or	27,72	30,96	29,72	33,78	32,73	30,38	28,64	26,26	27,28
Ab	29,50	24,83	25,91	18,92	30,29	24,25	26,96	31,26	28,68
An	1,98	1,30	0,27	–	1,89	–	2,85	2,68	1,21
Bi	5,03	3,33	4,67	2,63	2,43	–	3,79	4,25	3,79
Hm	–	–	–	–	–	4,50	–	–	–
Mt	0,60	1,01	1,33	2,36	1,64	0,58	1,92	1,07	0,56
Il	–	–	–	0,29	–	0,24	–	–	–
Tn	0,36	0,32	0,60	–	0,45	0,08	0,56	0,47	0,52
Cc	0,70	0,36	1,30	0,27	0,52	0,51	0,26	0,52	0,26
Ap	0,06	0,04	0,13	0,02	0,13	0,04	0,04	0,11	0,11
DI	91,27	93,63	91,70	94,42	92,96	94,05	90,58	90,91	93,55

Sample No.	72/53	72/83	72/105	72/104	72/103	72/101	72/155	72/280	72/146
SiO_2	73,00	76,50	76,30	77,50	74,20	72,90	71,80	76,10	71,10
TiO_2	0,26	0,15	0,14	0,07	0,06	0,11	0,19	0,11	0,14
Al_2O_3	12,20	11,10	11,50	11,90	12,90	12,90	12,50	11,30	13,80
Fe_2O_3	1,10	1,50	1,80	0,23	1,98	1,00	1,92	0,52	1,35
FeO	2,40	0,90	1,00	0,60	0,40	1,40	1,60	1,60	0,90
MnO	0,06	0,04	0,01	0,01	0,01	0,03	0,01	0,01	0,01
MgO	0,10	0,10	0,10	0,10	0,10	0,10	0,10	0,10	0,10
CaO	0,97	0,47	0,27	0,17	0,30	1,60	1,13	0,78	1,48
Na_2O	3,20	2,80	2,60	3,90	3,80	3,40	3,40	3,20	4,00
K_2O	5,19	4,93	5,33	5,14	5,55	5,23	5,55	5,23	5,15
H_2O^+	0,90	0,60	0,90	0,40	0,70	1,00	0,10	0,80	0,90
H_2O^-	0,30	0,10	0,20	0,20	0,30	0,20	0,20	0,20	0,20
P_2O_5	0,06	0,03	0,06	0,04	0,04	0,04	0,04	0,02	0,02
CO_2	0,20	0,10	0,20	0,20	0,10	0,50	1,00	0,40	0,10
ZrO_2	460	270	320	280	290	500	350	250	310
Ni	260	11	10	340	68	62	130	51	110
BaO	560	600	730	520	520	640	450	375	300
SrO	70	48	62	37	36	55	34	30	11
Rb_2O	230	240	200	290	230	230	290	360	240
TOTAL	100,10	99,44	100,54	100,07	100,55	100,56	99,76	100,48	99,35
Qtz	31,74	39,12	38,90	32,73	28,75	29,40	29,04	35,00	24,03
Cor	0,51	0,86	1,64	–	0,52	0,10	1,00	0,05	-0,68
Zir	0,05	0,03	0,03	0,03	0,03	0,05	0,04	0,03	0,03
Or	28,68	29,59	32,10	29,92	33,03	29,94	32,41	29,51	30,49
Ab	29,58	26,05	24,05	34,87	34,62	31,09	31,11	29,35	36,76
An	2,43	1,13	–	–	0,48	4,32	–	0,92	6,29
Bi	4,62	0,95	0,54	1,12	0,37	2,44	1,61	3,28	1,04
Hm	–	–	–	–	0,76	–	–	–	–
Mt	1,18	1,63	1,94	0,11	0,97	1,06	2,05	0,56	1,44
Il	–	–	0,20	0,10	–	–	0,27	–	–
Tn	0,56	0,33	–	–	0,13	0,23	–	0,24	0,30
Cc	0,52	0,26	0,52	0,38	0,26	1,29	2,32	1,02	0,26
Ap	0,13	0,07	0,07	–	0,09	0,09	–	0,04	0,04
DI	90,56	95,64	96,71	97,54	96,95	90,57	93,60	93,94	90,63

Sample No.	72/242	72/243	72/227	72/226	72/251	72/185	72/209	72/256	72/216
SiO_2	75,75	74,33	75,04	75,07	75,25	75,73	75,60	75,76	76,34
TiO_2	0,21	0,23	0,23	0,18	0,22	0,14	0,13	0,12	0,08
Al_2O_3	13,35	12,93	12,66	12,06	12,50	12,21	12,67	12,72	12,51
Fe_2O_3	0,32	1,32	0,82	1,36	0,64	0,61	0,69	0,64	0,71
FeO	0,14	1,00	1,06	0,56	1,34	1,01	0,80	0,67	0,56
MnO	0,01	0,02	0,03	0,02	0,04	0,03	0,02	0,02	0,02
MgO	0,19	0,06	0,03	0,48	0,21	0,20	0,20	0,03	0,11
CaO	0,33	0,49	0,59	0,30	0,97	0,72	0,61	0,66	0,44
Na_2O	4,29	3,28	3,32	3,20	3,34	3,43	3,86	3,39	3,76
K_2O	4,78	5,20	5,19	5,20	4,57	4,71	4,73	4,97	4,91
H_2O^+	0,36	0,77	0,60	0,79	0,48	0,57	0,35	0,33	0,22
H_2O^-	0,14	0,15	0,17	0,14	0,11	0,15	0,13	0,15	0,13
P_2O_5	0,03	0,03	0,04	0,18	0,04	0,03	0,02	0,03	0,01
CO_2	0,07	0,05	0,05	0,24	0,05	0,11	0,05	0,15	0,05
ZrO_2	332	330	349	349	330	273	244	212	170
Ni	12	14	40	36	10	22	20	6	8
BaO	744	577	504	245	364	297	262	199	252
SrO	99	54	77	41	65	51	43	37	19
Rb_2O	311	480	465	444	454	421	489	584	487
TOTAL	100,12	100,01	99,97	99,89	99,88	99,76	99,79	99,82	99,91
Qtz	19,99	33,12	33,68	34,71	34,68	34,76	32,03	34,15	32,83
Cor	1,06	1,64	1,25	1,31	0,84	0,72	0,45	1,25	0,48
Zir	0,03	0,03	0,03	0,03	0,03	0,03	0,02	0,02	0,02
Or	27,98	30,41	30,39	30,36	25,67	27,00	27,68	29,14	28,90
Ab	38,78	30,40	29,72	29,46	30,67	31,52	35,25	31,02	34,25
An	0,42	1,27	1,71	–	3,65	2,30	2,22	1,78	1,60
Bi	0,72	2,10	1,64	1,81	3,10	2,37	1,18	1,26	0,85
Hm	–	–	–	0,31	–	–	–	–	–
Mt	0,34	0,35	0,88	1,00	0,68	0,65	0,73	0,68	0,75
Il	–	–	–	0,26	–	–	–	–	–
Tn	0,44	0,50	0,49	–	0,47	0,30	0,28	0,26	0,17
Cc	0,18	0,13	0,13	0,62	0,13	0,29	0,13	0,39	0,13
Ap	0,06	0,07	0,09	–	0,09	0,06	0,04	0,06	0,02
DI	97,84	95,60	95,07	95,86	91,88	94,03	95,42	95,57	96,48

Sample No.	72/223	72/238	72/255	72/237	72/208	72/211	72/211a	72/212
SiO_2	76,41	75,48	77,01	74,61	75,16	75,03	73,58	74,11
TiO_2	0,10	0,14	0,08	0,20	0,22	0,20	0,20	0,19
Al_2O_3	12,55	12,61	12,33	12,88	12,96	12,85	13,66	13,10
Fe_2O_3	0,44	0,61	0,29	0,90	0,52	1,18	0,64	0,53
FeO	0,30	0,81	0,20	0,85	0,36	0,63	1,41	1,45
MnO	0,01	0,01	0,03	0,01	0,03	0,03	0,03	0,03
MgO	0,08	0,24	0,06	0,05	0,03	0,12	0,25	0,16
CaO	0,33	0,64	0,23	0,62	0,86	0,54	0,76	0,81
Na_2O	2,67	3,74	3,33	3,37	3,73	3,40	3,57	3,40
K_2O	6,31	4,94	5,75	5,41	5,33	5,04	5,03	5,06
H_2O^+	0,51	0,42	0,46	0,58	0,29	0,60	0,59	0,58
H_2O^-	0,12	0,17	0,12	0,09	0,17	0,14	0,14	0,12
P_2O_5	0,02	0,02	0,06	0,03	0,04	0,04	0,04	0,04
CO_2	0,05	0,11	0,11	0,05	0,05	0,05	0,05	0,19
ZrO_2	173	244	323	359	316	326	343	316
Ni	14	10	6	4	10	6	12	16
BaO	277	358	181	687	823	542	548	573
SrO	33	63	21	73	90	54	89	88
Rb_2O	575	507	428	490	353	420	521	510
TOTAL	100,17	99,90	100,13	99,81	99,91	99,98	100,10	99,92
Qtz	34,24	31,91	33,49	31,49	29,64	33,27	30,40	32,07
Cor	1,11	0,44	0,70	0,83	-0,09	1,40	1,54	1,43
Zir	0,02	0,02	0,03	0,03	0,03	0,03	0,03	0,03
Or	37,29	28,80	34,33	31,94	31,66	29,97	28,12	28,49
Ab	24,44	34,16	30,36	30,92	33,96	31,19	32,59	31,15
An	0,91	2,00	–	2,07	3,14	1,53	2,66	2,07
Bi	1,14	1,41	0,25	1,15	0,44	0,73	3,36	3,22
Hm	–	–	–	–	–	–	–	–
Mt	0,47	0,65	0,31	0,96	0,55	1,26	0,68	0,57
Il	–	–	0,08	–	–	–	–	–
Tn	0,21	0,30	0,06	0,43	0,47	0,43	0,43	0,41
Cc	0,13	0,28	0,28	0,13	0,13	0,13	0,13	0,49
Ap	0,04	0,04	0,13	0,06	0,09	0,09	0,09	0,09
DI	97,10	95,32	98,90	95,20	95,19	92,67	95,85	93,17

Sample No.	72/236	72/241	72/240	72/189	72/207	72/159	72/160	R152A
SiO_2	73,74	75,30	74,78	75,58	73,94	72,43	72,14	72,47
TiO_2	0,27	0,17	0,20	0,18	0,21	0,25	0,25	0,21
Al_2O_3	13,28	12,65	13,56	12,95	13,24	13,42	13,44	14,30
Fe_2O_3	0,74	0,71	0,40	0,62	0,48	0,45	0,56	0,47
FeO	1,43	1,01	0,72	0,45	1,01	1,84	1,97	1,70
MnO	0,04	0,04	0,03	0,01	0,02	0,02	0,03	0,03
MgO	0,29	0,12	0,08	0,63	0,61	0,89	0,85	0,46
CaO	1,00	0,80	0,95	0,65	0,96	1,24	1,35	1,38
Na_2O	3,28	3,38	3,85	3,10	3,16	2,87	2,88	3,75
K_2O	5,06	4,98	4,76	5,26	5,21	4,84	4,95	4,22
H_2O^+	0,48	0,35	0,19	0,22	0,43	0,70	0,67	0,69
H_2O^-	0,11	0,08	0,10	0,28	0,16	0,19	0,19	0,09
P_2O_5	0,05	0,04	0,04	0,03	0,04	0,07	0,06	0,05
CO_2	0,05	0,11	0,14	0,06	0,08	0,30	0,53	0,11
ZrO_2	403	289	353	140	160	210	230	313
Ni	14	12	12	15	15	10	10	30
BaO	640	517	903	590	600	820	850	789
SrO	91	75	120	55	70	95	85	176
Rb_2O	433	442	257	210	400	290	280	320
TOTAL	99,98	99,87	99,96	100,12	99,67	99,65	100,02	100,09
Qtz	31,70	33,37	30,60	34,19	32,12	33,91	33,36	30,14
Cor	1,25	0,86	1,05	1,51	1,29	2,60	2,80	1,80
Zir	0,04	0,03	0,04	0,01	0,02	0,02	0,03	0,03
Or	28,31	28,75	27,50	29,84	28,90	25,04	25,57	22,24
Ab	30,04	30,94	34,94	28,26	28,95	26,44	26,41	34,18
An	3,58	2,59	3,09	2,19	3,47	3,18	2,32	5,37
Bi	3,49	1,99	1,49	2,74	4,00	6,87	6,89	4,90
Hm	–	–	–	–	–	–	–	–
Mt	0,79	0,76	0,42	0,66	0,51	0,48	0,60	0,50
Il	–	–	–	–	–	–	–	–
Tn	0,58	0,36	0,42	0,38	0,45	0,54	0,53	0,45
Cc	0,13	0,28	0,36	0,15	0,21	0,78	1,37	0,28
Ap	0,11	–	0,09	0,06	0,09	0,15	0,13	0,11
DI	91,33	93,94	94,13	93,82	91,27	88,00	88,16	88,39

Sample No.	72/124	72/197	72/199A	72/199B	72/198	72/X1	72/257	72/228
SiO_2	76,31	75,59	76,50	73,60	74,30	72,00	70,73	72,84
TiO_2	0,15	0,16	0,11	0,25	0,28	0,24	0,46	0,38
Al_2O_3	11,59	11,87	11,20	11,70	11,70	14,02	13,90	12,75
Fe_2O_3	0,60	0,70	0,93	2,97	1,83	0,45	0,77	0,78
FeO	0,97	1,16	1,00	1,00	2,00	1,68	2,22	1,99
MnO	0,02	0,03	0,04	0,03	0,05	0,02	0,06	0,03
MgO	0,92	0,66	0,10	0,30	0,10	0,10	0,98	0,08
CaO	0,54	0,70	0,88	0,53	0,54	1,51	1,42	1,09
Na_2O	2,69	2,92	2,70	3,30	2,90	3,34	3,08	3,62
K_2O	5,22	5,18	5,48	4,67	5,14	4,33	4,73	4,86
H_2O^+	0,53	0,61	0,70	1,20	1,10	0,63	0,80	0,63
H_2O^-	0,23	0,19	0,30	0,40	0,30	0,17	0,17	0,21
P_2O_5	0,01	0,01	0,04	0,05	0,04	0,06	0,12	0,07
CO_2	0,14	0,16	0,20	0,20	0,30	0,17	0,12	0,17
ZrO_2	180	250	250	630	470	200	370	511
Ni	20	20	24	50	61	20	20	16
BaO	280	280	265	245	210	720	850	677
SrO	15	15	12	14	11	170	160	119
Rb_2O	310	300	350	290	285	270	380	492
TOTAL	100,00	100,03	100,26	100,32	100,68	99,86	99,74	99,68
Qtz	37,85	35,87	36,80	34,70	35,90	31,58	30,94	30,12
Cor	1,49	0,86	-0,11	1,29	1,54	2,08	2,47	0,61
Zir	0,02	0,03	0,03	0,06	0,05	0,02	0,04	0,05
Or	28,36	28,61	32,22	27,82	29,55	21,50	23,79	27,04
Ab	24,66	26,84	24,93	30,64	26,83	30,53	28,36	33,33
An	1,29	1,94	2,58	0,21	–	5,47	4,22	2,78
Bi	5,00	4,34	1,70	1,14	2,78	7,27	7,80	3,84
Hm	–	–	–	0,47	–	–	–	–
Mt	0,64	0,75	1,00	2,50	1,97	0,48	0,83	0,84
Il	–	–	–	–	0,17	–	–	–
Tn	0,32	0,34	0,24	0,54	0,35	0,51	0,99	0,81
Cc	0,36	0,41	0,52	0,52	0,78	0,44	0,31	0,44
Ap	0,02	0,02	0,09	0,11	0,09	0,13	0,26	0,15
DI	92,37	92,20	93,88	94,50	93,86	85,71	85,60	91,15

72/114	Sekhukhuni granite from Leeuwdraai 184 JR
72/22	Sekhukhuni granite from Enkeldoorn 217 JR
72/7	Sekhukhuni granite from Sybrandskraal 244 JR
72/29	Sekhukhuni granite from Klipspruit 245 JR
72/31	Sekhukhuni granite from Klipfontein 205 JR
72/38A	Sekhukhuni granite from Kameelpoort 202 JR
72/89	Sekhukhuni granite from Pieterskraal 190 JR
72/51	Sekhukhuni granite from Leeuwfontein 188 JR
72/52	Sekhukhuni granite from Wolvenkraal 192 JR
72/53	Sekhukhuni granite from Tweefontein 154 JR
72/83	Sekhukhuni granite from Klipplaatdrift 193 JR
72/105	Sekhukhuni granite from Rietfontein 214 JR
72/104	Sekhukhuni granite from Rietfontein 214 JR
72/103	Sekhukhuni granite from Springfontein 213 JR
72/101	Sekhukhuni granite from Hartebeestspruit 235 JR
72/155	Sekhukhuni granite from Boekenhoutkloof 37 JR
72/280	Sekhukhuni granite from Klipdrift 121 JR
72/146	Sekhukhuni granite from Klipdrift 90 JR
72/242	Verena granite from Gemsbokspruit 229 JR
72/243	Verena granite from Gemsbokspruit 229 JR
72/227	Verena granite from Roodepoortje 250 JR
72/226	Verena granite from Bultfontein 94 JS
72/251	Verena granite from Leeuwkop 228 JR
72/185	Fine-grained Makhutso Granite from Vlaklaagte 221 JR
72/209	Fine-grained Makhutso Granite from Hartebeestfontein 224 JR
72/256	Fine-grained Makhutso Granite from Hartebeestfontein 224 JR
72/216	Fine-grained Makhutso Granite from Rhenosterfontein 227 JR
72/223	Fine-grained Makhutso Granite from Leeuwkop 228 JR
72/238	Fine-grained Makhutso Granite from Gemsbokspruit 229 JR
72/255	Fine-grained Makhutso Granite from Gemsbokspruit 229 JR
72/237	Aplite in Makhutso Granite from Gemsbokspruit 229 JR
72/208	Makhutso Granite from Hartebeestfontein 224 JR
72/211	Makhutso Granite from Hartebeestfontein 224 JR
72/211a	Makhutso Granite from Hartebeestfontein 224 JR
72/212	Makhutso Granite from Hartebeestfontein 224 JR
72/236	Makhutso Granite from Gemsbokspruit 229 JR
72/241	Makhutso Granite from Gemsbokspruit 229 JR
72/240	Makhutso Granite from Gemsbokspruit 229 JR
72/189	Makhutso Granite from Vlaklaagte 221 JR
72/207	Makhutso Granite from Hartebeestfontein 224 JR
72/159	Makhutso Granite from Kameelrivier 160 JR
72/160	Makhutso Granite from Kameelrivier 160 JR
R152A	Makhutso Granite from Waterval 34 JS
72/124	Klipvoor granite from Houtenbek 194 JR
72/197	Klipvoor granite from Houtenbek 194 JR
72/199A	Klipvoor granite from Houtenbek 194 JR
72/199B	Klipkloof granite from Houtenbek 194 JR
72/198	Klipkloof granite from Houtenbek 194 JR
72/X1	Leptite in Makhutso Granite from Hartebeestfontein 224 JR
72/257	Leptite in Makhutso Granite from Vlaklaagte 221 JR
72/228	Leptite in Makhutso Granite from Gemsbokspruit 229 JR

6.3 GEOCHEMISTRY

6.3.1 Introduction

Chemical analyses were obtained from 18 samples of Sekhukhuni granite, 5 of Verena granite, 20 of Makhutso Granite, 2 of Klipkloof granite, 3 of Klipvoor granite and 3 of leptite (Table 6.7).

The samples from the Sekhukhuni, Klipvoor and Klipkloof granites were analysed by Bergström and Bakker, while the others were done by the General Superintendence Company (N.I.M. project No. 92773). Analyses were done by wave-length dispersive X-ray spectrometry on all elements, except for FeO which was determined by volumetric titration and H_2O and CO_2 which were determined gravimetrically.

6.3.2 Sekhukhuni and younger granites

An AFM-diagram (Fig. 6.19) for the Sekhukhuni, Klipvoor and Klipkloof granites indicates a spread along the alkali-iron axis which corresponds to the tholeiitic trend as defined by Nockolds and Allen (1954, 1956), with the Sekhukhuni granite at the top followed by the Klipvoor granite. The Klipkloof granite, however, plots near the top of the trend and can therefore not be regarded as the differentiation product of the Sekhukhuni granite.

When CaO, FeO and $Fe^{+2}/Fe^{+2} + Fe^{+3}$ are plotted against SiO_2 (Fig. 6.20), a decrease in CaO and FeO and an increase in the iron-ratio from Sekhukhuni to Klipvoor granite is illustrated; the Klipkloof granite plots midway along these trends. This corroborates the conclusion reached above, i.e. that the Klipkloof granite is not a differentiation product of the Sekhukhuni granite.

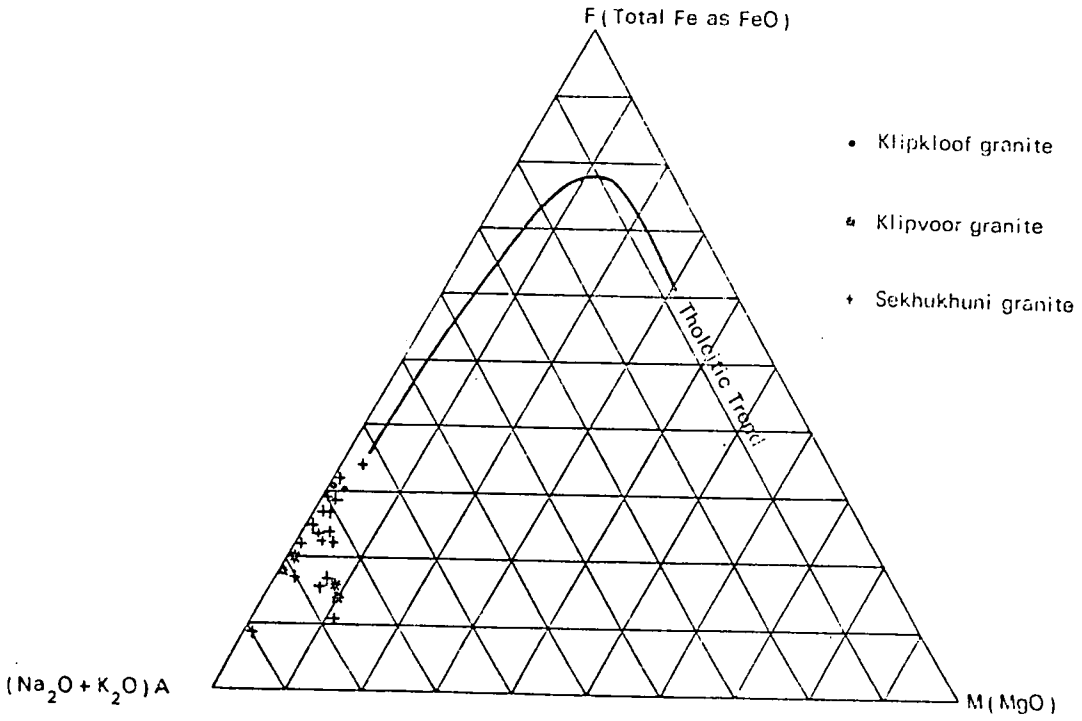

Fig. 6.19. AFM-diagram of the Sekhukhuni, Klipvoor and Klipkloof granites in the study area (tholeiitic differentiation trend after Nockolds and Allen, 1954, 1956).

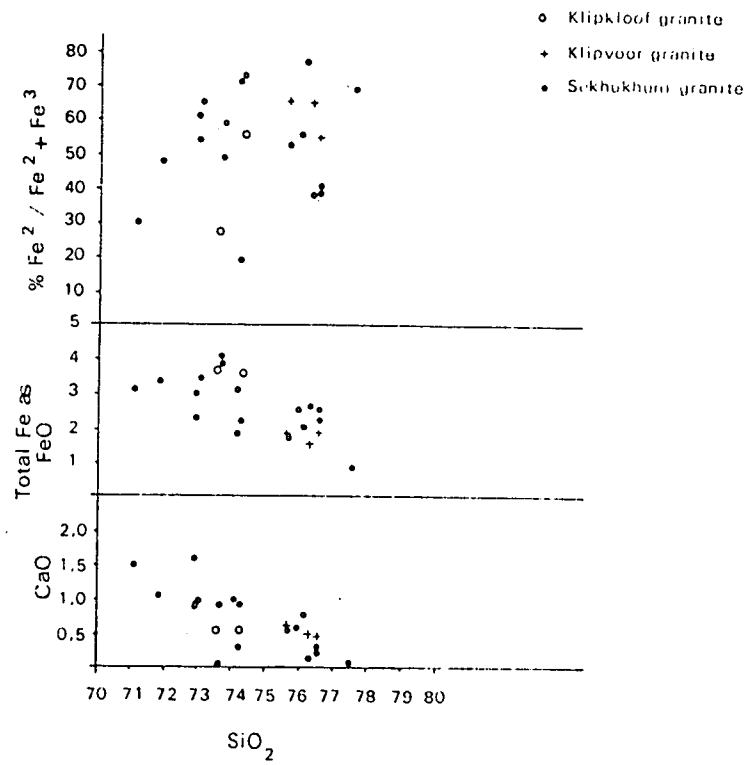

Fig. 6.20. Plots of CaO, FeO and $Fe^2/Fe^2 + Fe^3$ against SiO_2 for the Sekhukhuni, Klipvoor and Klipkloof granites of the study area.

The variation in chemical compositions, as illustrated by the various diagrams (Figures 6.19 and 6.20), shows a possible differentiation from Sekhukhuni to Klipvoor granite. The same trend is illustrated by the trace elements Ba, Sr and Rb (Fig. 6.21). The Klipkloof granite plots in the same positions as the Klipvoor granite and this, together with the break in the Sr to Rb ratio (Fig. 6.21), may indicate that both these granites represent later intrusions.

Geochronological data for the various granites in the area (Table 6.8) support the idea that the Sekhukhuni granite is the first crystalline phase of the Lebowa Granite Suite followed by the Klipvoor and Klipkloof granites.

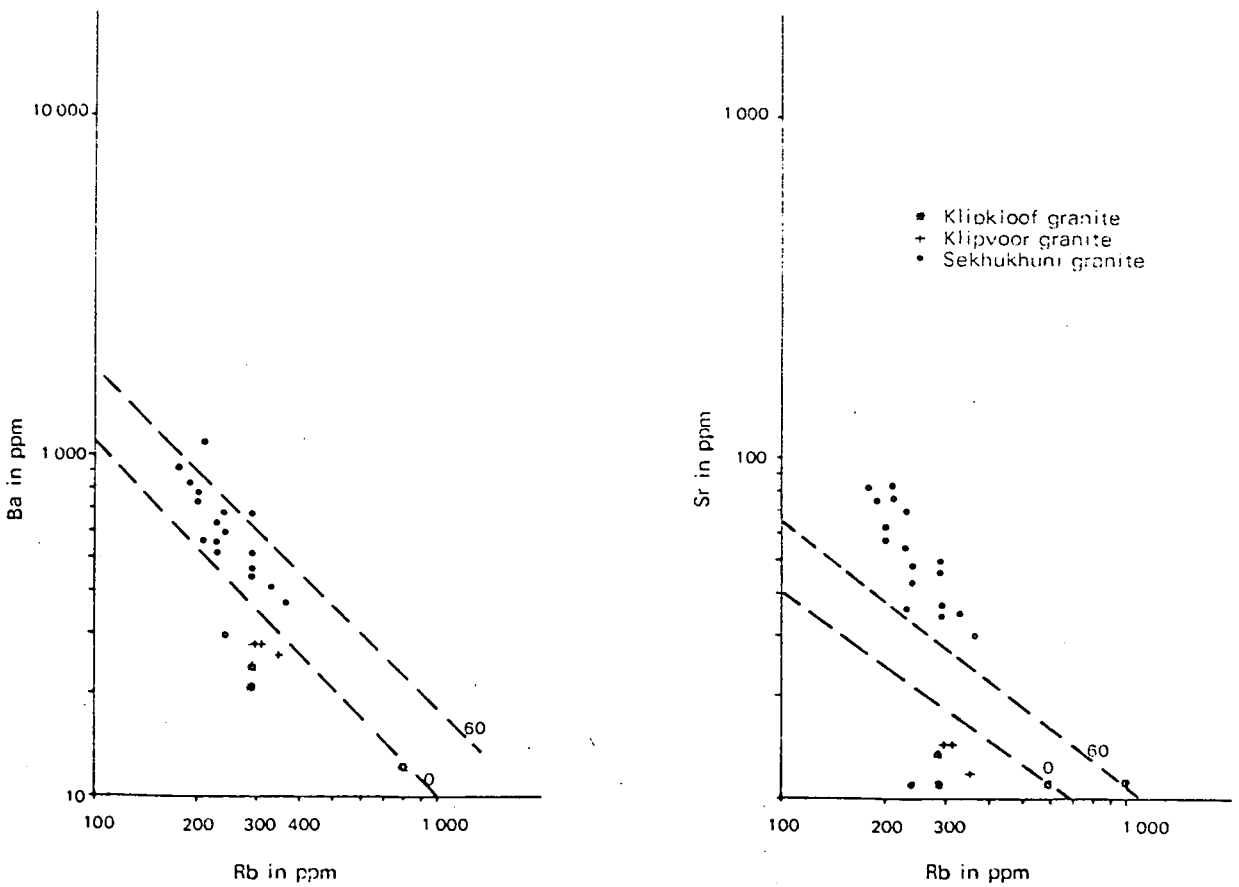

Fig. 6.21. Trace element distribution in the Sekhukhuni, Klipvoor and Klipkloof granites in the study area.

TABLE 6.8 : CONCORDIA AGES OF THE SEKHUKHUNI AND YOUNGER GRANITES IN THE STUDY AREA (AFTER COERTZE, *et al*, 1978)

Sample number	Granite type	$\frac{206_{Pb}}{238_U}$	$\frac{207_{Pb}}{235_U}$	Concordia age
HB 74/3	Klipkloof	0,03524	0,4362	1 400 my
HB 74/1	Klipvoor	0,0693	0,9254	1 670 my
HB 74/4	Sekhukhuni	0,2129	3,3748	1 920 my

6.3.3 Makhutso and Verena granites

Attempts to differentiate between these granites on the basis of geochemistry was unsuccessful, as the chemical composition as well as the normative compositions are very similar; even a highly discriminative technique such as cluster analysis was unable to accomplish this goal.

It was, however, possible to identify two chemically different suites within the southern pluton of the Makhutso Granite by means of cluster analysis, which is based on pair group average clustering by distance functions as described by Davis (1973). The pair group average clustering is given in Table 6.9, while Table 6.10 gives a similarity/distance matrix for the various samples of the Makhutso Granite. From these tables it is evident that the granites building the southern pluton of the Makhutso Granite, can be separated chemically from one another. This difference in chemical composition can also be illustrated diagrammatically as seen in Figure 6.22.

Field observations suggest that the southern pluton of the Makhutso Granite represents a zoned body consisting of a coarse-grained, porphyritic core and a fine-grained marginal facies. The zonation in granitic plutons can be explained in different ways:- by multiple intrusion (Taubeneck, 1957; 1967); by rapid chilling of the magma against colder country rocks (Vance, 1961), as well as by assimilation of country rocks (Reesor, 1958; Compton, 1955; Mursky, 1972) or through convection as proposed by Karner (1970).

TABLE 6.9 : PAIR GROUP AVERAGE CLUSTERING BASED ON DISTANCE COEFFICIENTS FOR SAMPLES FROM THE SOUTHERN PLUTON OF MAKHUTSO GRANITE

3	9	29.96165
4	7	12.23033
5	8	8.65063
6	17	19.95514
11	16	19.72956
12	13	17.60219
4	5	22.88349
10	12	24.55381
4	6	33.60720
10	14	25.75569
1	2	42.92625
10	11	34.50086
1	4	62.40621
10	15	43.70030
1	3	73.91203
1	10	122.27464

Columns 1 and 2 – observations combined into clusters

Column 3 – similarity level of clustering

TABLE 6.10 : CORRELATION MATRIX AND DISTANCE MATRIX OF ANALYSES OF THE MAKHUTSO GRANITE. (DATA ABOVE DIAGONAL THAT OF CORRELATION MATRIX AND THAT BELOW DIAGONAL THAT OF DISTANCE MATRIX).

	1	2	3	4	5	6	7	8	9	10	11	12	13	14	15	16	17
1		0.96	0.98	0.91	0.90	0.92	0.91	0.88	0.98	0.77	0.58	0.70	0.70	0.79	0.60	0.68	0.93
2	42.92		0.97	0.96	0.97	0.95	0.97	0.95	0.93	0.88	0.76	0.85	0.85	0.91	0.75	0.84	0.97
3	73.13	61.93		0.96	0.94	0.97	0.95	0.93	0.99	0.83	0.65	0.77	0.75	0.84	0.69	0.73	0.97
4	63.67	39.78	65.14		0.99	0.99	0.99	0.99	0.92	0.95	0.82	0.91	0.89	0.95	0.86	0.87	0.99
5	78.34	43.42	66.17	23.10		0.98	0.99	0.99	0.89	0.96	0.86	0.93	0.92	0.97	0.87	0.90	0.99
6	78.42	55.83	48.88	29.43	30.00		0.98	0.98	0.94	0.93	0.78	0.88	0.85	0.92	0.84	0.83	0.99
7	63.97	35.60	71.62	12.23	20.94	37.76		0.99	0.90	0.96	0.85	0.93	0.91	0.96	0.87	0.89	0.99
8	84.06	50.74	72.48	24.61	8.65	31.49	22.87		0.88	0.97	0.87	0.94	0.92	0.97	0.90	0.91	0.98
9	86.55	87.18	29.96	90.00	93.66	71.96	97.30	99.24		0.77	0.55	0.69	0.66	0.77	0.62	0.63	0.93
10	86.06	72.60	119.33	56.17	66.21	82.64	49.91	63.18	142.37		0.94	0.98	0.96	0.99	0.96	0.95	0.93
11	122.14	99.63	151.06	88.83	89.18	113.33	80.22	85.42	177.39	44.92		0.98	0.98	0.95	0.95	0.98	0.80
12	99.13	80.66	130.51	67.09	72.39	93.25	59.33	68.98	155.34	18.91	26.52		0.99	0.99	0.97	0.98	0.89
13	98.29	81.06	136.08	75.55	80.59	103.22	66.92	78.70	161.30	30.18	26.74	17.60		0.98	0.94	0.99	0.87
14	87.48	62.12	110.90	49.14	51.06	74.53	39.80	48.41	136.87	24.84	40.59	22.43	30.89		0.94	0.97	0.94
15	111.70	101.35	145.36	81.09	90.97	105.46	76.59	86.31	167.53	29.30	43.18	29.20	40.00	47.84		0.93	0.83
16	107.90	82.62	136.23	76.87	75.96	102.04	67.27	73.67	163.24	41.57	19.72	25.44	20.77	29.28	51.80		0.85
17	82.53	52.63	44.42	37.00	28.11	19.95	42.53	32.49	71.85	90.85	116.16	98.68	106.74	78.07	114.88	102.86	

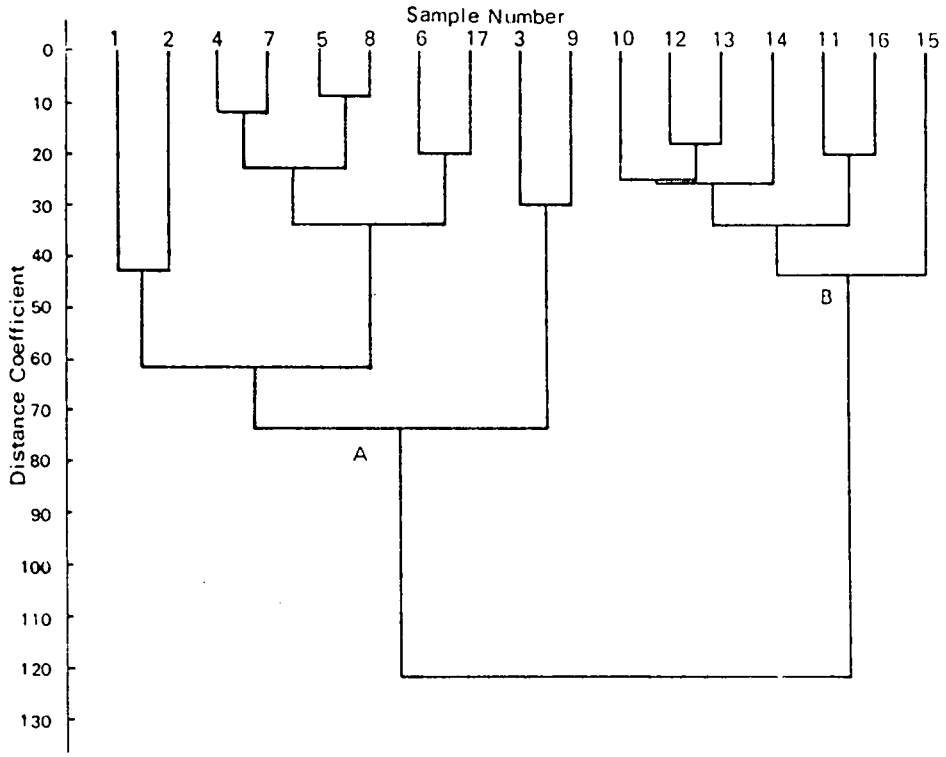

Fig. 6.22. Dendrogram indicating two different fields in the geochemical data from the southern pluton of Makhutso Granite. (A) corresponds to the coarse-grained porphyritic core of the pluton and (B) represents the fine-grained marginal facies.

Variation diagrams for the rocks of the southern pluton indicate a reversed differentiation trend. According to Vance (1961) the granitic magma will become progressively more siliceous as differentiation progressed, but in the case of the Makhutso Granite it is clear from Figure 6.23 that the fine-grained marginal facies is enriched in SiO_2, while the TiO_2 and CaO contents decrease. This consequently rules out the possibility of a chill phase being formed against colder country rocks, while the possibility of multiple intrusion is also countered by the gradational nature of the contact between the two facies. From the chemical characteristics of the two facies, it can be deduced that the coarse-grained porphyritic core probably crystallized before the finer grained marginal facies.

This feature can be explained by *in situ* crystallization and differentiation of the main body, while the residual magma is filter-pressed towards the margin of the pluton where it then crystallizes as an aplitic phase. Taubeneck (1967) explained the zonation of the Cornucopia Stock of the Wallow Mountains by means of a similar process.

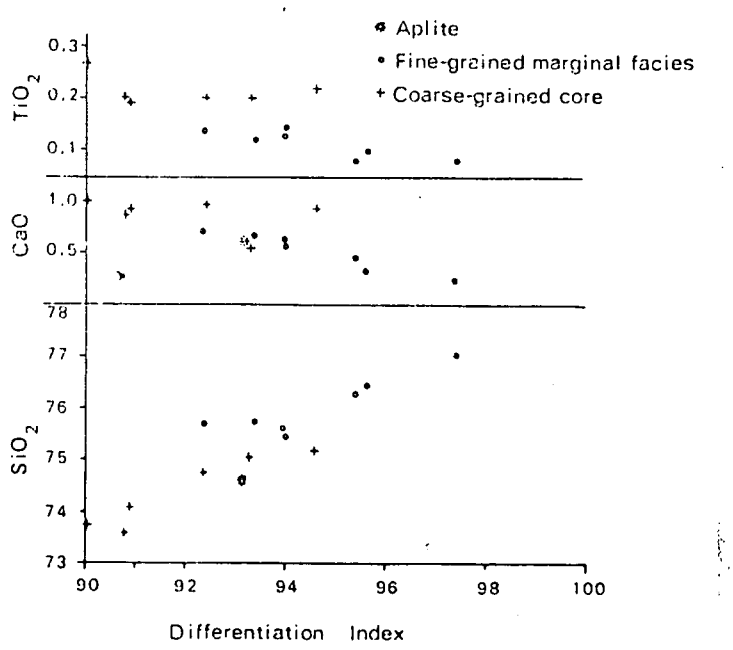

Fig. 6.23. CaO, TiO_2 and SiO_2 as a function of the differentiation index for the southern pluton of Makhutso Granite.

6.3.4 Leptite assimilation and chemical composition

Plots of Ba, Rb and Sr ratios of the granites in the Zaaiplaats area led McCarthy (1977) to the conclusion that the variation in the chemical composition of the granites was the result of fractional crystallization. When the data from the study area are plotted on similar diagrams (Fig. 6.24), a similar trend to that described by McCarthy (1977) can be seen. According to this trend the Sekhukhuni granite crystallized first, while the Klipvoor and Klipkloof granites represent the differentiation products. This diagram, however, shows a marked enrichment of Ba, Sr and Rb in the Makhutso and Verena granites (Fig. 6.24).

According to Krauskopf (1979), Ba and Sr are concentrated in the early phases of crystallization, while Rb enters the later formed K-minerals and concentrates during differentiation, while the melt becomes depleted in Ba and Sr. If this is taken into account for the granites of the study area, the Verena and Makhutso Granites, which represent an older marginal phase of the Sekhukhuni granite and a younger granite respectively, should display much higher Ba/Rb and Sr/Rb and lower Ba/Rb and Sr/Rb ratios respectively than is the case.

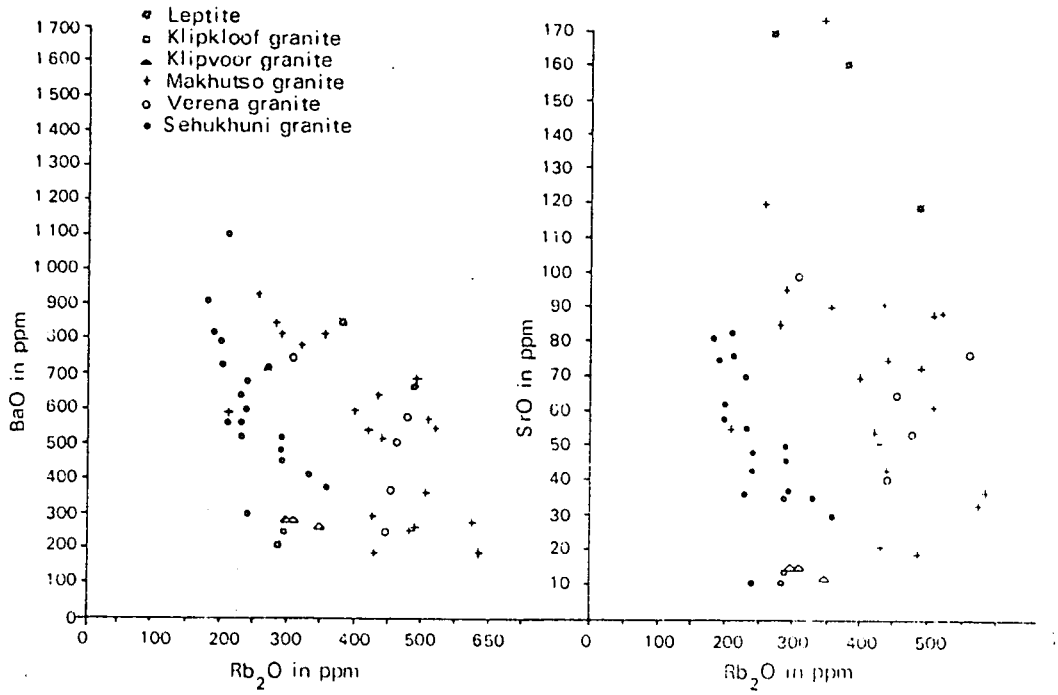

Fig. 6.24. Ba and Sr as functions of Rb for the granites from the study area.

To cater for this anomalous distribution, various options were investigated, including the effect of leptite assimilation as leptite xenoliths are only present in these two granites. When the chemical composition of the leptite (Table 6.7) is treated with the data from the granites, a very interesting picture emerges from this comparison. A diagram of the BaO/Rb_2O and SrO/Rb_2O ratios of the granites as well as that of the leptite xenoliths (Fig. 6.25) shows a marked enrichment in BaO, SrO and Rb_2O for the leptites. The assimilation of leptite could therefore satisfactorily explain the enrichment of trace elements in the granites.

A magma will assimilate a rock higher in the reaction series by chemically and mineralogically altering it to correspond to the composition of the magma (Bowen, 1928), while the overall composition of the magma will change towards that of the assimilated material (Woodard, 1957; Leake

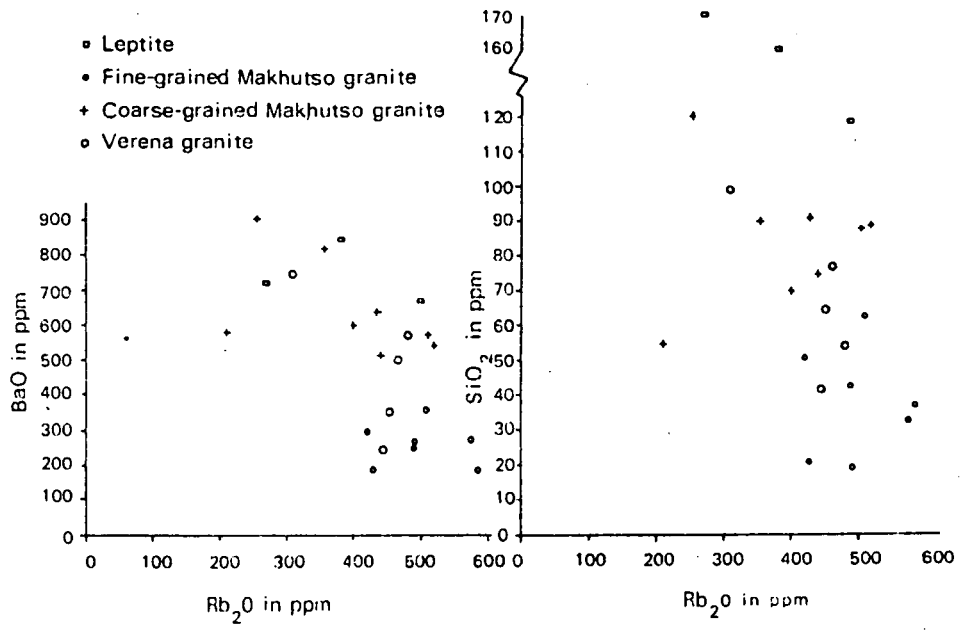

Fig. 6.25. BaO and SrO as functions of Rb_2O in the granites and leptite of the study area.

and Skirrow, 1960). The mineralogical composition of the inclusions will therefore approach that of the magmatic rock (Reesor, 1958). Evidence of this is the presence of feldspar megacrysts in the leptite xenoliths.

According to Heier and Billings (1972), Rb is a mobile element in granitic metamorphic aureoles and in xenoliths within granite. It was also found by Bowler (1959) that metamorphosed shales in close proximity to a granitic intrusion show much greater Rb enrichment than shales outside the metamorphic aureole. As the leptite analised in this investigation was present as inclusions in the granite and no leptite was investigated away from the granite contact, it was not possible to determine the amount of enrichment in the trace elements in the leptite by granite assimilation in this case.

The above is probably the reason why the Makhutso and Verena granites do not correspond to the general differentiation trend as exhibited by the other granites in the study area. De Bruiyn and Rhodes (1975) concluded on field and chemical evidence that the Makhutso Granite does not form part of the Sekhukhuni granite and in the light of the new evidence, this conclusion is probably invalid.

7 STRUCTURAL GEOLOGY

7.1 INTRODUCTION

A review of the general structural pattern of the Bushveld Complex and the structural features controlling its setting, is necessary to clarify the structural features of the study area. Hall (1931) regarded the fundamental structural control for the positioning of the Bushveld Complex as being the intersection of the Murchison lineament and the southward extension of the Great Dyke. This was, however, disputed by the gravity survey which indicates an absence of the Mafic Phase underneath the central part of the complex (Smit *et al,* 1962).

The Bushveld Complex is located within the Transvaal depositional basin, to the east of the Vryburg arch (Hunter, 1975). Deposition in the basin was influenced by linear and domal structures, which played a role during early sedimentation, as seen in the Wolkberg Group (Button, 1973), the Witwatersrand Basin (Brock and Pretorius, 1964) and the Waterberg and Transvaal sequences (Jones, 1968). In some cases the deformation was contemporaneous with deposition as found by Crockett (1971) in the Transvaal sediments in Botswana. Hunter (1975) regards the Vryburg arch as being of major importance in the development of structures in the Transvaal basin, as revealed by the sedimentation in the Transvaal and adjacent areas. Sharpe and Von Gruenewaldt (1979), however, reach the conclusion that the arch was relatively unimportant in the initial stages of emplacement of the Bushveld Complex and that this arch post-dates the emplacement of the mafic rocks. The younger alkaline intrusions along the north-eastern flank of the arch is cited as evidence by Sharpe and Von Gruenewaldt, (1979). North - north-east and north - north-west trending warps, which have influenced the structural evolution of the Kaapvaal Province from the earliest times, are also present (Hunter, 1963, 1970; Pretorius, 1964; Brock and Pretorius, 1964; Roering, 1968). The structural features in the western Bushveld Complex, where anticlinal folding was responsible for the doming of the granitic and mafic rocks in the Crocodile River fragment area, is

attributed to the Johannesburg fold as described by Ferguson (1973) and later by Walraven (1974). Similar domal structures are also present in the eastern Bushveld Complex.

Clubley-Armstrong and Sharpe (1979) are of the opinion that the coinciding trends of major displacements and the compressive stress direction prohibits the formation of domes by the emplacement of magma bodies, a situation which was previously described by De Waal (1970). The development of a regional stress system synchronous with the subsidence of the Transvaal basin, prior to and during the emplacement of the Bushveld Complex, could have resulted in the development of the Moos River Dome (Clubley-Armstrong and Sharpe, 1979). According to Clubley-Armstrong (1977), the structural highs are the result of regional stress systems which developed prior to the emplacement of the Bushveld Complex, but synchronous with the subsidence of the Transvaal basin. Similar explanations are given for the origin of the Molope Dome by Marlow and Van der Merwe (1977) in the Sekhukhuni Plateau. The age of the doming is unknown, but Clubley-Armstrong and Sharpe (1979) are of the opinion that an incipient pre-Bushveld dome existed which was produced by crustal depression and subsidence of the Transvaal Basin and was superimposed on a pre-existing basement feature. Von Gruenewaldt (1966) found evidence that the doming in the Dennilton area continued after the intrusion of the Upper and Main zone gabbros, but stopped before the intrusion of the granites.

The reactivation of the Dennilton Dome caused minor and later master joint systems, which continued into upper Waterberg times (Clubley-Armstrong and Sharpe, 1979). The master joint system was also found by Coertze *et al,* (1978) to be present in the sediments of the Waterberg Group which post-date the Bushveld granite. Vermaak (1970) reported strikes of 163° and 073° for the conjugate joints of the western Bushveld Complex, while Hunter (1975) described strikes of 150° and 160° as the most common direction in the Potgietersrust/ Marble Hall areas. Clubley-Armstrong (1977) was able to differentiate between systematic and non-systematic joints; the latter he attributed to contraction due to cooling. The systematic joints have strike directions of 102° and 042°, which is in agreement with the work of Von Gruenewaldt (1966) who found directions of 115° and 037°.

Previous investigations, therefore, indicate that the Bushveld Complex was structurally controlled by various features of which the pre-Transvaal basement structure and the development of structural highs and lows during the evolution of the Transvaal basin, are probably the most important.

The present investigation was conducted in order to unravel the tectonic setting of the granites and felsites in the study area and to contribute to our knowledge of the structural pattern of the complex in general.

7.2 JOINTS

No distinction was made between systematic and non-systematic joints in the study area. The well developed, clearly defined joints in the granites have strike directions which correspond well with the results of Vermaak (1970). The most prominent direction falls in the interval 135° to 150°, while the other major direction is approximately 060° (Fig. 7.1a).

A study of the orientation of the aplite veins and dykes indicates a close correspondence with that of the joints (Fig. 7.1b). This may indicate that the aplite intruded along pre-existing joints. The dilatational origin of the aplites indicate that the joints in the granites are to a certain extent contractional, not indicative of stress.

7.3 FAULTS AND QUARTZ FILLED LINEAMENTS

Faults are not very well developed in the study area, except in the vicinity of Rust de Winter Dam, where numerous small faults are present. On Prince Anna 234 JR (Folder I) a fault zone, which is located in the granite, is marked by oxidation and boxwork structures.

A large number of quartz-filled shear zones are present on the farms Roodepoortje 250 JR, Zandspruit 189 JR and Kameelrivier 202 JR. The amount of displacement along these structures is uncertain as they all occur within granite.

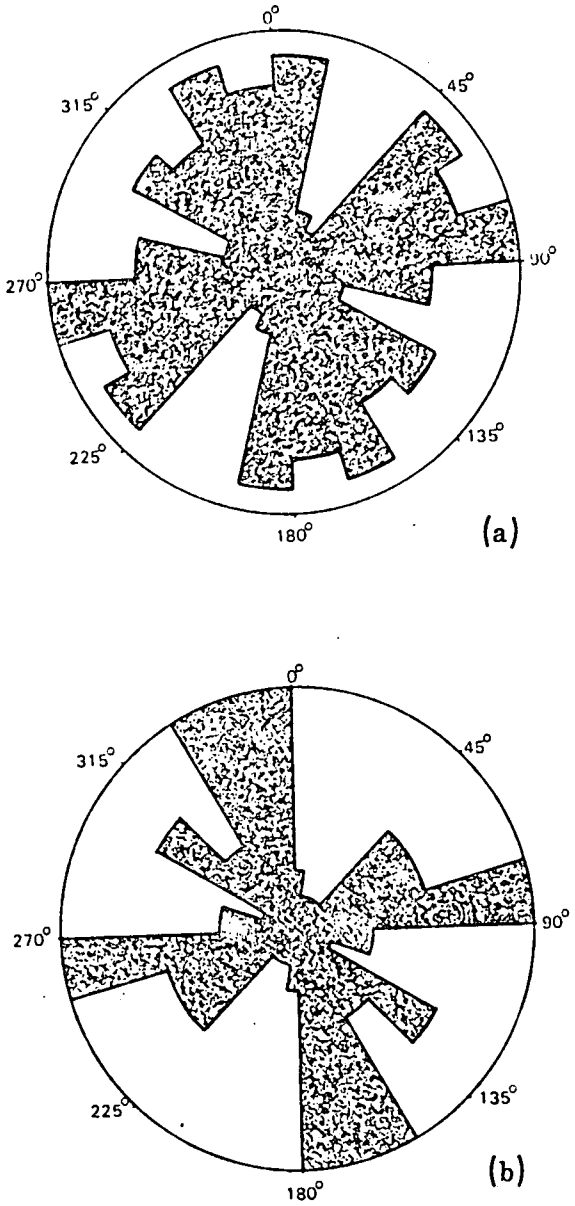

Fig. 7.1. Rose diagrams of the strike directions of joints (a) and aplite dykes (b) in the granites of the study area.

A graben-like structure, in which sediments of the Karoo Sequence were deposited, is present in the western part of the study area. The depression is bounded on the east and the west by very clearly defined lineaments (Fig. 7.2 and Fig. 7.3). Field relationships indicate that this structure possibly formed after the intrusion of the granite, but due to poor exposure in this area, it was not possible to determine the amount of displacement along the lineaments.

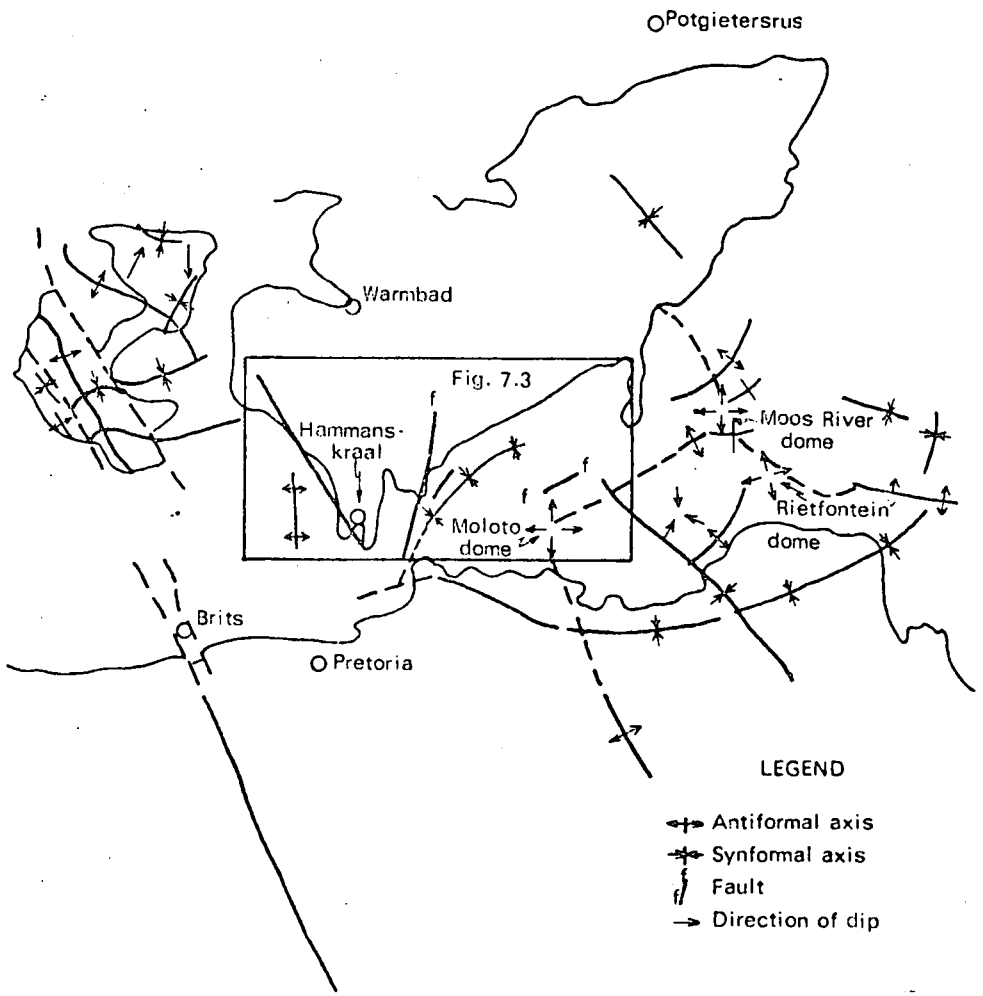

Fig. 7.2. Structural map of the Transvaal (after Hunter, 1975).

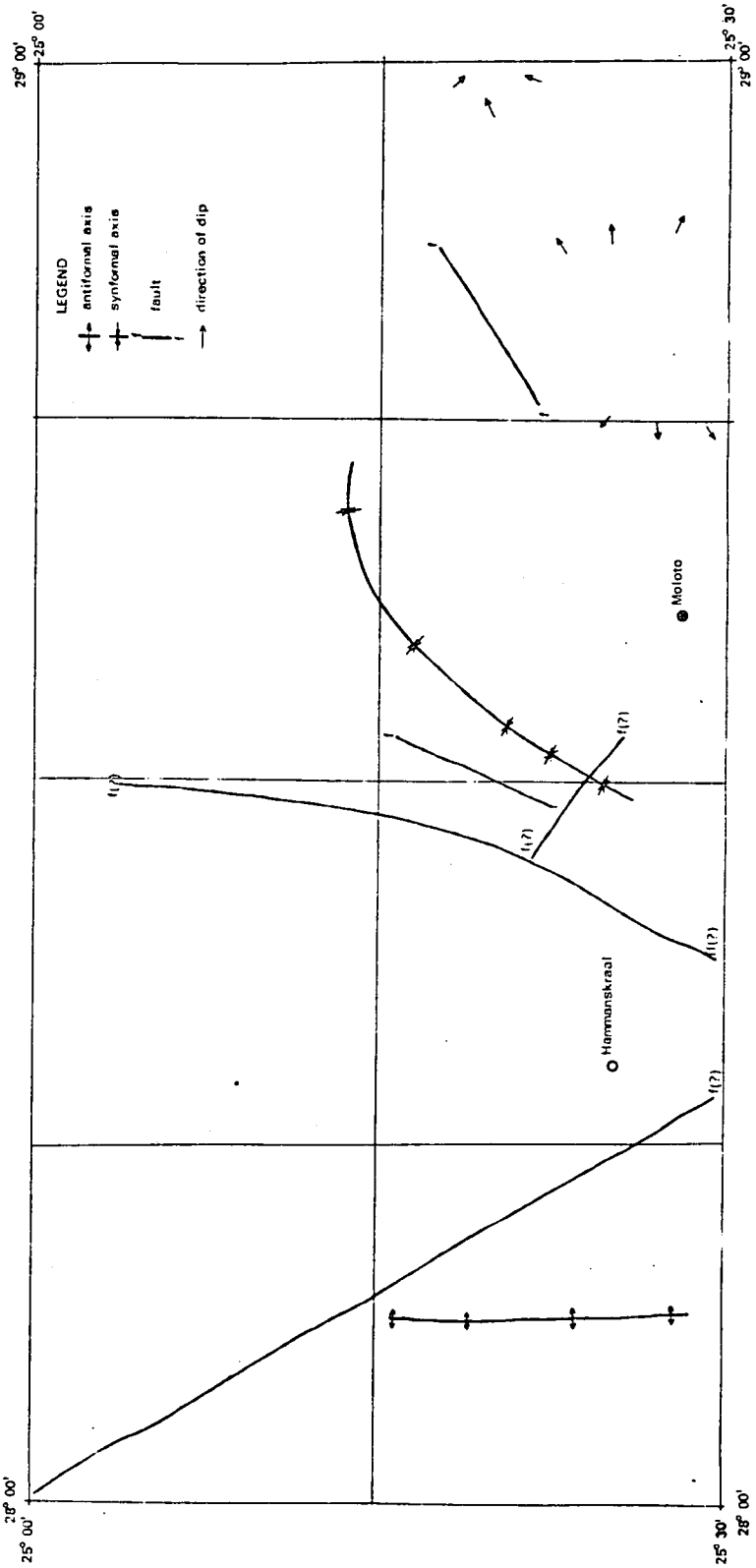

Fig. 7.3. Structural map of the study area.

7.4 FOLDS

Hunter (1975) and Clubley-Armstrong (1977) described north-east and north-west trending folds (Fig. 7.2) in the areas immediately east and west of the study area. Some of these folds can be extended into the study area. One of the most prominent structures in the study area is a large open synform in the Rooiberg felsite with dips of up to 45°, while the strike direction of the fold axis is north-east. Due to poor outcrops, it was not possible to link this fold axis with any other known axis in the surrounding area (Fig. 7.2). In the south-western corner of the area, the structure is marked by prominent highs and lows in the floor. The Moloto Dome is situated on the intersection of north-west and north-east trending fold axes.

An antiformal structure, which could not be linked to any known fold axis outside the study area, is present in the vicinity of Hammanskraal, while just to the east a synform intersects the Roodeplaat Complex just to the south of the study area. When the synformal axis of the fold structure in the felsite is extended in a southerly direction, it intersects the other fold axis in the near vicinity of the Roodeplaat Complex. The intersection of these two features, therefore, could have led to the positioning of the latter (Fig. 7.2).

7.5 STRUCTURAL FORM LINES

Badgley (1959) as well as Krumbein and Sloss (1963) describe a method by which the shape of a stratigraphic unit, using structural form lines, can be determined. This is done by contouring points of intersection between elevation contours and lithological contacts. As most of the structures in the study area are obscured by younger and superficial deposits, this technique was used to unravel the tectonic setting of the acid rocks.

In this study the upper contacts of the granites and the intersection of the contacts with the contour lines were used as control points. A two-dimensional plot of the data (Fig. 7.4) , using the computer programme of Davis

(1973), as well as a three-dimensional plot, (Fig. 7.5), using the programme of Watkins (1973), gives a general picture of the structural features of the area. The computed structural maps show all the major structures already described in the area, but also reveal a number of structural features hitherto not shown by regional mapping.

From these computed structural patterns, it can be seen that an antiformal ridge in the south-west of the area, which corresponds with the antiform mapped in Figure 7.4, is truncated by a linear feature along the side of the graben, which extends in a north-westerly direction (Fig. 7.5). This lineament corresponds fairly well with the directions of faulting in the Crocodile River Fragment and in the area around Brits. Farther to the east, another north-east trending lineament can be seen. These features define the sides of the graben-like structure already described.

A structural high, of which the centre is developed approximately half-way between Moloto and Verena (Fig. 7.2) is present in the south-western part of the area. The northern margin of this high is cut by a lineament indicated by the closely spaced contours on the two-dimensional and three-dimensional plots (Figures 7.4 and 7.5). This lineament corresponds with a quartz filled shear zone on surface.

A domal feature, which is very sharply bounded by high density contours, is present to the west of Moloto. The actual existence of this feature is, however, attributed to the volcanic activity in the vicinity of the Roodeplaat Complex. The central part of the area is marked by structural undulations in the granite floor and in the central part of the area a broad depression can be observed. In the north-east a north-west trending lineament occurs, which represents a zone of weakness pre-dating the faulting in the Moloto dome, as it does not extend into or past the fault zone (Fig. 7.5).

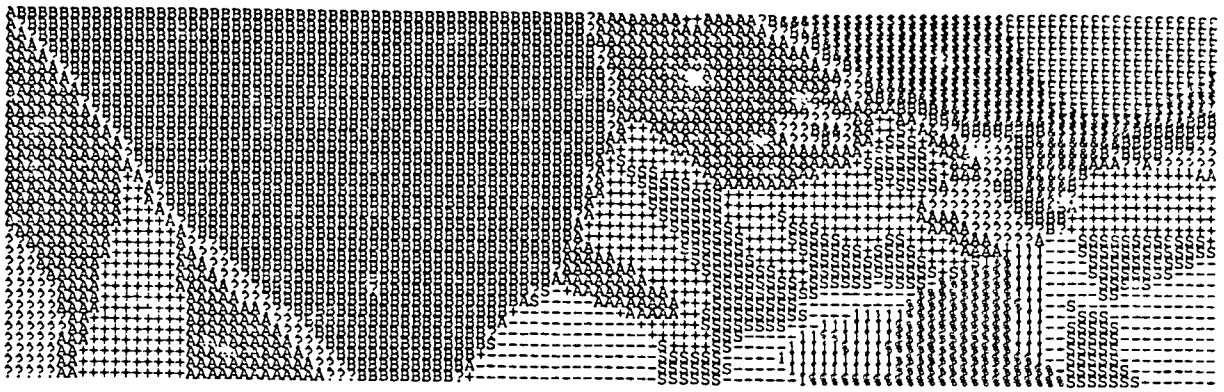

LEGEND

% = 4650 - 1500		A = 3900 - 3750	
1 = 4500 - 4350		? = 3750 - 3600	
- = 4350 - 4200		B = 3600 - 3450	
S = 4200 - 4050		& = 3450 - 3300	
+ = 4050 - 3900		$ = 3300 - 3150	
	£ = 3150 - 3000		

Fig. 7.4. Two-dimensional contour map of the top of the granite in the study area.

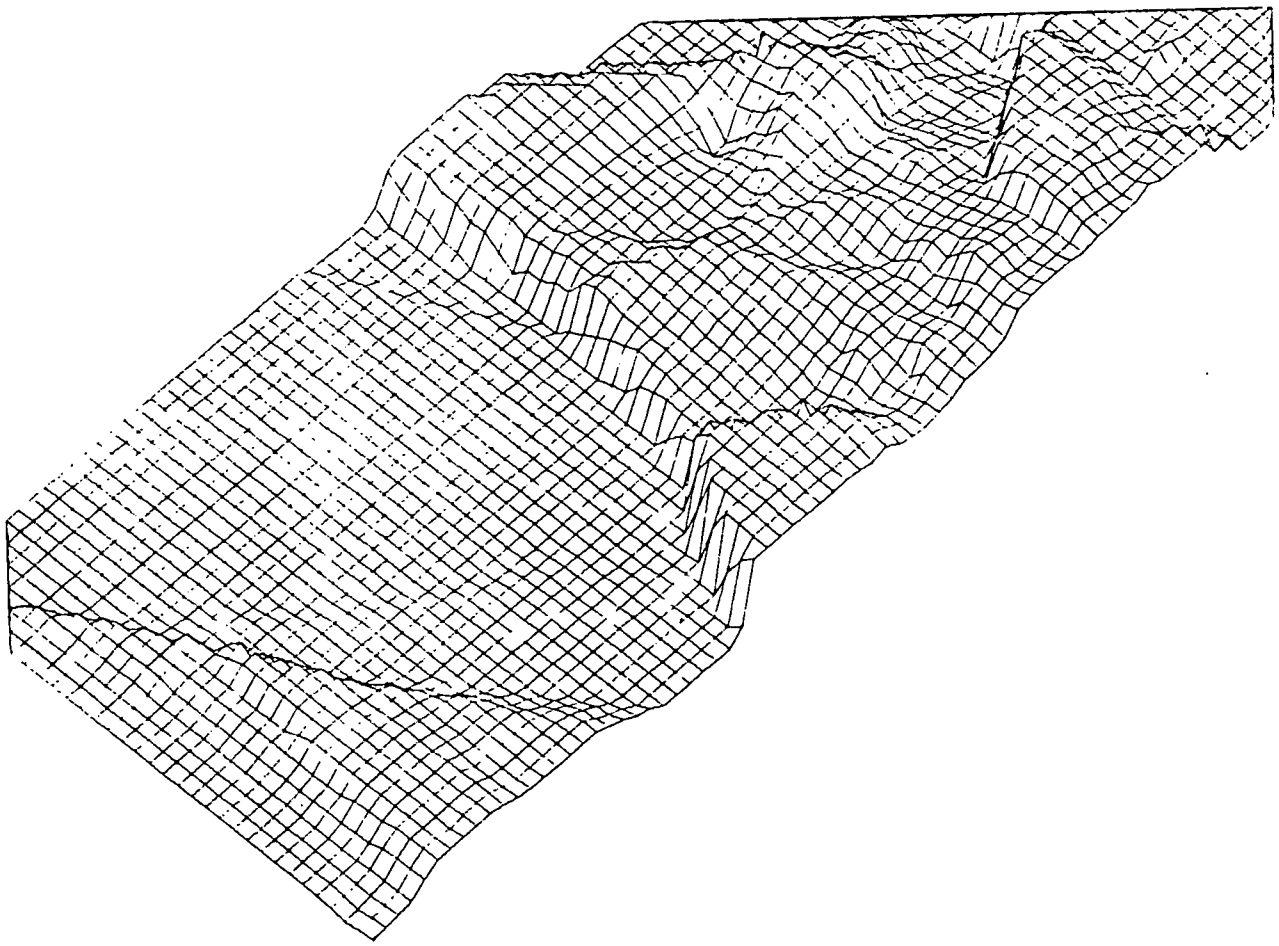

Fig. 7.5. Three-dimensional contour map of the top of the granite in the study area.

7.6 CONCLUSIONS

The structural evidence indicates that the area was subjected to structural instability during and after the intrusion of the granite, as indicated by the structural highs and lows in the granite floor. These structural features may represent cogenetic structures in the floor of the Bushveld Complex, as stated by previous investigators.

Folding in the felsite, as well as warping in the granites, indicate the existence of stress systems prior to and during the emplacement of the Bushveld granite. The presence of faults and other zones of crustal weakness in the granite point towards late to post-emplacement movements in the floor of the complex. This gives rise to the formation of graben structures in which sediments of the Karoo Sequence were deposited.

Prominent joint systems in the granite is most probably the result of contraction on cooling and serves as channels for the intrusion of late magma in the form of aplite veins.

8 SYNTHESIS AND MODEL

8.1 INTRODUCTION

A number of theories have been proposed for the formation of the felsic rocks in the Bushveld Complex. It was generally accepted that the felsite represents lava flows (Hall, 1932; Lombaard, 1932; Willemse, 1969; Von Gruenewaldt, 1972), although no clarity exists as to the mode of eruption of these rocks (Willemse, 1964). Due to the rather homogeneous nature of the Rooiberg felsites, as described by Von Gruenewaldt (1972) and Rhodes and Du Plessis (1975), Rhodes (1975) concluded that the lower part of the Rooiberg Group represents a meteoritic shock induced impact melt (as first suggested by Dence, 1971), which is analogous to the Onaping Formation of the Sudbury Complex (Peredery, 1972).

Although French and Hargraves (1971) could not find any evidence for this theory, Rhodes (1975) found similarities between the structure of the Bushveld Complex and other large impact features, for example that described by Howard *et al* (1972). Rhodes (1974) also found petrogenetic evidence that the Rooiberg Group and the Bushveld granites are unrelated, a factor which he attributed to the astrobleme origin of the former (Rhodes, 1975).

Work by Clubley-Armstrong (1977), however, indicates that the Rooiberg Group, as defined by Rhodes and Du Plessis (1976) has a thin formation at its base, which gradually changes into the upper formations, indicating differentiation of the parental magma.

The origin of the granophyre has been regarded as metasomatic by Iannello (1970) and Walraven (1977); a palingenetic product of the Rooiberg felsite by Irvine (1970), Von Gruenewaldt (1972) and Marlow (1976); a recrystallization product of the felsite (De Bruiyn, 1975), similar to an origin postulated for the leptite (Von Gruenewaldt, 1968; Molyneux, 1970); and highly metamorphosed Transvaal sediments (Strauss, 1947), which corresponds to another origin proposed for the leptite (Kushke, 1950; Steyn, 1950; Strauss,

1955; Truter, 1955; Willemse, 1964). Rhodes (1975a) and Walraven (1976, 1977) proposed that the granophyre is the product of eutectic crystallization, which is in agreement with ideas advanced by Lombaard (1932) and Hall (1932) who believed that the granophyre formed from a felsitic melt which crystallized under its own roof. There is distinct evidence for the different modes of granophyre formation with the result that each granophyre occurrence must be regarded in its own right.

The origin and mode of intrusion of the granites in the Bushveld Complex poses another problem. The majority of the granites have sheet-like forms, with the exception of the younger granites, for example the Makhutso Granite. The 'average' Bushveld granite displays initial rubidium-strontium ratios which indicate that the magma responsible for their formation was crust derived (Davis, 1973). It would, therefore, seem that the model as proposed by Iannello (1970) of a metasomatic granite, although it may not be excluded, may well be regarded as of only local importance. The contact relationships of the younger granites indicate that these granites are of igneous origin and were intruded as sheet-like bodies under the roof-rocks, while the younger granites intruded into these sheets as well as into the roof-rocks.

With the above theories in mind, a model based on geochemical and petrographical data, is postulated for the Acid Phases of the Bushveld Complex in the study area.

8.2 SYNTHESIS

Geochemical results show that the lower Damwal Formation differs significantly from the Kwaggasnek and Schrikkloof Formations (Fig. 4.28) and that the latter two probably formed consecutively from the same parental magma (Figures 4.24, 4.25 and 4.30).

The Damwal Formation is only present in the vicinity of Loskop Dam and is separated from the younger formations by a sandstone which signifies a hiatus in the volcanic activity. The presence of the sandstone, together with the significant break in chemical composition, indicate that the Damwal Formation may represent an older volcanic sequence. The significant differences in the lithologies between the Kwaggasnek and Schrikkloof Formations may have resulted from an increase in the water content of the magma of the Schrikkloof Formation resulting in explosive eruptions, which is manifested in the large number of tuffs and agglomerates present in this formation. The presence of flow-banding in the Schrikkloof Formation and the general lack of these features in the Kwaggasnek Formation also indicate a build-up of water content in the magma as flow-banding is more likely to occur in less viscous magma (Lacy, 1960).

The intercalated sandstones and shaly tuffs in the Schrikkloof Formation are indicative of interruptions in the volcanic cycle. These sediments were deposited in small isolated basins in the lava topography. The end of such a hiatus is marked by the development of features where high volatile content played a role, such as the flattened bombs in the shaly tuff on Groenfontein 125 JR.

The extrusion of the Rooiberg Group is problematic in the sense that no vents have yet been found. The shards in ash-flow tuffs as defined by Ross and Smith (1961), was used by Hoover (1964), Walker and Swanson (1968), Elston and Smith (1970) and Rhodes and Smith (1972) in other areas to define the position of vents, but no data could be obtained from the ash-flow tuffs in the Rooiberg felsites to determine the position of possible vents in the study area.

The alkali-iron-magnesium ratios of the granophyre, on an AFM-diagram (Fig. 5.9), and plots of other oxides (Fig. 5.10), show that the granophyre, in part, formed as a differentiation product of the granitic magma which gave rise to the felsite and later also to the Sekhukhuni granite in the area (Fig. 8.1). The granophyre which has an age of 2 090 my. (Faurie, 1977) probably formed by eutectic crystallization, similar to that described by Rhodes (1975a) and Walraven (1976, 1977). Walraven (1979) regards the granophyre as the shallow intrusive equivalent of the extrusive volcanic rocks of the Rooiberg Group. As eutectic crystallization in the system

quartz-orthoclase-albite will produce granophyre and as the composition of the granophyre in the study area corresponds with m, which is the temperature of minimum eutectic melt (Fig. 5.8), the conclusion is drawn that the granophyres of the present study represent the products of eutectic crystallization and not of assimilation or metasomatism. This is corroborated by the observed differentiation trends (Figures 5.9 and 5.10). The granitic magma, when it came into contact with the colder roof-rocks, gave rise to a chill phase against the upper contact, similar to that of the Enerdale granophyre (Dunham, 1965). The marginal facies, while of a similar composition as the overlying felsite, was subjected to devitrification caused by the generation of heat from the hotter magma below. Bow-tie granophyric spherulites in the lower part of the Kwaggasnek Formation indicate that this part of the formation was also subject to devitrification according to the mechanism described by Lofgren (1971), which also resulted in a devitrification front, converting part of the lower felsite to granophyre. Continuing crystallization of the melt resulted in the crystallization of quartz and feldspar from nuclei of plagioclase phenocrysts, thus giving rise to granophyre. The release of heat, due to crystallization, would in turn reduce supercooling, while the increase of water vapour pressure would lower the liquidus, causing the intergrowth to become coarser (Dunham, 1965). The combination of these factors would have the liquid at a temperature where the rate of nucleation is smaller, but the rate of crystal growth is still high, resulting in a granitic texture. This explains the gradational nature of both the upper and lower contacts of the granophyre.

After formation of the granophyre, the remainder of the magma intruded in a number of steps displaying differentiation as indicated by the major element (Fig. 6.19 and Fig. 6.20), as well as the trace element distributions (Fig. 6.21). The first granite to intrude was the Sekhukhuni granite (with an age of 1 920 my., Coertze *et al*, 1978), which formed large sills and locally developed a marginal facies of porphyritic granite, i.e. the Verena granite. These sills were later subjected to warping, thus forming domes of which the Moloto dome is a good example. The differentiation of the magma of this granite suite led to the formation of the Makhutso Granite magma, which intruded at 1 670 my. (Coertze *et al*, 1978). The trace element geochemistry of the Makhutso Granite does not follow the differentiation trend, due to the assimilation of leptite, which was responsible for the alteration of the geochemistry of this granite.

The variation diagrams reveal a continuous trend from the Sekhukhuni granite to the Klipvoor granite, while the Klipkloof granite plots near the beginning of the differentiation trend (Figures 6.19 and 6.20). This may indicate that the Klipvoor granite, which has an age of 1 670 my. (Coertze *et al,* 1978), represents the end member of magmatic differentiation of the granite melt which formed the acid phase of the Bushveld Complex. The Klipkloof granite, however, has an age of 1 400 my. (Coertze *et al,* 1978), which may indicate that it represents a younger, independant intrusion not related to the main acid phase of the Bushveld Complex.

The chemical data, illustrated in an AFM-diagram (Fig. 8.1) of all the acid rocks within the study area, indicate a differentiation along the tholeiitic trend, starting with the rocks of the Rooiberg Group and proceeding to the granophyre. Analyses of the Sekhukhuni granite slightly overlap with that of the granophyre and continue towards the Makhutso Granite. The Klipvoor granite plots near the end of the Sekhukhuni trend (or the beginning of the Makhutso trend). The Verena granite, which on field evidence is regarded as a marginal phase of the Sekhukhuni granite, shows a considerable scatter, possibly due to assimilation of leptite (Fig. 8.1).

The distribution of trace elements (Fig. 8.2) reveal that the felsite of the Rooiberg Group and the granophyre of the Rashoop Suite overlap within the field of normal granite as defined by El Bouseily and El Sokkary (1975). This indicates that the felsite and the granophyre may have had a common parental magma. As the result of prolonged crystallization, however, the granophyre shows a slight differentiation trend, as observed in Figure 8.1.

The trace elements of the Sekhukhuni granite defines a differentiation trend (Fig. 8.2) from the field of normal granite into the field of strongly differentiated granite (fields defined by El Bouseily and El Sokkary, 1975). Both the Klipvoor and Klipkloof granites fall within the field of strongly differentiated granite and define a continuation of the Sekhukhuni trend on this diagram (Fig. 8.2).

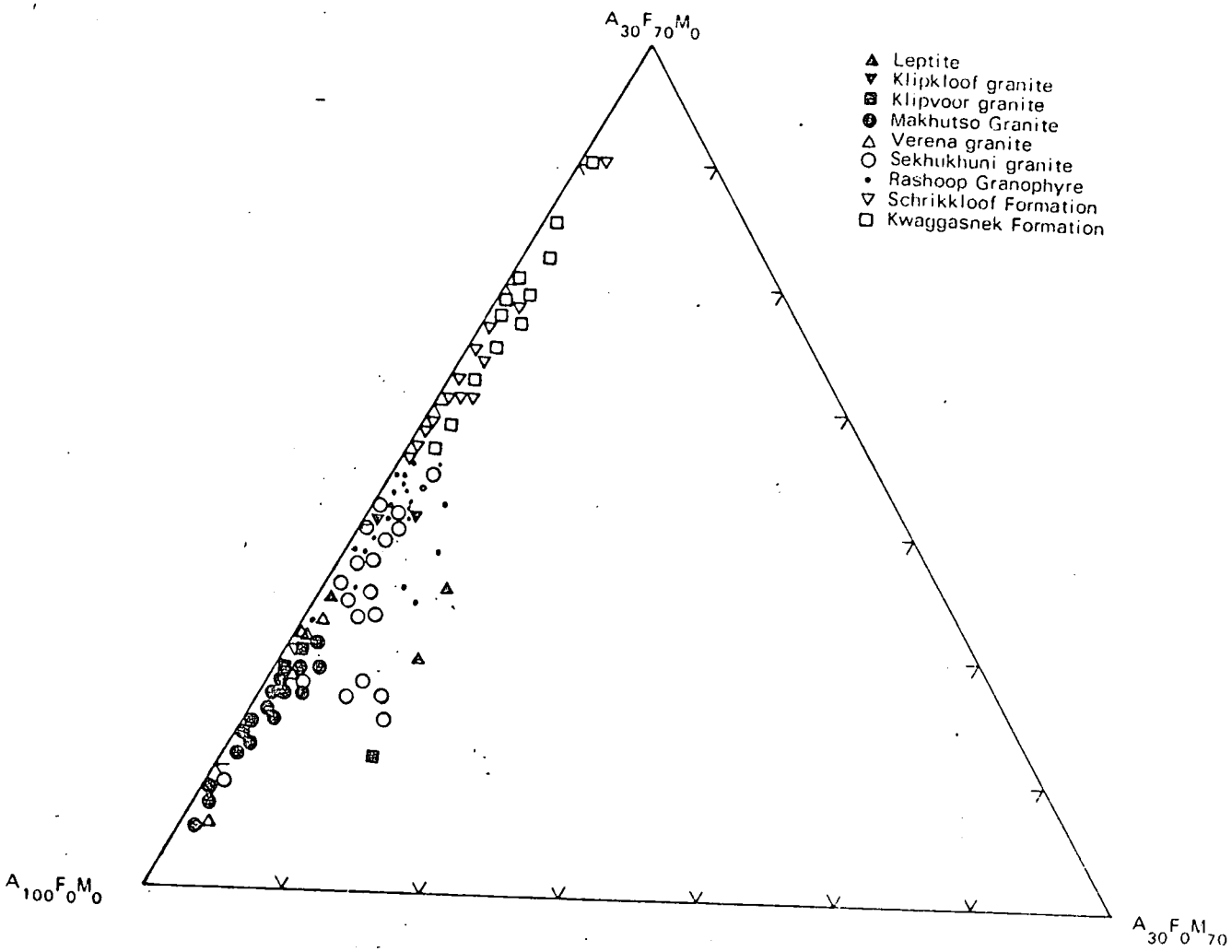

Fig. 8.1. AFM-diagram of the felsic rocks in the study area.

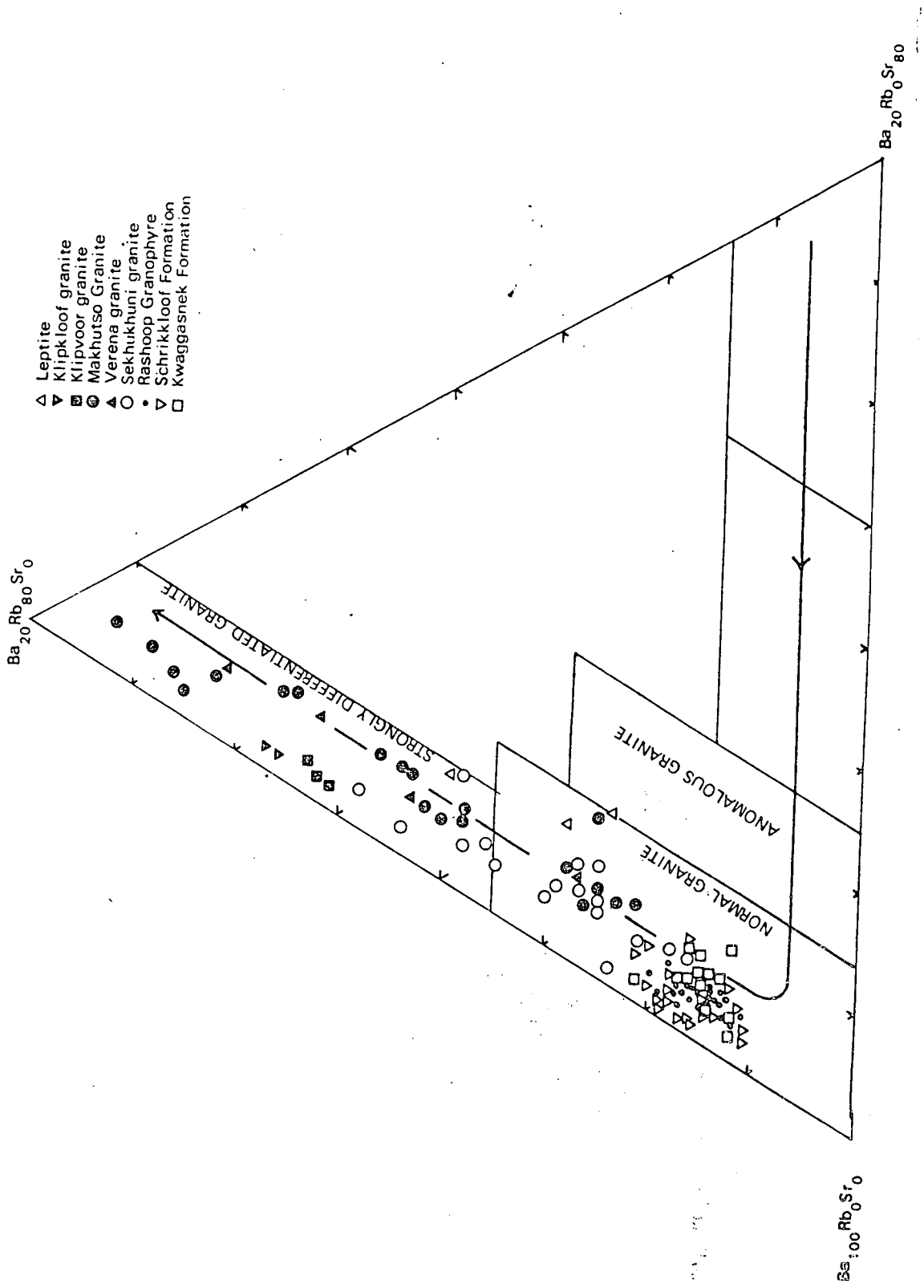

Fig. 8.2. Ba Rb Sr-diagram of the felsic rocks in the study area (fields and differentiation trend after El Bouseily and El Sokkary, 1975).

The Verena and Makhutso Granites fall in the fields of normal and strongly differentiated granite, following the trend of the Sekhukhuni granite. The relative position of both is, however, anomalous. This is due to enrichment of Ba and Sr, which is probably the result of assimilation of leptite.

8.3 MODEL

The final stages of the deposition of the Transvaal Sequence was marked by downwarping. This resulted in the formation of zones of weakness along which first extrusion of mafic magma (represented by the Hekpoort and Dullstroom lavas), followed by the extrusion of acid magma (represented by the Rooiberg felsite and its intrusive equivalent the Rashoop granophyre), followed by the intrusion of large volumes of mafic magma (represented by the Layered Sequence of the Bushveld Comples) and finally by the intrusion of acid magma (represented by various granites) could occur. In the study area, no equivalents of the first mafic magmatic pulse is present. The intrusion of the second pulse of acid lava is represented by the Damwal Formation near Loskop Dam (to the east of the study area) (Fig. 8.3), which formed in an incipient graben-like depression. This was followed by a hiatus of unknown length, which is represented by the deposition of sandstone in the Loskop Dam area. On further warping of the crust magma extruded to form the Kwaggasnek Formation, which is the basal unit in the study area (Fig. 8.4). The water content of this acid magma was probably relatively low, resulting in a homogeneous unit without flow-banding and with relatively small phenocrysts, which may indicate a rapid ascend of the magma. The extrusion of the Kwaggasnek volcanics was followed by a quiet period, during which considerable pressure was built up within the magma chamber. This resulted in explosive eruptions, which gave rise to the Schrikkloof Formation. The volcanic activity was often interrupted by periods of sedimentation resulting in a volcano-sedimentary sequence (Fig. 8.5).

A balance, under tensional conditions, between the litho- and hydrostatic pressures of the overburden and of the intruding magma, caused the magma to spread out laterally without reaching the surface. This granitic magma, responsible for the formation of the Sterk River and Blinkwater granophyres thus intruded underneath the roof-rocks in various stratigraphic positions. The magma crystallized below the roof of felsite and formed the Sterk River

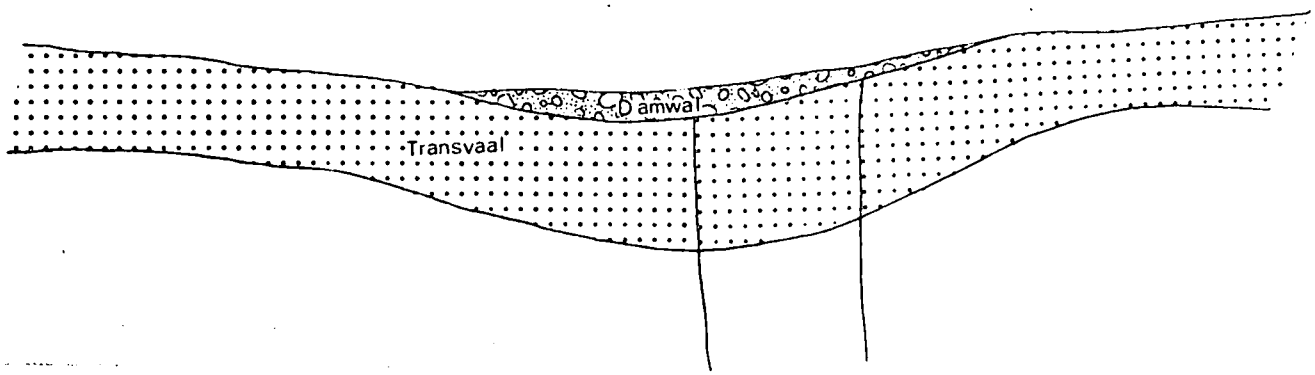

Fig. 8.3. Schematic diagram illustrating the extrusion of the Damwal Formation.

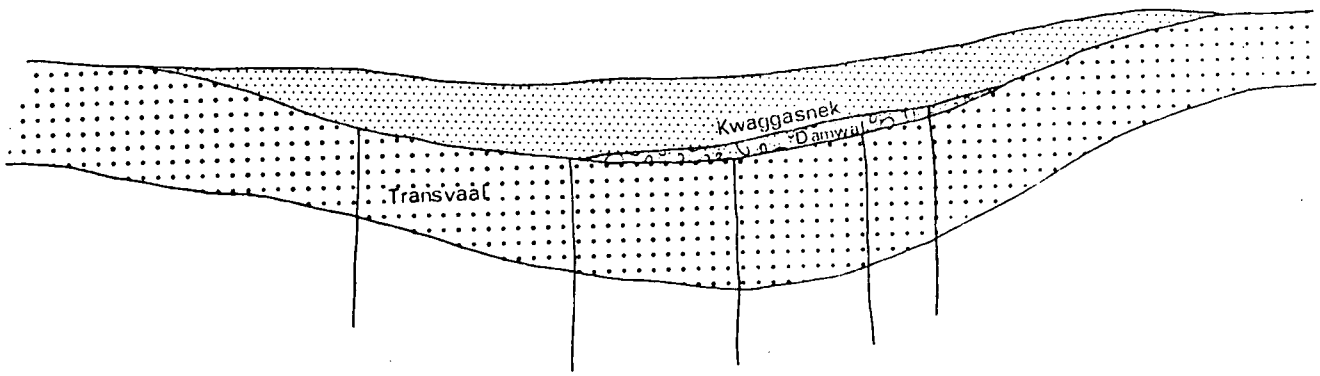

Fig. 8.4. Schematic diagram illustrating the extrusion of the Kwaggasnek Formation.

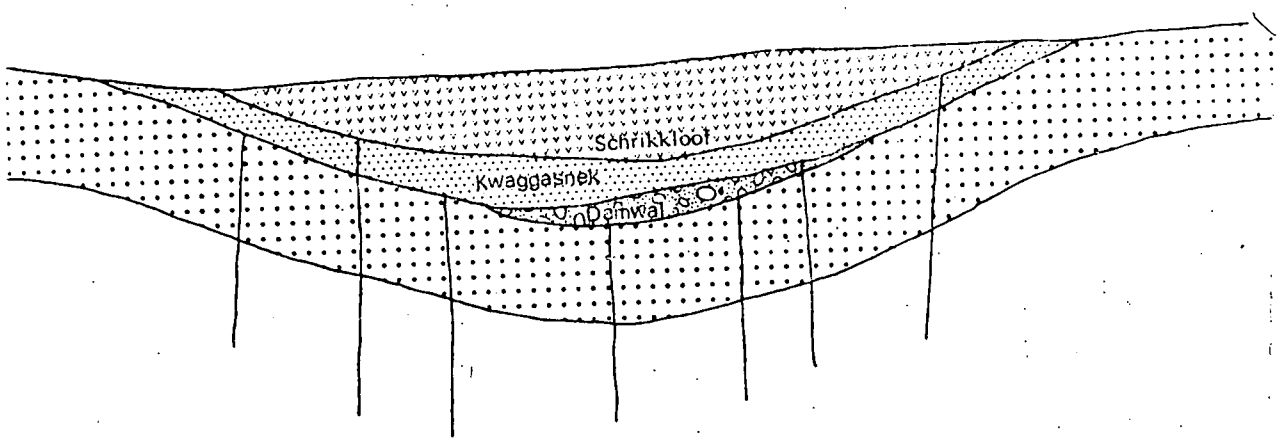

Fig. 8.5. Schematic diagram illustrating the extrusion of the Schrikkloof Formation.

granophyre (Fig. 8.6). The gradational contacts between the felsite and the granophyre resulted from devitrification and alteration of the felsite near the contact with the granophyre. In the study area the roof-rocks of the Blinkwater granophyre were removed by erosion, but in other areas it crystallized underneath a roof of Transvaal sediments.

No equivalents of the intrusion of the third pulse of mafic magma are present in the study area, although these layered, sill-like bodies outcrop over large areas of the complex (Fig. 8.6). According to Walraven (1976, 1977), the intrusion of the mafic bodies locally transformed the Transvaal sediments to form the Zwartbank pseudogranophyre. In other areas the intrusion of the mafic phase of the complex transformed the Rooiberg felsite by palingenesis to form granophyre (Von Gruenewaldt, 1972).

The fourth and final pulse of acid magma resulted in the intrusion of various granites, i.e. the Sekhukhuni granite and its marginal facies, the Verena granite and the Makhutso and Klipvoor granites (Fig. 8.7). The granite also locally transformed the Transvaal sediments into granophyre (Strauss, 1947, 1955; Iannello, 1971), i.e. the Stavoren granophyre. The granophyre in the Bushveld Complex thus has at least four different origins.

The intrusion of the Makhutso Granite was accompanied by large scale assimilation of roof-rocks (Fig. 8.7). The end of the entire magmatic event is characterized by the development of contraction joints into which rest magma in the form of aplite and other late magmatic fluids were emplaced.

The sequence of events described above is one of downwarping, followed by isostatic rebound and emplacement of magma. The Bushveld Complex was emplaced in the central part of the Kaapvaal Craton, thus into the thickest part of the sialic Precambrian crust. A combination of thick crust, downwarping, isostatic rebound and magmatism thus explains the uniqueness of the Bushveld Complex.

The Bushveld event was followed by renewed tectonic instability during which large scale vertical movements gave rise to horst and graben structures. The faults flanking the grabens served as feeders for the emplacement of alkaline bodies, such as the one on Groenfontein 120 JR. Some grabens also served as depositories of Karoo sediments.

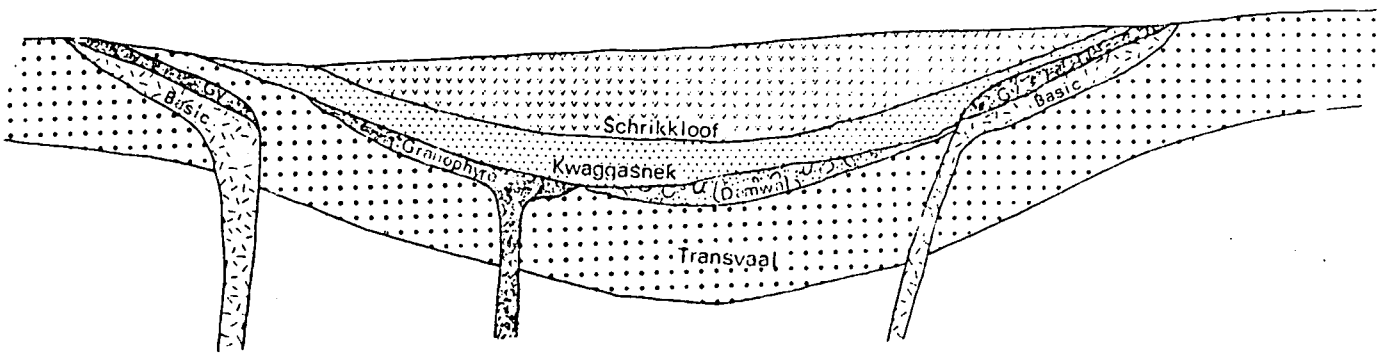

Fig. 8.6. *Schematic diagram illustrating the intrusion of the magmas responsible for the formation of the granophyre and the Mafic Phase of the Bushveld Complex.*

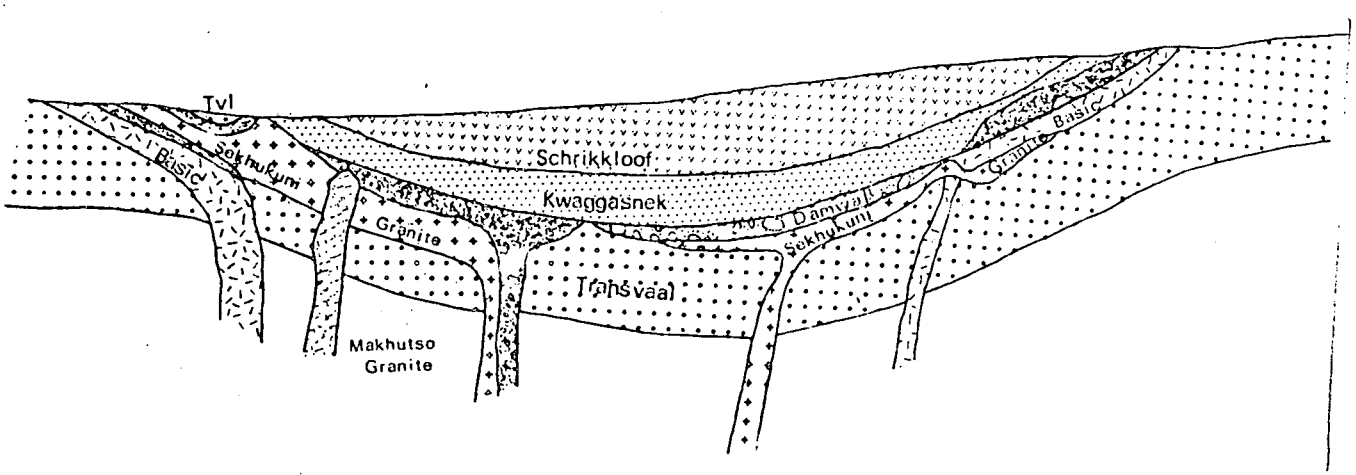

Fig. 8.7. *Schematic diagram illustrating the intrusion of the magmas responsible for the formation of the Sekhukhuni granite as well as the Makhutso Granite.*

9 ACKNOWLEDGEMENTS

The author wishes to express his sincere gratitude and appreciation to the following persons and institutions :

The Director of the Geological Survey, Dr. W.L. van Wyk, for permission to use information obtained during the course of mapping for the Geological Survey.

The Rector of the University of the North for funds for chemical analyses of samples and the use of facilities.

Prof. H.J. Oosthuizen of the University of the North for assistance in computer programming and computer time.

Mr. G.J. van Tonder and Mr. G.N. Bakkes for assistance in computer programming and the use of some of their programmes.

Mrs. M.J. Botha for typing the manuscript and Mr. J.J. Mouton for the preparation of the illustrations.

Prof. B.J.V. Botha for permission to enroll at the University of the Orange Free State and constant support in this project.

Dr. G.J. Geringer for his advice and suggestions during the study, critical reading of this thesis and valuable time spent in discussions.

My wife, Edney, for her encouragement when completion of this task seemed impossible.

---

10 REFERENCES

ALPER, A.M. and POLDERVAART, A., (1957). Zircons from the Animas Stock and associated rocks, New Mexico. *Econ. Geol., 52, 952–997.*

BADGLEY, P.C., (1959). *Structural Methods for the Exploration Geologist :* Harper and Row, New York, 280 pp.

BAILEY, E.H. and STEVENS, R.E., (1960). Selective staining of K-feldspar and plagioclase on rock slabs and thin sections. *Am. Mineral., 45, 1020–1026.*

BARING-HORWOOD, C., (1909). Notes and analyses of some typical Transvaal rocks. *Trans. geol. Soc. S. Afr., XIII, 29–55.*

BARTH, T.F.W., (1962). A final proposal for calculating the mesonorm of metamorphic rocks. *J. Geol., 70, 497–498.*

BERRY, L.G., (1974). *Selected Powder Diffraction Data for Minerals.* First ed., Joint Committee on Powder Diffraction Standards, Pennsylvania, 833 pp.

BLACK, G.P., (1954). The acid rocks of western Rhum. *Geol. Mag., 91, 257–272.*

BLACK, R.H., (1953). Analysis of bauxite exploration samples; an X-ray diffraction method. *Anal. Chem., 25, 743–748.*

BONEAU, C.A., (1960). Violations of assumptions underlying the t-test. *Psch. Bull., 51, 49–63.*

BOSHOFF, J.C., (1942). *The Upper Zone of the Bushveld Complex at Tauteshoogte.* Unpubl. D.Sc. thesis, Univ. Pretoria, 79 p.

BOWLER, C.M.L., (1959). *The distribution of the five alkali elements and fluorine in some granites and associated aureoles from the south-west of England.* Unpubl. Ph.D. thesis, Univ. Bristol.

BOWEN, N.L., (1928). *The Evolution of Igneous Rocks.* Princeton University Press, Princeton, N.J., 332 pp.

BROCK, B.B. and PRETORIUS, D.A., (1964). Rand basin sedimentation and tectonics; p. 549–599. In : Haughton, S.H., Ed., *The Geology of Some Ore Deposits in Southern Africa, Volume 1. Geol. Soc. S. Afr., Johannesburg, 625 pp.*

BUTTON, A., (1973). *A regional study of the stratigraphy and development of the Transvaal basin in the eastern and north-eastern Transvaal.* Unpubl. Ph.D. thesis, Univ. Witwatersrand, 352 pp.

CHAYES, F., (1956). *Petrographic Modal Analysis.* Chapman and Hall, London, 113 pp.

CLUBLEY-ARMSTRONG, A.R., (1977). *The geology of the Selonsrivier area, north of Middelburg, Transvaal, with special reference to the regions south-east of the Dennilton dome.* Unpubl. M.Sc. thesis, Univ. Pretoria, 107 pp.

---------- and SHARPE, M.T., (1979). The structural evolution of the Dennilton Dome and its relationship to the intrusion of the Bushveld Complex. *Trans. geol. Soc. S. Afr., 82, 23–36.*

COERTZE, F.J., (1962). The relationship between the Pretoria Series and the Bushveld Igneous Complex, north-east of Pretoria. *Ann. geol. Surv. S. Afr., 1, 67–70.*

COERTZE, F., JANSEN, H. and WALRAVEN, F. (1977). The transition from the Transvaal Sequence to the Waterberg Group. *Trans. geol. Soc. S. Afr., 80, 145–156.*

COERTZE, F.J., BURGER, A.J., WALRAVEN, F., MARLOW, A.G. and MACCASKIE, D.R., (1978). Field relations and age determinations in the Bushveld Complex. *Trans. geol. Soc. S. Afr., 81, 1–12.*

COETZEE, G.L., (1970). The Rooiberg felsite north of Nylstroom. *Spec. Publ. geol. Soc. S. Afr., 1, 312–325.*

COHEN, E., (1896). Über eine nördliche von Pretoria (Transvaal) gelegene Salzpfanne. *Tscherm. Miner. Petr. Mitt., 2, 15, 1–8.*

COMPTON, R.R., (1955). Trondhjemite batholith near Bidwell Bar, California. *Geol. Soc. Am. Bull., 66, 9–44.*

COOLEY, W.W. and LOHNES, P.R., (1962). *Multivariate Procedures for the Behavioural Sciences.* John Wiley and Sons, New York, 364 pp.

CROCKER, I.T., (1976). *Fluorite mineralisation in the Bushveld granites, south-east of Rooiberg, Transvaal.* Unpubl. M.Sc. thesis, Univ. Stellenbosch, 118 pp.

CROCKETT, R.N., (1971). Some aspects of post-Transvaal System tectogenesis in south-eastern Botswana with particular reference to the Lobatsi and Ramotswa areas. *Trans. geol. Soc. S. Afr., 74, 211–236.*

DAVIS, J.C., (1973). *Statistics and Data Analysis in Geology.* John Wiley and Sons, New York, 550 pp.

DAVIS, R.D., ALLSOPP, H.L., ERLANK, A.J. and MANTON, W.I., (1970). Sr-isotopic studies on various layered mafic intrusions in Southern Africa. *Spec. Publ. geol. Soc. S. Afr., 1, 576–593.*

DE BRUIYN, H., (1974). *The geology of the Bushveld Complex between Winterveld and Dennilton, Northern Transvaal, areas 2528A (Pienaarsrivier) and B (Rust der Winter).* Unpubl. Rep. geol. Surv. S. Afr., 44 pp.

(1975). Phenocryst analysis : A technique for determining the origin of granophyre in the Bushveld Complex. *Trans. geol. Soc. S. Afr., 78, 185–190.*

and RHODES, R.C., (1975). A new variety of Bushveld granite in the Dennilton area, Transvaal. *Trans. geol. Soc. S. Afr., 78, 89–95.*

DEER, W.A., HOWIE, R.A. and ZUSSMAN, J., (1974). *An Introduction to the Rock Forming Minerals.* Longmans, London, 528 pp.

DENCE, M.R., (1971). Impact melts. *J. Geophys. Research, 76, 5552–5565.*

DE VILLIERS, S.B., (1963). *Die geologie van die noordwestelike gedeelte van gebied 2428B.* Unpubl. Rep. geol. Surv. S. Afr., 30 pp.

DE WAAL, S.A., (1970). Interference-folding of Bushveld Igneous Complex age in the Transvaal System north of Marble Hall, Transvaal. *Spec. Publ. geol. Soc. S. Afr., 1, 283–298.*

(1972a). The Bushveld granites in the Zaaiplaats area. *Trans. geol. Soc. S. Afr., 75, 135–148.*

(1972b). Replies to discussions by D.H. Lenthall and P. Iannello. *Trans. geol. Soc. S. Afr., 76, 175–179.*

DIXEY, F., (1942). Notes on the erosion cycles of the Southern Transvaal. *S.A. Geog. J., xxiv, 35–40.*

DOWNIE, N.M. and HEATH, R.W., (1970). *Basic Statistical Methods* : Harper and Row, New York, Third ed., 356 pp.

DUNHAM, A.C., (1965). The nature and origin of the groundmass textures in felsites and granophyres from Rhum, Inverness-shire : *Geol. Mag., 102, 8–23.*

DU PLESSIS, M.D., (1976). *The Bushveld granites and associated rocks in the area north-west of Warmbaths, Transvaal* : Unpubl. M.Sc. thesis, Univ. Pretoria, 85 pp.

EL BOUSEILY, A.M. and EL SOKKARY, A.A. (1975). The relation between Rb, Ba and Sr in granitic rocks. *Chem. Geol., 16, 207–219.*

ELSTON, W.E. and SMITH, E.I., (1970). Determination of flow-direction of rhyolite ash-flow tuffs from fluidal textures : *Geol. Soc. Am. Bull., 81, 3393–3406.*

FAURIE, J.N. (1977). *Uraan-lood ouderdomsbepalings op granitiese gesteentes van die oostelike Bosveldkompleks.* Unpubl. M.Sc. thesis, Univ. Pretoria, 72 pp.

FERGUSON, J., (1973). The Pilansberg Alkaline Province, South Africa : *Trans. geol. Soc. S. Afr., 76, 249–270.*

FRENCH, B.M. and HARGRAVES, R.B., (1971). Bushveld Igneous Complex, South Africa : Absence of shock metamorphic effects in a preliminary search : *J. Geol., 79, 616–620.*

GAU, W.J., (1906). Geological notes on a portion of the Bushveld in the neighbourhood of the junction of the Elands and Olifants Rivers : *Trans. geol. Soc. S. Afr., 9, 67–73.*

GEOLOGICAL MAP OF THE UNION OF SOUTH AFRICA (1955). *Geol. Surv. S. Afr., Government Printer, Pretoria.*

GEOLOGICAL MAP OF THE REPUBLIC OF SOUTH AFRICA (1970). *Geol Surv. S. Afr., Government Printer, Pretoria.*

GEOLOGICAL MAP OF PRETORIA (2528) (1:250 000) (1978). *Geol. Surv. S. Afr., Government Printer, Pretoria.*

GLATTHAAR, C.W., (1956). *Die verysterde piroklaste en 'n na-Waterbergse graniet, suidoos van die dam Rust Der Winter :* Unpubl. M.Sc. thesis, Univ. Pretoria, 80 pp.

HALL, A.L., (1904). The geological survey of the north-east portion of the Pretoria District, including the tin fields : *Ann. Rep. geol. Surv. Transvaal for 1904, 37–44.*

(1905). *Report on a survey of Pretoria and neighbourhood. An explanation of the geological map and the environs.* Geol. Surv. Transvaal, Mem. 1.

(1909). The geology of the country west and north-west of Lydenburg, including Western Sekukuniland : *Ann. Rep. geol. Surv. Transvaal for 1909, 55–72.*

(1932). *The Bushveld Igneous Complex of the Central Transvaal :* Mem. geol. Surv. S. Afr., 28, 560 pp.

HARBAUGH, J.W. and MERRIAM, D.F., (1968). *Computer Applications in Stratigraphic Analysis* : John Wiley and Sons, New York, 282 pp.

HARKER, A., (1909). *The Natural History of Igneous Rocks* : Macmillan, New York.

HATCH, F.H. and CORSTORPHINE, G.S., (1909). *The Geology of South Africa :* Second ed., London.

HAWKES, D.D., (1967). Order of abundant crystal nucleation in a natural magma : *Geol. Mag., 104, 473–486.*

HAWKES, L., (1930). On rock glass, and the solid and liquid states. *Geol. Mag., LXVII, 17–24.*

HEIER, K.S. and BILLINGS, G.K., (1972). Rubidium : in WEDEPOHL, K.H., ed., *Handbook of Geochemistry,* II/3, 37, B1-N9; Springer Verlag, Berlin.

HOOVER, D.L., (1964). Flow structures in a welded tuff, Nye County, Navada (abs.): *Geol. Soc. Am. Spec. Paper 76, 83.*

HOWARD, K.A., OFFIELD, T.W. and WILSHIRE, H.G., (1972). Structure of the Sierra Madera, Texas, as a guide to central peaks of lunar craters : *Geol. Soc. Am. Bull., 83, 2795–2808.*

HUGHES, C.J., (1960). The Southern Mountains Igneous Complex, Isle of Rhum : *Quart. J. Geol. Soc. Lond., 116, 111–131.*

HUNTER, D.R., (1963). The Mozaan Series in Swaziland : *Geol. Surv. Swazild. Bull., 3, 5–16.*

(1970). The Ancient Gneiss Complex in Swaziland : *Trans. geol. Soc. S. Afr., 73, 107–150.*

(1972). The regional setting and extent of the Bushveld Complex : *Ann. Rep. Econ. Geol. Res. Unit, Univ. Witwatersrand, 25–26.*

(1975). *The Regional Geological Setting of the Bushveld Complex (An Adjunct to the Provisional Tectonic Map of the Bushveld Complex)* : Econ. Geol. Res. Unit, Univ. Witwatersrand, 18 pp.

HUTCHISON, C.S. and JEACOCKE, J.E., (1971). FORTRAN IV computer programme for calculation of the Niggli Molecular Norm : *Geol. Soc. Malaysia Bull., 4, 91–95.*

IUGS, Subcommission on the Systematics of Igneous Rocks. 25th Circular, Contribution No. 60, 1976.

IANNELLO, P. (1970). *The geology of the country between the Boshofsberg and the Crocodile River :* Unpubl. M.Sc. thesis, Univ. Pretoria.

IANNELLO, P., (1971). The Bushveld granites around Rooiberg, Transvaal : *Geol. Rdsch., 60, 630–655.*

IRVINE, T.N., (1970). Heat transfer during solidification of layered intrusions. I. Sheet and sills *: Can. J. Earth Sci., 7, 1031–1061.*

JONES, M.T., (1968). Explanation of the geology of quarter degree sheet 2326D and part of 2327C : Notwani and Limpopo river area : *Geol. Surv. Botswana.*

JORISSEN, E., (1905). Notes on some intrusive granites in the Transvaal, the Orange River Colony and in Swaziland : *Trans. geol. Soc. S. Afr., VII, 151–160.*

KARNER, F.R., (1970). Evidence for convection as a cause of zoning in granitic plutons *: Geol. Soc. Am. Abst., 2, No. 7, 590 pp.*

and BERTRAM, R.E., (1972). Modal variation in granitic units of the White Mountain Plutonic-Volcanic Series, New Hampshire *: 24th Int. Geol. Con., Section 2, 164–170.*

KING, L.C., (1962). *The Morphology of the Earth :* Oliver and Boyd, London.

KLUG, H.P. and ALEXANDER, L.E., (1954). *X-ray Diffraction for Polycrystalline and Amorphous Materials :* John Wiley and Sons, New York, 716 pp.

KOEN, G.M., (1955). Heavy minerals as an aid to the correlation of sediments of the Karoo System in the northern part of the Union of South Africa : *Trans. geol. Soc. S. Afr., 58, 281—366.*

KOSTOV, I., (1968). *Mineralogy* : Oliver and Boyd, London, 587 pp.

KRAUSKOPF, K.B., (1979). *Introduction to Geochemistry :* Second Ed., McGraw-Hill, New York, 617 pp.

KRUMBEIN, W.C. and SLOSS, L.L., (1963). *Stratigraphy and Sedimentation* : 2nd Ed., Freeman, 660 pp.

KUSHKE, O.H., (1950). *Granitic rocks of the Bushveld, north-west of Brits :* Unpubl. M.Sc. thesis, Univ. Pretoria, 45 pp.

KYNASTON, H., (1907). *The geology of a portion of the Bushveld north of Pretoria :* Expl. Sheet 2, geol. Surv. S. Afr., 28 pp.

(1909). *The Geology of the Waterberg Tinfields :* Mem. geol. Surv. S. Afr., 4, 114 pp.

(1929). *The Geology of the country surrounding Pretoria :* Expl. Sheet 1, geol. Surv. S. Afr.

and MELLOR, E.T., (1905). On a traverse from Pretoria to Pietersburg: *Annual Rep. for 1904, Geol. Surv. Transvaal, 11—25.*

LACY, E.D., (1960). Melts of granitic composition, their structure, properties and behaviour : *Repr. Int. Geol. Cong. Norden, Part 14, 7—15.*

LARSEN, L.H. and POLDERVAART, A., (1957). Measurement and distribution of zircons in some granitic rocks of magmatic origin : *Miner. Mag., 31, 544—564.*

LEAKE, B.E. and SKIRROW, G., (1960). The pelitic hornfelses of the Cashel-Lough Wheelaon Intrusion, County Galway, Eire : *J. Geol., 68, 23—40.*

LEIGHTON, M.W., (1954). Petrogenesis of a gabbro-granophye complex in northern Wisconsin : *Geol. Soc. Am. Bull., 65, 401—442.*

LEITH, M.J. and RHODES, R.C., (1971). Granitic rocks in the Basement Complex around Mapumulo, Natal, in the light of zircon studies : *Trans. geol. Soc. S. Afr., 74, 57—68.*

LENTHALL, D.H., (1972a). *The application of discriminatory and cluster analysis as an aid to the understanding of the Acid Phase of the Bushveld Complex :* Econ. Geol. Res. Unit, Univ. Witwatersrand, Inf. Circ., 72, 33 pp.

(1972b). A tentative model for the evolution and development of the Bushveld granites : *In Annual Rep. Econ. Geol. Res. Unit, Univ. Witwatersrand, 14, 32–34.*

(1973). A proposed nomenclature system for the granophyres associated with the Bushveld Complex : *Trans. geol. Soc. S. Afr., 76, 75–76.*

(1975). *Aspects of the geochemistry of the Acid Phase of the central and eastern Bushveld Complex :* Econ. Geol. Res. Unit, Univ. Witwatersrand, Inf. Circ., 99, 20 pp.

LEROUX, J., LENNOX, D.H. and KAY, K., (1953). Direct quantitative X-ray analysis by diffraction-absorption technique : *Anal. Chem., 25, 740–743.*

LI, C.C., (1964). *Introduction to Experimental Statistics :* McGraw-Hill, New York, 460 pp.

LINTON, D.L., (1955), The problem of tors : *Geogr. J., 124, 289–291.*

LOFGREN, G., (1971). Experimentally produced devitrification textures in natural rhyolitic glass : *Geol. Soc. Am. Bull., 82, 111–124.*

LOMBAARD, B.V., (1929). The geology of a centrocline, 18 miles north-east of Pretoria : *Trans. geol. Soc. S. Afr., 32, 151–164.*

(1931). *The geology of the north-eastern Pretoria District and adjoining country :* Expl. Sheet 18, geol. Surv. S. Afr., 48 pp.

(1932). The felsites and their relations in the Bushveld Complex : *Trans. geol. S. Afr., 37, 5–52.*

MACDONALD, G.A. and KATSURA, T., (1964). Chemical composition of Hawaiian lavas : *J. Petrol., 5, 82–133.*

MARLOW, A.G., (1976). *The geology of the Bushveld Complex on the Sekhukhune Plateau, Eastern Transvaal :* Unpubl. M.Sc. thesis, Univ. Pretoria, 105 pp.

and VAN DER MERWE, M.J., (1977). The geology and the potential economic significance of the Malope area, north-eastern Bushveld Complex : *Trans. geol. Soc. S. Afr., 80, 117–124.*

McCARTHY, T.S., (1977). *Geochemical studies of selected granitic terraines in South Africa :* Unpubl. Ph.D. thesis, Univ. Witwatersrand, 350 pp.

MELLOR, E.T., (1906). Evidence of contemporaneous volcanic activity in the lower portion of the Waterberg Formation : *Trans. geol. Soc. S. Afr., VIII, 38—41.*

MENGE, G.F.W., (1963). *The cassiterite deposits on Doornhoek 342 KR and vicinity, west of Naboomspruit, Transvaal :* Unpubl. M.Sc. thesis, Univ. Pretoria, 56 pp.

MERENSKY, H., (1909). The rocks belonging to the area of the Bushveld Granite Complex in which tin may be expected with descriptions of the deposits actually found : *Trans. geol. Soc. S. Afr., XI, 25—42.*

MILLER, R.L. and KAHN, J.S., (1962). *Statistical Analysis in the Geological Sciences :* John Wiley and Sons, New York, 483 pp.

MOLENGRAAFF, G.A.F., (1905). Inter Colonial Irrigation Commission : *Pretoria, 90 pp.*

MOLYNEUX, T.G., (1970). *A geological investigation of the Bushveld Complex in Sekhukhuneland and part of the Steelpoort valley, Eastern Transvaal, with particular reference to the oxide minerals :* Unpubl. D.Sc. thesis, Univ. Pretoria, 123 pp.

MURSKY, G., (1972). Origin and significance of zonation in a granitic intrusion : *24th Int. Geol. Con., Section 2, 181—190.*

NOCKOLDS, S.R. and ALLEN, R., (1954). The geochemistry of some igneous rock series. Part II : *Geochim. Cosmochim. Acta., 5, 245—285.*

(1956). The geochemistry of some igneous rock series. Part III : *Geochim. Cosmochim. Acta., 9, 34—77.*

ORVILLE, P.M., (1967). Unit cell parameters of the microcline-low albite and the sanidine-high albite solid solution series : *Am. Miner., 52, 55—86.*

PEREDERY, W.V., (1972). Chemistry of fluidal glasses and meld bodies in the Onaping Formation : *in New Developments in Sudbury Geology; Spec. Paper, Geol. Assoc. Canada, 10, 45—59.*

POLDERVAART, A. and PARKER, A.B., (1964). The Crystallization Index as a parameter of igneous differentiation in binary variation diagrams : *Am. J. Sci., 262, 281—289.*

PRETORIUS, D.A., (1964). *The geology of the South Rand Gold Field :* Econ. Geol. Res. Unit, Univ. Witwatersrand, Inf. Circ., 17, 86 pp.

REESOR, J.E., (1958). Dewar Creek map area with special emphasis on the White Creek Batholith, British Columbia : *Mem. Geol. Surv. Canada, 292, 58—60.*

RHODES, R.C., (1973). Petrologic framework of the Mogollon Plateau Volcanic Ring Complex : *Univ. New Mexico, Publ. in Geology, 8, 12–26.*

(1974). Petrochemical characteristics of Bushveld granite and Rooiberg felsite : *Trans. geol. Soc. S. Afr., 9, 119–126.*

(1975). New evidence for impact origin of the Bushveld Complex : *Geology, 3, 549–554.*

(1975a). Bushveld granophyre in the Stavoren tin District, Transvaal : *Trans. geol. Soc. S. Afr., 78, 71–74.*

and BORNHORST, T.J., (1975). Application of discriminant function analysis to the felsic rock of the Bushveld Complex : *Lithos, 8, 193–198.*

and DU PLESSIS, M.D., (1976). Notes on some stratigraphic relations in the Rooiberg felsite : *Trans. geol. Soc. S. Afr., 79, 183–185.*

and SMITH, E.I., (1972). Distribution and directional fabric of ash-flow sheets in the north-western Mogollon Plateau, New Mexico : *Geol. Soc. Am. Bull., 83, 1863–1868.*

ROERING, C., (1968). *Non-orogenic granites and the age of the Precambrian Pongola Sequence* : Econ. Geol. Res. Unit, Univ. Witwatersrand, Inf. Circ., 46, 34 pp.

ROSS, C.S. and SMITH, R.L., (1960). *Ash-flow tuffs : Their origin, geologic relations and identification* : U.S. Geol. Surv. Prof. Paper, 366, 81 pp.

SHAND, S.J., (1921). The nepheline rocks of Sekhukhuniland : *Trans. geol. Soc. S. Afr., 24, 111–149.*

(1922). The alkaline rocks of the Franspoort line, Pretoria District : *Trans. geol. Soc. S. Afr. 25, 81–100.*

SHARPE, M.R. and VON GRUENEWALDT, G., (1979). A structural framework for the emplacement of the Bushveld Complex (abs.) : *18th Cong. geol. Soc. S. Afr., 337–338.*

SMALL, R.L., (1972). *The Study of Landforms* : University Press, Cambridge, 486 pp.

SMIT, P.J., HALES, A.C. and GOUGH, D.I., (1962). *The gravity survey of the Republic of South Africa* : Handbook geol. Surv. S. Afr., 3, 486 pp.

SNYMAN, A.A., (1953). *Die geologie van 'n gebied ten ooste van Hammanskraal, Transvaal* : Unpubl. Rep. geol. Surv. S. Afr., 18 pp.

SPIEGEL, M.L., (1972). *Theory and Problems of Statistics* : Schaum's Outline Series, McGraw-Hill, New York, 359 pp.

SPIES, J.J., (1952). *Die geologie van die gebied in die omgewing van Hammanskraal, Distrik Pretoria :* Unpubl. Rep. geol. Surv. S. Afr., 18 pp.

STEYN, J.G.D., (1950). *Die geologie van die Bosveldkompleks in die omgewing van Magneethoogte :* Unpubl. M.Sc. thesis, Univ. Pretoria, 66 pp.

(1962). *The mineralogy of the more important tin-bearing pipes on Stavoren :* Mem. geol. Surv. S. Afr., 51, 103 pp.

STORMER, J.C., (1975). A practical two-feldspar geothermometer : *Am. Mineral., 60, 667–674.*

STRAHLER, A.N., (1952). Hypsometric (area-altitude) analysis of erosional topography : *Geol. Soc. Am. Bull., 63, 1117–1142.*

(1969). *Physical Geography :* 3rd ed., John Wiley, New York, 732 pp.

STRAUSS, C.A., (1947). Granitization and rheomorphism associated with the granite near the Leeuwpoort Tin Mine : *Trans. geol. Soc. S. Afr., 50, 161–170.*

(1955). *Die geologie en mineraalafsettings van die Potgietersrustinvelde :* Mem. geol. Surv. S. Afr., 46, 268 pp.

and TRUTER, F.C., (1944). The Bushveld granites in the Zaaiplaats Tin Mining area : *Trans. geol. Soc. S. Afr., 47, 47–77.*

STRECKEISEN, A., (1967). Classification and nomenclature of igneous rocks : *Neues Jahrb. Mineral. Abhandl., 107, 144–240.*

TATLOCK, D.B., (1966). *Rapid modal analysis of some felsic rocks from calibrated X-ray diffraction patterns :* Geol. Surv. *Am.* Bull., 1209, 41 pp.

TAUBENECK, W.H., (1957). Geology of the Elkhorn Mtn., north-eastern Oregon, Bald Mountain Batholith : *Geol. Soc. Am. Bull., 68, 181–238.*

(1967). *Petrology of the Cornucopia tonalite unit, Cornucopia Stock, Wallow Mountains, north-eastern Oregon :* Geol. Soc. *Am.* Spec. Paper, 91, 56 pp.

TEICHMAN, R.F.H., (1962). *Die geologie van die gebied noord van Kameelfontein, Distrik Pretoria :* Unpubl. Rep. geol. Surv. S. Afr., 8 pp.

TILL, R., (1974). *Statistical Methods for the Earth Scientist, an Introduction :* Macmillan, London, 154 pp.

TOENS, P.D., (1952). *The geology around Leeuwfontein, north-east of Pretoria :* Unpubl. M.Sc. thesis, Univ. Pretoria.

TRUTER, F.C., (1943). *Interim report on tin and associated minerals of parts of the Bushveld Igneous Complex, Central Transvaal :* Unpubl. Rep. geol. Surv. S. Afr.

(1949). A review of volcanism in the geological history of South Africa : *Proc. geol. Soc. S. Afr., 52, XXIX–LXXXIX.*

(1955). Modern concepts of the Bushveld Igneous Complex : *C.C.T.A. South reg. Comm. Geol., 1, 77–87.*

TUTTLE, O.F. and BOWEN, N.L., (1958). *The origin of granite in the light of experimental studies in the system* $NaAlSi_3O_8$-$KAlSi_3O_8$-SiO_2-H_2O *:* Mem. Geol. Surv. Am., 74, 153 pp.

TYRRELL, G.W., (1958). *The Principles of Petrology.* Methuen and Company Ltd., London, 349 pp.

VAN BILJON, S., (1949). The transformation of the Pretoria Series in the Bushveld Complex : *Trans. geol. Soc. S. Afr., 39, 45–76.*

VANCE, J.A., (1961). Zoned granitic intrusions – an alternative hypothesis of origin : *Geol. Soc. Amer. Bull., 72, 1723–1727.*

VAN DER KAADEN, G., (1951). *Optical studies on natural plagioclase feldspars with high- and low-temperature optics :* Unpubl. thesis, State Univ. Utrecht, 150 pp.

VAN DER WESTHUIZEN, J.M., (1945). *Die geologie van Bothasberg, Bosveldkompleks* : Unpubl. M.Sc. thesis, Univ. Pretoria, 27 pp.

VAN ZIJL, J.S.V., (1965). *A geological-geophysical investigation of the Albert Silver Mine, north of Bronkhorstspruit, Transvaal* : Bull. geol. Surv. S. Afr., 43, 84 pp.

VENTER, F.A., (1933). Breccias and associated rocks occurring north-east of Pretoria : *Trans. geol. Soc. S. Afr., 36, 41–63.*

VERMAAK, C.F., (1970). The geology of the lower portion of the Bushveld Complex and its relationship to the floor rocks in the area west of the Pilanesberg, Western Transvaal *: Spec. Publ. geol. Soc. S. Afr., 1, 242–262.*

VERWOERD, W.J., (1967). *The carbonatites of South Africa and South West Africa :* Handbook geol. Surv. S. Afr., 6, 452 pp.

VOGT, J.H.L., (1930). The physical chemistry of the magmatic differentiation of igneous rocks III Part 2. On the granitic rocks : *Skr. Norske Vidensk. Akad., I Mat.-Naturv., Kl., 8.*

VON GRUENEWALDT, G., (1966). *The geology of the Bushveld Igneous Complex east of the Kruis River Cobalt occurrence, north of Middelburg, Transvaal :* Unpubl. M.Sc. thesis, Univ. Pretoria, 104 pp.

(1968). The Rooiberg felsite north of Middelburg : *Trans. geol. Soc. S. Afr., 71, 153–172.*

(1972). The origin of the roof-rocks of the Bushveld Complex between Tauteshoogte and Paardekop in the Eastern Transvaal : *Trans. geol. Soc. S. Afr., 75, 121–134.*

VON PLATEN, H., (1965). Kristallisation granitischer Schmetzen : *Contrib. Miner. Petr., 11, 334–381.*

WAGER, L.R., (1961). A note on the origin of ophitic texture in the chilled olivine gabbro of the Skaergaard Intrusion : *Geol. Mag., 98, 353–366.*

WAGNER, P.A., (1920). Note on the volcanic origin of the salt pan on the farm Zoutpan 467 : *Trans. geol. Soc. S. Afr., 23, 52–58.*

(1921). *The Mutue Fides-Stavoren Tinfields :* Mem. geol. Surv. S. Afr., 16, 192 pp.

(1922). *The Pretoria Saltpan. A soda caldera :* Mem. geol. Surv. S. Afr., 20, 136 pp.

(1927). *The geology of the north-eastern part of the Springbok Flats and surrounding country :* Explan. Sheet 17, geol. Surv. S. Afr., 104 pp.

(1929). *The Pretoria Saltpan :* 15th Int. Geol. Cong., Excursion Guide B11, 6.

WALKER, G.W. and SWANSON, D.A., (1968). Laminar flowage in a Pleistocene soda rhyolite ash-flow tuff, Lake and Harney Counties, Oregon : *U.S. Geol. Surv. Prof. Paper, 600B, B37–B47.*

WALRAVEN, F., (1974). Tectonism during the emplacement of the Bushveld Complex and the resulting fold structures : *Trans. geol. Soc. S. Afr., 77, 323–328.*

(1976). Notes on the late-stage history of the western Bushveld Complex : *Trans. geol. Soc. S. Afr., 79, 13–21.*

(1977). *The transition between the Mafic and the Acid Phase of the Bushveld Complex in the Rustenburg-Brits area :* Unpubl. M.Sc. thesis, Univ. Pretoria, 111 pp.

(1979). Granophyre – lava relations in the Bushveld Complex : *Ann. geol. Surv. S. Afr., 13, 59–80.*

WATKINS, S.L., (1973). Masked three-dimensional plot program with rotations (J6) : *Collected Algorithms from CACM, 483, 1–4.*

WELLINGTON, J.H., (1926a). The physical and economical geography of the central Magaliesberg region of the Southern Transvaal : *S.A. Geogr. J., 9, 37–44.*

(1926b). The present cycle of erosion in the Magaliesberg region : *S.A. J. of Sci., 23, 197–203.*

(1937). The Pre-Karoo peneplain in the south-central Transvaal : *S.A. J. of Sci., 33, 281–295.*

WHITNEY, J.A. and STORMER, J.C., (1976). Geothermometry and geobarometry in epizonal granite intrusions : a comparison of iron-titanium oxides and coexisting feldspars : *Am. Mineral., 61, 751–761.*

WILKE, D.P., (1963). *Die geologie van die suidelike gedeelte van blad 2428B :* Unpubl. Rep. geol. Surv. S. Afr., 47 pp.

WILLEMSE, J. (1964). A brief outline of the geology of the Bushveld Complex. *p. 91–128 in Haughton, S.H., Ed., The Geology of some Ore Deposits of Southern Africa, Vol. II: Geol. Soc. S. Afr., Johannesburg, 739 pp.*

(1969). The geology of the Bushveld Igneous Complex, the largest repository of magmatic ore deposits in the world : *Econ. Geol. Mon., 4, 1–22.*

WINKLER, H.G.F., (1976). *Petrogenesis of Metamorphic Rocks :* 4th Ed., Springer-Verlag, New York, 334 pp.

WOLHUTER, L.E., (1954). *The geology of the country surrounding Loskop Dam, Transvaal* : Unpubl. M.Sc. thesis, Univ. Pretoria, 66 pp.

WOODARD, H.H., (1957). Diffusion of chemical elements in some naturally occurring silicate inclusions : *J. Geol., 65, 61–84.*

WRIGHT, T.L., (1968). X-ray and optical study of alkali feldspar : II. An X-ray method for determining the composition and structural state from measurement of 2Θ values for three reflections : *Am. Mineral., 53, 88–104.*

and STEWART, D.B., (1968). X-ray and optical study of alkali feldspar : I. Determination of composition and structural state from refined unit-cell parameters and 2V *: Am. Mineral., 53, 38–87.*

APPENDIX I

DETERMINATION OF THE ANORTHITE CONTENT OF PLAGIOCLASE AND THE COMPOSITION OF ALKALI FELDSPARS

A curve which yields the composition of plagioclase feldspars up to labradorite, was compiled from the data in Kostov (1968). This part of the curve represents the most common compositions of the plagioclases obtained from granites (Fig. I.1). The powder sample was scanned at a $\frac{1}{4}$ degree 2θ per minute at 15 mA and 35 kV tube settings, while the recorder was set at 5 mm/minute and a time constant of 5. The diffracted curve (Fig. I.2) may be read off and the anorthite content estimated.

Data obtained from a diffraction pattern, when correlated with data obtained from thin sections, determined by the method of Van der Kaaden (1951), indicate that the difference between these two methods is less than 2 per cent (Table I.1). A statistical t-value of 0,14 satisfies the null hypothesis and signifies that this method may be used for a rapid determination of the anorthite content of plagioclase.

The composition of the alkali feldspars were determined by the three peak method, described by Wright (1968). In this method the (002), ($\bar{2}$04) and (060) reflections were used to determine the position of the ($\bar{2}$01) reflection, which gives an indication of the composition of the feldspars. If the position of the calculated ($\bar{2}$01) peak, as determined by the above method, differs by more than 0,1 degree 2θ from the measured peak, the cell has abnormal dimensions and cannot be determined by this method.

All samples were subjected to heat treatment (Orville, 1967), while the structural state of the feldspars were determined by using the position of the ($\bar{2}$01) reflection, based on the data of Wright and Steward (1968).

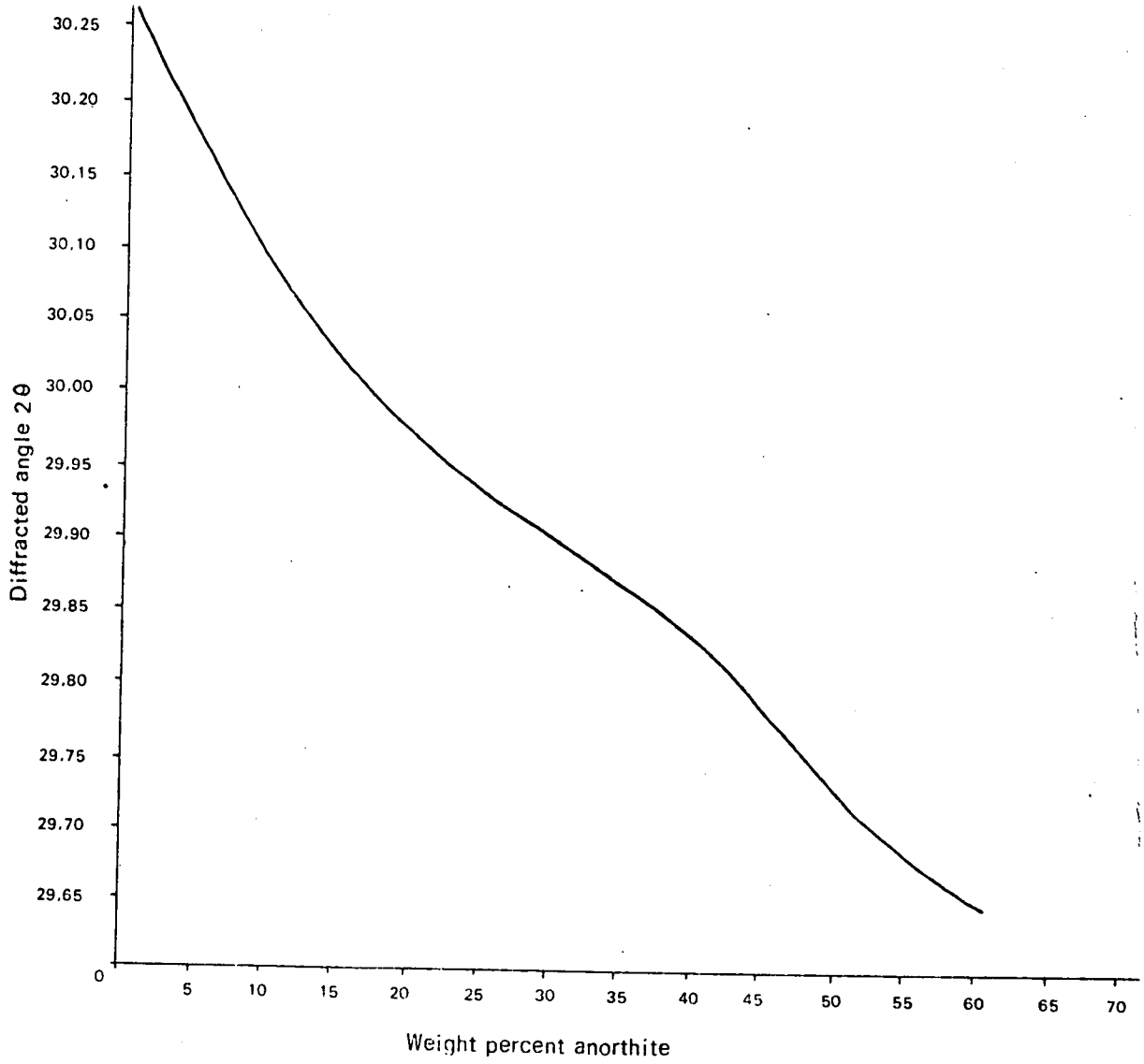

Fig. I.1. Plot of diffracted angle 2Θ against weight per cent anorthite.

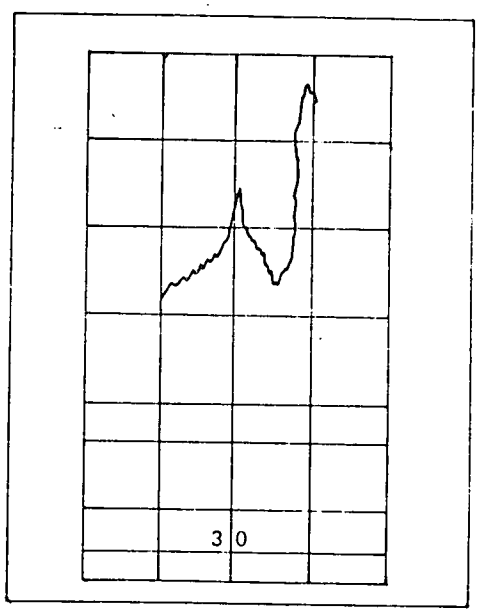

Fig. I.2. Example of diffractogram of peak at 30,05° 2Θ.

TABLE I.1 : PLAGIOCLASE COMPOSITION AS DETERMINED BY CONVENTIONAL MICROSCOPIC METHODS (VAN DER KAADEN, 1951) AND BY MEANS OF X-RAY DIFFRACTOMETRY

SAMPLE NUMBER	1	2
2/240	15	13
2/238	12	10
2/209	13	11
2/208	15	13
2/158	14	15
2/160b	16	14
2/160	13	12
3/15	12	14
2/216	10	12
2/188	16	15
2/185	14	12
2/223	13	15
2/137	10	10
2/133	12	8
2/242	12	14
2/42	14	16
2/252	15	15
2/105	10	10
2/164	15	13
3/48	10	7
$\bar{X}$	13,05	12,45
s	2,01	2,48

1) Plagioclase composition as determined by microscopic means

2) Plagioclase composition as determined by X-ray diffractometer

$\bar{X}$ = mean of series

s = standard deviation of series

APPENDIX II

MODAL ANALYSIS OF THE FELSIC ROCKS

Modal analysis was carried out on stained samples using a Swift Point Counter (Bailey and Stevens, 1960), in order to determine the accuracy of the X-ray diffractometric methods. The number of points which were counted was determined by the method of Chayes (1956).

X-ray diffractometric techniques have been employed quantitatively in the determination of one or more components in mineral mixtures (Black, 1953; Leroux *et al,* 1953; Klug and Alexander, 1954; Karner and Bertram, 1972).

Minerals from samples from the study area were separated and standards prepared. The diagrams of Tatlock (1966) were used to determine the weight fraction of each component after adjusting the 4,26 A^{o} peak height of quartz to correspond to the 70 and 30 per cent standards respectively. The setting was checked by measuring the background intensity for pure magnetite at 4,26 A^{o}, as this mineral may effect the quartz peak height (Tatlock, 1966) and must be eliminated.

Calibration was done to comply with the curves of Tatlock (1966) for quartz (Fig. II.1a), plagioclase (Fig. II.1b) and K-feldspar (Fig. II.1c). In the case of the K-feldspar, it is necessary to determine the crystal system (monoclinic or triclinic) before analysis, as a distinct difference exists between the reflected intensity of the 3,25 A^{o} peak for monoclinic and triclinic feldspar.

Determination of quartz requires that both the background intensity and the peak height above the background be known. The peak height is first plotted (Fig. II.1a), then the background correction must be applied and only then can the amount of quartz be read off. This is not true for the plagioclase or K-feldspar curves (Figures II.1b and II.1c), where only the peak height above background must be known.

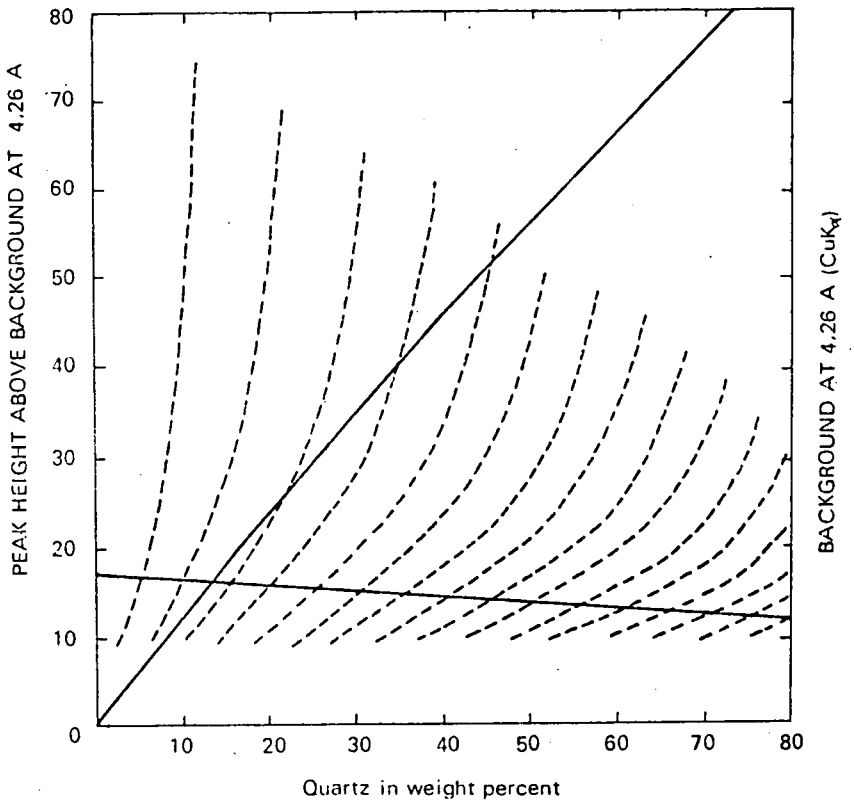

(a)

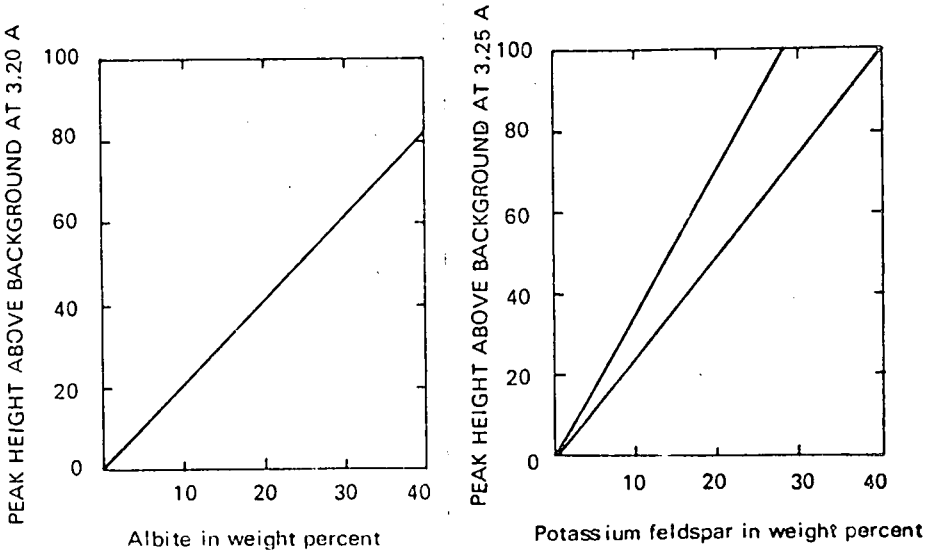

(b) (c)

Fig. II.1. Curves to determine the modal composition of samples containing quartz (a), plagioclase (b) and K-feldspar (c) (after Tatlock, 1966).

A reasonable correlation (95 per cent) was obtained between the X-ray derived data and those obtained by point counting, providing that the samples do not contain large amounts of perthite. This can be ascribed to the fact that the perthite lamella could not be measured individually under the microscope, thus making the X-ray method more accurate.

Instrument settings and angles at which measurements were done, are as follows :

INSTRUMENT : Rigaku Geigerflex with scintillation counter and automatic sample changer.

TUBE : Copper with nickel filter.

COUNTER : Time constant 4 seconds, 1 degree divergence and anti-scatter slits, 0,5 mm receiving slit.

RECORDER : Chart speed 10 mm/minute.

Mineral	kV	mA	Count rate full scale	A°
Quartz	40	15	4000 cps	4,26
Plagioclase	42	20	2000 cps	3,20
K-feldspar	42	20	2000 cps	3,25

APPENDIX III

TEXTURAL ANALYSIS

Textural analysis, as proposed by Hawkes (1967), is based on the number of crystals per cm^3, deduced from the number of crystals per cm^2. This analysis can be used to determine the amount of magmatic undercooling in a system, which will result in the formation of large phenocrysts in the eventual rock. Tyrrell (1958, p. 59) defines two regions; a metastable region where the crystallization is slow and the development of large crystals can take place and the labile region in which the crystallization is rapid, with consequent small crystal development.

The method as proposed by Hawkes (1967), was only applicable to phanerocrystalline rocks, however, and could not be used for aphanitic or cryptocrystalline rocks. This scheme was amended by Rhodes (1973) for use in volcanic rocks. In the case of phanerocrystalline rocks, this unit was termed the whole rock index (WRI) and in the case of volcanic rocks, it was called the crystallinity index (CI). The latter abbreviation differs from that used by Poldervaart and Parker (1964) for the Crystallization Index (CI).

The W.R.I. can be determined from the equation

$$\text{W.R.I.} = \frac{(n) \times (10)}{(\bar{s})}$$

where (n) = number of crystals per cm^2

$(\bar{s})$ = mean diameter of the crystals

The latter could be determined from the number of crystals per cm^2 as follows :

$$(\bar{s}) = \sqrt{(100)/(n)}$$

This equation is only valid for phanerocrystalline rocks, however, and had to be amended for use in cryptocrystalline rocks. This was accomplished by calculating $(\bar{s})$ in a different manner :

$$(\bar{s}) = \{\Sigma(\sqrt{lb})\}/n$$

where l = (the long axis of a phenocryst in mm)

b = (the short axis of a phenocryst in mm)

$\{\Sigma(\sqrt{lb})\}$ = the sum of all the square roots of (all the long axes)x(the short axes) of all the phenocrysts present in the section

n = (the total number of phenocrysts that have been measured)

In the latter formula 'n' must not be confused with that in the earlier part of the calculation. The number of phenocrysts per cm^2 must still be considered. The rest of the equation remains the same.

These calculations do not, however, reflect the degree of porphyriticness, so that another variable, the porphyritic index (PI) (De Bruiyn and Rhodes, 1975), was used. This can be calculated by the formula :

$$PI = \bar{x}/\bar{s}$$

where $\bar{s}$ = mean calculated diameter as used in the determination of WRI

$\bar{x}$ = mean diameter of the ten largest crystals in the thin section

The latter variable can be calculated according to the equation :

$$\bar{x} = (\Sigma\sqrt{lb})/10$$

where l = the long axis of a crystal

b = the short axis of a crystal

The PI can, under ideal conditions where the rock is completely equigranular, approach unity. This is very seldomly the case and therefore this could be used in conjunction with the WRI in correlating rocks from different areas.

APPENDIX IV

FORTRAN IV PROGRAMME FOR DETERMINATION OF CORRELATION PARAMETERS FOR PHENOCRYSTS

```
C       PROGRAM CORRELATION PARAMETERS
C
C     PROGRAM TO CALCULATE CORRELATION PARAMETERS FROM THE
C     LONG AND SHORT AXES OF CRYSTALS IN AN IGNEOUS ROCK
C     WHICH ARE MEASURED IN THIN SECTION OR GRAIN MOUNT.
C
      DIMENSION NL(500),NB(500),NS(500),NE(500),NV(500)
      DIMENSION X(4),Y(4)
C
C       READ MULTIPLICATION CONSTANT (C)
C       AND NUMBER OF CRYSTALS (N)
C
      READ(5,19)C,N
   19 FORMAT(1X,F6.3,I3)
      WRITE(6,1)C,N
C
C        READ HISTOGRAM INTERVAL (HL2) AND
C       MAXIMUM LENGTH OF CRYSTAL (HL3)
C       AS WELL AS HISTOGRAM INTERVAL (HV2)
C       AND MAXIMUM VOLUME (HV3) WHICH IS
C       CALCULATED BY X(MAX)*Y(MAX)*Y(MAX)
C
      READ(5,40)HL2,HL3,HV2,HV3
   40 FORMAT (4F7.3)
    1 FORMAT(5X,'C=',F6.3,5X,'N=',I3)
      HL1=0.000
      HE1=1.00
      HE2=0.50
      HE3=6.00
      HV1=0.000
    2 FORMAT(2F6.3,5X,2F6.3,5X,2F6.3,5X,2F6.3)
      DO 20 JJ=1,100
      NL(JJ)=0.
      NB(JJ)=0.
      NS(JJ)=0.
      NE(JJ)=0.
   20 NV(JJ)=0.
      SUMX=0.
      SUMY=0.
      SUME=0.
      SUMS=0.
      SUMV=0.
      SUMXX=0.
      SUMYY=0.
      SUMXY=0.
      FN=N
```

```
C
C       READ (LONG AXIS,SHORT AXIS) OF CRYSTALS,
C       FOUR ANALYSES PER CARD
C
      DO 6 K=1,N,4
      READ(5,2)X(1),Y(1),X(2),Y(2),X(3),Y(3),X(4),Y(4)
      IF(N-K-3)4,3,3
    3 M=4
      GO TO 5
    4 M=N-K+1
    5 DO 6 J=1,M
      X(J)=X(J)/C
      Y(J)=Y(J)/C
      E=X(J)/Y(J)
      S=SQRT(X(J)*Y(J))
      V=X(J)*Y(J)*Y(J)
      JJ=(X(J)-HL1)/HL2+1.0
      NL(JJ)=NL(JJ)+1
      JJ=(Y(J)-HL1)/HL2+1.0
      NB(JJ)=NB(JJ)+1
      JJ=(S-HL1)/HL2+1.0
      NS(JJ)=NS(JJ)+1
      JJ=(E-HE1)/HE2+1.0
      NE(JJ)=NE(JJ)+1
      JJ=(V-HV1)/HV2+1.0
      NV(JJ)=NV(JJ)+1
      SUMX=SUMX+X(J)
      SUMY=SUMY+Y(J)
      SUME=SUME+E
      SUMS=SUMS+S
      SUMV=SUMV+V
      SUMXX=SUMXX+X(J)*X(J)
      SUMYY=SUMYY+Y(J)*Y(J)
    6 SUMXY=SUMXY+X(J)*Y(J)
      XBAR=SUMX/FN
      YBAR=SUMY/FN
      EBAR=SUME/FN
      SBAR=SUMS/FN
      VBAR=SUMV/FN
      WRITE(6,7)XBAR,YBAR,EBAR
    7 FORMAT(1X,'XBAR=',F10.7,3X,'YBAR=',F10.7,3X,'EBAR=',F10.7)
      WRITE(6,15)SBAR,VBAR
   15 FORMAT(1X,'SBAR=',F10.7,3X,'VBAR=',F10.7)
      RATIO=XBAR/YBAR
      SX=SQRT(SUMXX/FN-XBAR*XBAR)
      SY=SQRT(SUMYY/FN-YBAR*YBAR)
      WRITE(6,8)RATIO,SX,SY
    8 FORMAT(1X,'RATIO=',F10.7,3X,'SX=',F10.7,3X,'SY=',F10.7)
      RD=SQRT((FN*SUMXX-SUMX*SUMX)*(FN*SUMYY-SUMY*SUMY))
      R=(FN*SUMXY-SUMX*SUMY)/RD
      SLOPE=SY/SX
      RECIP=1.0/SLOPE
      WRITE(6,9)R,SLOPE,RECIP
    9 FORMAT(1X,'R=',F10.7,3X,'SLOPE=',F10.7,3X,'RECIP=',F10.7)
      SE=SLOPE*SQRT((1.0-R*R)/FN)
      DS=2.0*(1.0-R)*(SX*SX+SY*SY)/(XBAR*XBAR+YBAR*YBAR)
```

```
      D=100.*SQRT(DS)
      WRITE(6,10)SE,D
   10 FORMAT(1X,'ST ERROR SLOPE=',F10.7,3X,'D=',F6.2)
      A=SLOPE
      B=YBAR-A*XBAR
      WRITE(6,11)A,B
   11 FORMAT(1X,'REG LINE Y=',F10.7,'X+',F10.7)
      WRITE(6,21)
   21 FORMAT(1X,'ELONGATION HISTOGRAM')
      JJ=1
      H1=HE1
   23 H2=H1+HE2
      HN=NE(JJ)
      PERC=HN/FN*100.
      WRITE(6,22)H1,H2,HN,PERC
   22 FORMAT(1X,F5.2,3X,F5.2,3X,F6.0,3X,F6.3)
      JJ=JJ+1
      H1=H1+HE2
      IF(H1-HE3)23,24,24
   24 CONTINUE
      WRITE(6,25)
   25 FORMAT(1X,'LENGTH AND BREADTH HISTOGRAMS')
      JJ=1
      H1=HL1
   27 H2=H1+HL2
      HNL=NL(JJ)
      PERCL=HNL/FN*100.
      HNB=NB(JJ)
      PERCB=HNB/FN*100.
      HNS=NS(JJ)
      PERCS=HNS/FN*100.
      WRITE(6,26)H1,H2,HNL,PERCL,HNB,PERCB,HNS,PERCS
   26 FORMAT(1X,2F8.3,F8.0,F8.2,10X,F8.0,F8.2,10X,F8.0,F8.2)
      JJ=JJ+1
      H1=H1+HL2
      IF(H1-HL3)27,28,28
   28 CONTINUE
      WRITE(6,30)
   30 FORMAT(1X,'VOLUME HISTOGRAM')
      JJ=1
      H1=HV1
   31 H2=H1+HV2
      HNV=NV(JJ)
      PERCV=HNV/FN*100.
      WRITE(6,32)H1,H2,HNV,PERCV
   32 FORMAT(1X,F7.3,3X,F7.3,3X,F6.0,3X,F7.3)
      JJ=JJ+1
      H1=H1+HV2
      IF(H1-HV3)31,34,34
   34 CONTINUE
      CALL EXIT
      END
```

GEOLOGICAL LEGEND

SEDIMENTARY COLUMN

IGNEOUS COLUMN

recent and superficial deposits

Trachyandesite, with sporadic ... and dykes ... porphyry

Diabase dykes undifferentiated

Mk ... granite porphyry

Porphyritic ... granite with ... facies

Porphyry

VERENA GRANITE

SEKHUKHUNI GRANITE

NEBO GRANITE

STERK RIVER GRANOPHYRE

STAVOREN GRANOPHYRE

BLINKWATER GRANOPHYRE

RASHOOP GRANOPHYRE SUITE

LEBOWA GRANITE SUITE

ROODEPLAAT COMPLEX

BUSHVELD COMPLEX

WATERBERG GROUP

WYLLIESPOORT FORMATION

Sandstone, pebbly sandstone, small conglomerate

lw

ROOIBERG GROUP

SCHRIKKLOOF FORMATION

KWAGGASNEK FORMATION

Black glassy ... agglomerate ... and quartzite

vs

vk

Dip and strike ...

Geological ...

Quartz-filled shear zone

Fault observed

Fault inferred

2528B RUST DE WINTER

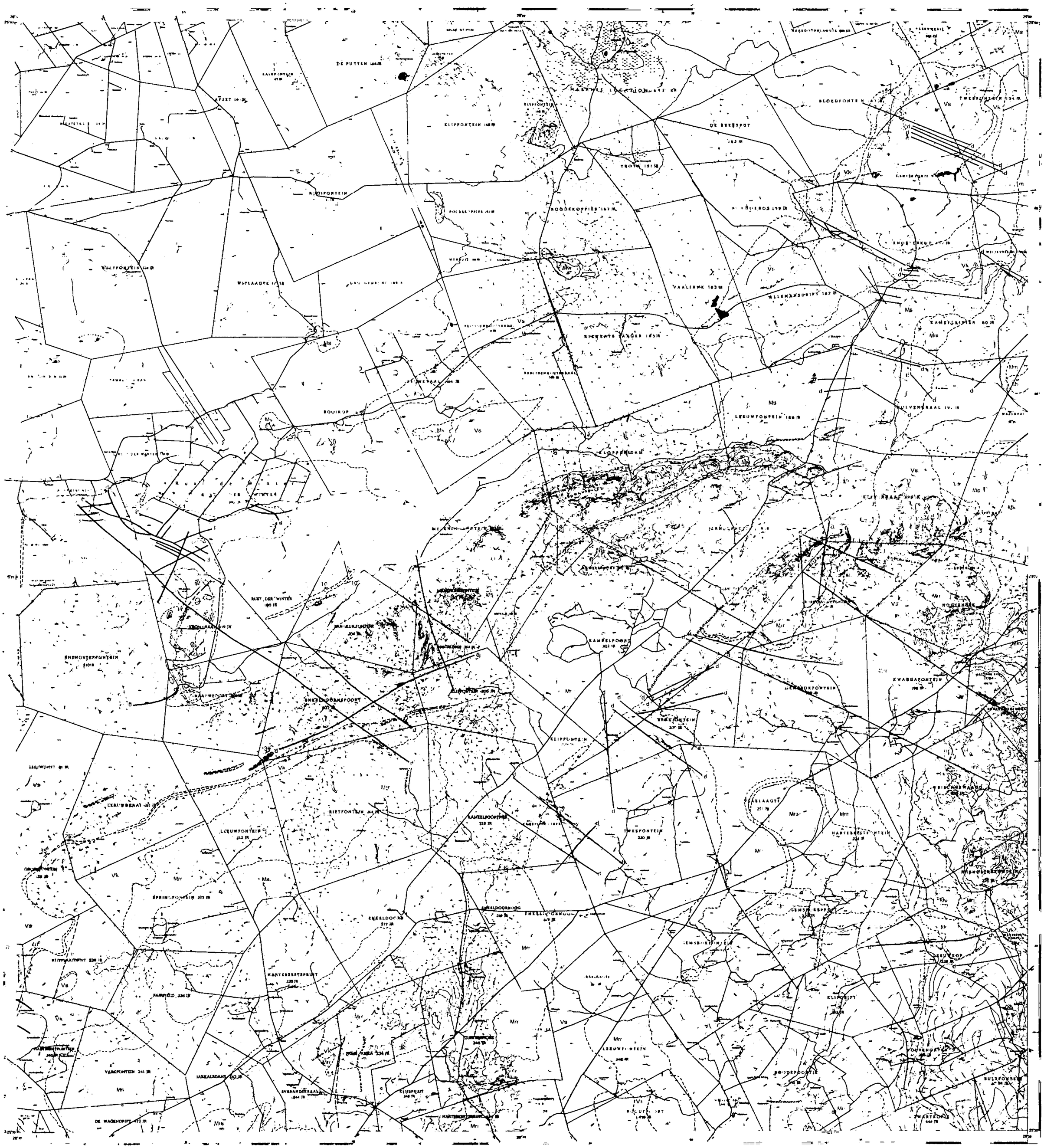

1 : 100 000

km 0 1 2 3 4 5 6 7 8 9 10 km

Miles 1 0 1 2 3 4 5 Myl

Topographical and cadastral information compiled from photographic reductions of the latest issues of the 1:50 000 topographical maps.

Topografie en kadastrale gegewens saamgestel vanaf fotografiese verkleinings van die mutste uitgawes van die 1:50 000 topografiese kaarte

2528A PIENAARSRIVIER

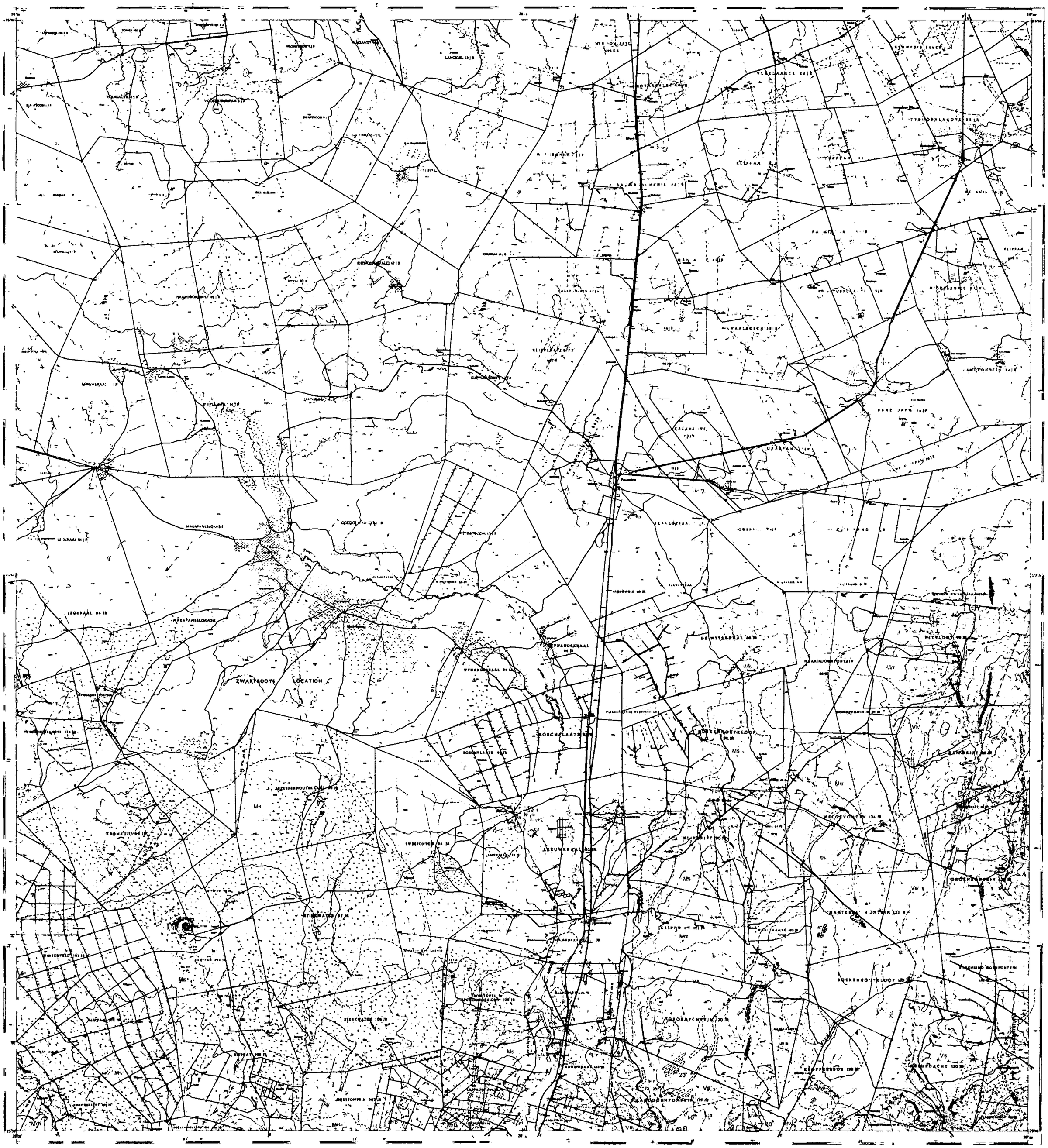

Topographical and cadastral information compiled from photographic reductions of the latest editions of the 1:50000 topographical maps.

Topografiese en kadastrale gegewens saamgestel vanaf fotografiese verkleinings van die nuutste uitgawes van die 1:50000 topografiese kaarte.

1:100000

km 0 1 2 3 4 5 6 7 8 9 10 km

miles 0 1 2 3 4 5 myl